NEURAL MECHANISMS OF GOAL-DIRECTED ACTION SELECTION BY PREFRONTAL CORTEX: IMPLICATIONS FOR BRAIN-MACHINE INTERFACES

By

Ali Mohebi

A DISSERTATION

Submitted to
Michigan State University
in partial fulfillment of the requirements
for the degree of

Electrical Engineering - Doctor of Philosophy

2014

ABSTRACT

NEURAL MECHANISMS OF GOAL-DIRECTED ACTION SELECTION BY PREFRONTAL CORTEX: IMPLICATIONS FOR BRAIN-MACHINE INTERFACES

By

Ali Mohebi

Initiating a movement goal and maintaining that goal throughout the planning and execution of a goal-directed action is an essential element of all goal-directed behavior. In the context of Brain Machine Interfaces (BMIs), a direct communication pathway between the brain and a man-made computing device, continuous access to movement goals is essential, so as to guide the control of neuroprosthetic limbs that provide neurologically impaired subjects with an alternative to their lost motor function. The Prefrontal cortex (PFC) has been suggested as an executive control area of the brain that bridges the temporal gap between incoming sensory information and ensuing motor actions. The mechanisms underlying the dynamics of PFC neural activity, however, remain poorly understood. The main objective of this dissertation is to elucidate the role of PFC neurons in mediating goal initiation and maintenance during goal-directed behavior.

Using a combination of electrophysiological recordings, optogenetic and pharmacological manipulation of population activity and behavioral assays in awake behaving subjects, we demonstrate that the PFC plays a critical role in the planning and execution of a two-alternative forced choice task. In particular, PFC neurons were mostly goal selective during the choice epoch of the task when subjects had to select the action with the highest utility while suppressing all other unrewarded actions. Decoding PFC neural activity using advanced machine learning algorithms showed robust single trial prediction of motor goals,

suggesting that PFC may be a candidate site for inferring volitional motor intent. In addition, results from inactivation experiments demonstrate a lateralized performance decline with respect to the inactivation site, further confirming the critical role of the PFC in mediating the motor- but not the sensory- information during the execution of goal-directed behavior. Taken together, our results suggest that the design of next generation BMIs could be further improved by incorporating goal information from cognitive control areas of the brain, thereby augmenting the capability of current designs that only rely on decoding the moment-by-moment kinematics of intended limb movements from motor areas of the brain.

To **Art** and **Philosophy**, the precogs of scientific endeavor
To **Maman** and **Baba**, who taught me
To my **Love**, whom in her presence love exists

ACKNOWLEDGMENTS

Of course I should start this dissertation by acknowledging **Karim**'s role in my past five years. He is the one who admitted me into his lab, provided funding for my research and scientific travels and throughout the years helped me to get hands on biomedical research. I should mention upfront that I may use singular subject pronouns in this dissertation explaining some of the work, but truth is Karim has been closely involved in the process of experimental design, analysis and interpretation of the results to the extent that I consider all these a common intellectual property of both of us. Besides his intellectual contributions, I have enjoyed being a student in his lab and he has been a good mentor and I hope for our professional and friendship relations to linger on.

Also I should thank my guidance committee members: Prof. *Jack Deller*, who taught me things beyond the *'Detection and estimation'* course I took with him in my sophomore year, Dr. *Devin McAuley* who reinforced my interest in *'basic cognitive processes'* through the course material he taught me and the series of seminars and workshops he managed to hold as the director of Cognitive Science program here at MSU, and last but not the least, Dr. *Joshua Berke*, professor of psychology at University of Michigan who devoted his time to guide me throughout my research, meet with me and travel to MSU campus for my comprehensive exam and defense session.

I also found myself lucky joining the NSEL lab and having the company of such great friends: Seif-Eldawlatly who guided me through the transition to a wet lab and always a great friend, Mehdi Aghagolzadeh who was always there for me as a brother and consultant, John Daly with whom I spent hours and hours debating about intellectual dilemmas in science, engineering, religion, politics etc, definitely an outstanding fellow, Erin Purcell the

brilliant research scientist in our lab who both helped and taught me . . . and all other friendly members of the lab who made this an exciting experience: Ki Yong Kwon, Karl Hedderich, Farzad Asgarian, Ahmed Eleryan, Islam Badreldin, May Mansy, Mehrdad Hashemi, Julian Alford and Wilfredo Cartagena.

During my first two years here at Michigan State I was involved with the leadership of the MSU Persian Student Association (PSA). I really enjoyed my time there, we initiated programs for helping newcoming Iranian students to help them settle and had a number of community wide and university wide outreach programs. I like to acknowledge all my friends in PSA especially Rouhollah Jafari, Mehdi Aghagolzade, Amir Khakpour, Fatemeh Noohi and Sohrab Soltani.

Later I joined LEEGS, the League of Electrical Engineering Graduate Students first as a member and then in a leadership role. That was a fantastic experience where I developed partnership with number of fellow EE graduate students from different backgrounds, we had a few successful initiatives and lots of joyful social gatherings. LEEGS was also a good opportunity to work with the department administration to foster better quality of graduate school experience for all graduate student. I would like to thank the chair of ECE department Prof. Tim Grotjohn for his continuous support of LEEGS and Prof. Shanker the advisor to our group and the department chair of graduate studies for the time he devoted for our group. And I like to acknowledge the friendship of my fellow ECE graduate students at LEEGS, Andrew Baczewski, Daniel Dault, Shannon Demlow, Andrew Pray, Nick Miller and others.

Council Of Graduate Students (COGS) is the student government body here at MSU. It was my pleasure to serve on the full council as the representative for ECE graduate students and through COGS on a number of university committees. Throughout many years in

academia I have been involved with a number of student organizations. COGS has been and probably will remain my best such experience. I like to thank Stefan Fletcher, Emily Bank, Shannon Demlow and Mandie Maxwell.It was through COGS that I gor the chance to serve on the search committee for the dean of engineering which was an extraordinary experience. I would also like to thank Dr. Thomas Voice, chair of the committee for all the effort he put forward for the committee.

This acknowledgment is growing large and I haven't yet talked about the role of my family. There is nothing I can mention to account for their sacrifice. This work, and I all have, will achieve and possess in future is dedicated to them; sweet fact is that I would still owe them.

PREFACE

A man is a success if he gets up in the morning and gets to bed at night, and in between he does what he wants to do.

— Bob Dylan

I used this quote from *Bob Dylan* in my comprehensive exam report and I am repeating it again here to emphasize the influence he had through his words and tunes on me during this period of my training as a doctoral student at Michigan State, aka the second half decade of my 20s, which will never come back. Of course I have enjoyed *'knocking on heavens door'* and *'like a rolling stone'*, but the most I learned from Bob is through his lifestyle depicted best in the amazing motion picture '**I am not there**' directed by *Todd Haynes*, staring the fabolous trio *Cate Blanchett*,*Christian Bale* and *Heath Ledger*. Bod Dylan taught me that you are a success if you do what you like to do in between getting in and out of the bed.

Like a Bob Dylan beavering away on finding some meaning for life, love and faith, I experienced many different and often apparently conflicting experiences to get to this point where I am and probably in future I would not remain still here. My first memories of existence in this world are all accompanied with books and novels. I was not a sports guy. I was not into dance and music. And for all not being these I regret, but this is how I grew up: being surrounded by books, spending hours and hours reading over and over. For all kids growing up in the same era I did, Jurassic Park and genetic engineering was a big fantasy. I remember reading that book and its sequels dozens of times, each time diving deeper and deeper, amazed by the chaos theory pieces that Ian Malcolm talked about throughout the book. Later in high school all those looked science-fiction to me. I distanced myself from biology and got into physics. I guess what made the awe in me for physics was the predictive

power of the theories I was studying in mechanics and the power of mathematical modeling of natural phenomenon. I was thrilled by the noticing that a mathematical formula can predict the trajectory of a flying ball, and same principles can be applied to predict the trajectory of a planet revolving around a star. This was amazing, I knew I wanted to become a physicist. But then physics was looked down back home. Smart, brilliant kids in my school all used to either pursue medical school or top engineering programs. Only those who couldn't get into these disciplines got science majors. So this time unlike Bob Dylan I followed the mainstream and got into a prestigious electrical engineering program.

College years awakened the rebel inside me. While attending the engineering courses I followed my *other* interests in literature, arts and philosophy, working as a freelance writer in a literature magazine of which I was elected later as the editor-in-chief. I finally got my diploma in electrical engineering with a concentration in control theory. This was where I steered back to some old thoughts I had and applied chaos theory to analysis of some biological phenomenon: heart-rate variability. Of course at the time I was a cocky ignorant young man, biological system was far more complex and my ambitious efforts of modeling were not predicting any real phenomenon. I got a chance to get to the nation's top biomedical engineering program and work on a thesis under the supervision of the brilliant Prof. Soltanian-Zadeh. Good times and great experiences.

Long story short, at the age of 25 I joined Michigan State electrical engineering program. I like to think that I had a role in this, but honestly it was a matter of luck that my PhD adviser and mentor had very similar interests in science of brain where I was starting to branch out at the end of my Master program. Five years later, here I am starting the fourth decade of my life, still know nothing about brain function but I now have more and more knowledge about my ignorance. Compared to where I was standing when joined this

program, I am now a much more educated ignorant and I like it this way.

This dissertation summarizes parts of my journey during the past 5 years. I would expect the reader to share some of my enthusiasm in discovering the unknowns of the most complicated computing machine that ever existed on the earth. I have tried to shed light on some aspects of its function, but the ocean of known unknowns and unknown unknowns of brain function stays unexplored ahead of us, calling for passionate and ambitious sailors. So read the diaries of one young cabin boy who has joined the exploratory trip. When you finish reading, you would not find me at the end. *I am not there*, I am sailing away.

Ali Mohebi — East Lansing, MI

TABLE OF CONTENTS

LIST OF TABLES

LIST OF FIGURES

KEY TO SYMBOLS AND ABBREVIATIONS

Abbreviation	Description
BMI	Brain-Machine Interface
MD	Medio Dorsal Nucleus
PFC	Prefrontal Cortex
mPFC	Medial Prefrontal cortex
PrL	Prelimbic area (of mPFC)
SVM	Support Vector Machine
LFP	Local Field Potential
WM	Working Memory
ChR2	Channel Rhodopsin (Version 2)
ArCh	Archaerhodopsin
M1	Primary motor cortex
M2	Secondary motor area
MSN	Medium Spiny Neurons
FSI	Fast Spiking Interneurons

Chapter 1

Introduction

Principles and logic do not give birth to reality. Reality comes first and the principles and logic follow.

— Haruki Murakami, *1Q84*

1.1 Motivation

Brian Kolfage is an Iraq war veteran, who lost his right arm in an insurgent attack back in 2004. Koni Dole, a Montana high school football player, suffered a compound fracture on the field that cost him his leg. Christopher Reeve, an American actor, film director and producer became a quadriplegic after being thrown from a horse during a competition in Virginia.

Partial or full loss of movement ability is not limited to these individuals and indeed is a widespread affliction. A report published by Christopher and Dana Reeve foundation in 2009, estimated that almost 5.6 million people in US only, are suffering from some form of paralysis, with the leading causes being stroke, spinal cord injury and multiple sclerosis [47]. Ziegler-Graham et al. [251] also estimated that there are nearly 2 million people living with limb loss in the United States, with main causes being vascular disease, trauma and cancer[1]. Amputations occur at the rate of 185,000 per year in the United States and is estimated to

[1]Like Augustus Waters, the male love interest in John Green's New York Times bestseller *The fault in our starts*, who suffered a limb loss due to cancer.

cost over $8.3 billion [82, 182].

What is common among all these different cases of movement disabilities is that the patients have lost their motor execution abilities, but their brain regions responsible for planning the movements and initiating a will to move is still intact. It has been proposed that one can utilize these intact brain signals to decode motor commands and drive prosthetic to restore motor function.

My first encounter with the idea that decoding thoughts and intentions is possible through electrodes implants on top of the skull was in third grade elementary school through the brilliant science-fiction trilogy by John Christoher: *The White Mountains (1967)*, *The City of Gold and Lead (1968)* and *The Pool of Fire (1968)*[2]. In this post-apocalyptic novel, humanity has been conqured and enslaved by *'The tripods'*. Humans are controlled by *Masters* through *caps* implanted on their skull at the age of 14. People who are capped happily follow and serve the masters, as their minds are controlled by them. The story rolls with the narrative of Will Parker, a rebellious teenagers who joins the rebels camouflaged in the white mountains working on a strike plan against the tripods.

Around the same time that John Christopher was writing his ingenious novels in England, Eb Fetz had recently graduated from Massachusetts Institute of Technology with a PhD in physics and had started a post-doctoral fellowship at University of Washington in Seattle where he later became a professor of physiology and biophysics[3]. Using the same idea that

[2]Here I should acknowledge my amazing creative writing teacher Mr.Adel who introduced me to these novels.

[3]In 2013 during his visit to Michigan State University, when I picked him up from the Lansing airport, during our brief trip to campus, he told me how strange it was back in 1965 for someone from department of physics at MIT to work on a dissertation topic barely related to the so called 'mainstream physics' and the hardship he had to go through to get the dissertation accepted. The trick was easy though, he changed the dissertation title to 'Physics of spinal cord injury'. Use of the term 'physics' in the title made the magic! And finally he joked to me and said you are in the department of electrical engineering, maybe you can title your dissertation as 'the circuits of

inspired Christopher, Fetz adopted the technique called electrophysiology to record activity of individual nerve cells from the motor cortex of awake behaving rhesus macaque monkeys. He discovered that the primates were able to volitionally control the activity of these motor cortex cells without eliciting any overt limb movement. Results of this study was published in the prestigious journal *Science*, brought him fame and kicked off the modern science of Brain-Machine Interface (BMI) [88–90, 171].

Brain Machine Interface (also called direct neural interface) is an interdisciplinary field of research where the main goal is to restore sensory and motor function of the brain using a direct communication pathway between brain and an external device. Since its infancy, the field has exploited on the capacities to restore impaired hearing and sight senses and motor functions. Although the underlying mechanism of BMI function is very poorly understood, but speculations are that BMIs work through the amazing properties of the brain tissue known as 'plasticity' [169], which in simple terms is attributed to changes in structural and functional properties of brain circuitry due to changes in the environment or learning and can occur at different levels.

Here at Neural System Engineering Lab (NSEL) where I am a contributing member, our research is focused around the Brain Machine Interfaces at multiple development areas. Although the idea of a BMI has been around for a long while, and early implementations of BMI have shown success, the progress in the field has been very incremental. Inception of the modern science of BMI idea can be traced back to Eb Fetzs work in 1967, where he showed volitional control of one degree of freedom using brain signals. State-of-the-art BMI from the BrainGate group reports 3 DoF control in 2012 which is still far from the 27 DoF required of natural hand control. This slow progress in BMI capabilities is puzzling and

prefrontal cortex'.

becomes more puzzling when one considers the progress in robotics which is the backbone of any BMI. Majority of current BMIs use brain signals from the motor cortex and apply regression algorithms to decode the trajectory of a robotic arm movement for multiple degrees of freedom. It has been suggested [166, 189] that BMIs can adopt an intermittent level of control where the job of the decoder be rapid realization of intended actions rather than decoding moment-by-moment changes of the trajectory. In this scheme, upon motor intent decoding, the robotic algorithm will take control of finding the optimal movement trajectory and the decoding algorithm will monitor the neural activity for any possible 'action switch'.

The question underlying this switch between or choice of different action plans has long been studied under different terminologies such as 'decision making', 'action selection' etc [200]. Different brain regions may contribute to the action selection process and thus signals collected from different brain regions have been suggested to be exploited on for the so called 'cognitive BMIs' [10]. Although the idea of 'modularity' in cognitive functions of the brain has been refuted and the whole brain as an entity is believed to be engaged in all aspects of our behavior, still some brain regions are *more* involved in certain tasks than others. Thus it makes sense to look for the optimal brain region for decoding motor intents.

Prefrontal cortex, sitting on top of the hierarchy of cognitive control in brain is one of the least understood regions of the neocortex. In this dissertation I will explore the role of prefrontal cortex of rodents in action selection through a delayed choice task. The results of this study can be insightful to for the design of next generation cognitive Brain Machine Interfaces.

1.2 Organization of this dissertation

This dissertation is organized into 6 independent but interconnected chapters. In the chapter following this introductory chapter, I *review* the related literature about Brain Machine Interfaces, prefrontal cortex and delayed reaction tasks. In this chapter only the basics and concrete concepts related to each topic will be covered. I have kept the more speculative studies for the discussion chapter. I also review a number of recent studies where a very similar experimental design was used to study roles and functions of different brain regions.

Chapter 3 has been dedicated to the *methods* used throughout this study. Given the extent and the number of different experiments and analysis used in this study, I have dedicated some good portion of the document elaborating on the techniques and analysis methods. The methods are in fact the key to collect the required empirical evidence in order to answer the scientific question I am after. Thus I paid attention to the choice of methods acquired for this dissertation and the reader may come across a body of references throughout the methods chapter.

Chapter 4 which is the heart of this dissertation showcases and compiles *results* from different experiment and analysis. Here I try to use graphics and statistics to summarize mass of information collected to answer research questions of my interest. To the extent that is possible I have interpreted the results as illustrating them, but thorough interpretation of the results were left to the next chapter. I tried to keep the order of the presented results in a way to make it more intuitively comprehensible and represent the line of thought that I followed during the design of the experiment. Wherever required I had highlighted and emphasized the most important results that the reader should pay careful attention to and gloss over the less important results.

Chapter 5 is the *discussion* chapter. The purpose of this chapter is to give meaning to the previously presented results by binding them to the previously established theories. I have also made an effort to extrapolate from the results and come up with explanations for still unknown mechanisms of action selection in brain.

And at last in chapter 6 I will have the *concluding remarks* where I try to recap the previous five chapters and provide suggestions for future works based on the results of this study. Limitations of the study will also be discussed in this chapter and suggestions are made to overcome these limitations.

Chapter 2

Literature Review

Contained within each of these articles is the joy of learning for its own sake... But research is only the first step, we can't ignore the lingering question of how we can -and should- use scientific evidence to our advantage.
— Dan Ariely, *The Best American Science and Nature Writing 2012*

2.1 Introduction

The main objective of this dissertation is to explore the role of prefrontal cortex circuits in initiating and processing information related to motor action selection and execution. The idea is to use the information as an input to cognitive motor prosthesis in form of flexible control signals, which will ultimately provide an unprecedented opportunity for patients suffering from amputation or paralysis. As mentioned earlier, this problem is mainly studied in the framework of Brain-Machine Interface (BMI) among the neural engineering community.

In this chapter dedicated to literature review, I will start with a brief introduction of the Brain-Machine Interface problem, its history, scope and challenges. Then I will review the literature related to cognitive neural prosthetic, which is a relatively newer concept trying to approach the BMI from a different perspective. I will describe the rationale supporting the use of cognitive prosthetic for the BMI application.

As will be described in the following sections of this chapter, different signal modalities from myriad of brain regions have been recruited for cognitive neural prosthetic. My proposal in this dissertation is to utilize neuronal signals from the prefrontal cortex for this purpose. Prefrontal cortex compared to other parts of the brain has been studied less, partly due to complexity of the anatomy and difficulty in interpretation of the results of recorded activity. Especially in the context of BMI, I am not aware of any study using signals from prefrontal cortex. Here I suggest recruiting prefrontal cortex to obtain a flexible drive signal for the BMI devices. Thus the final section of this review will be dedicated to explore the literature of theories of prefrontal cortex function in order to endorse our suggestion.

2.2 Brain-Machine Interfaces

2.2.1 Introduction

Over 10 million people are suffering from different types of motor disabilities, in US only. These disabilities range from paralysis to limb amputation [47, 82, 182, 251]. A common feature of many of these disabilities is that although their motor apparatus is impaired but the regions in the cortex responsible for voluntary movement planning and execution are intact. The main idea behind the Brain-Machine interfaces is to use brain signals from these regions, decode the motor volition using computer algorithms and use the information to drive prosthetic arms [123] for amputees or to use Functional Electrical Stimulation (FES) to move the paralyzed limb, bypassing the spinal cord [84]. An FES system uses electrical pulses to activate muscles in an orderly fashion in order to drive the limbs [188].

Use of prosthetic limbs to replace amputated arm/leg is not a modern invention. In fact historical references for such prosthetic can be traced back to 1500 BCE, in a Hindu

holy book that mentioned the warrior queen Vishpala who had a leg amputation in a battle that was replaced by an iron limb [168, 183]. However, the idea of using brain signals to derive movement information used for prosthetic is not more than half a century old. Miguel Nicolelis, himself one of the front runners of this field, considers [171] the seminal study of Eberhard Fetz of the University of Washington as a game changer for the field [88–90].

In these series of experiments, Fetz and others recorded activity of single cells from intact brain of an awake behaving monkey using a single metal microelectrode. The activity was conditioned by reinforcing higher rates of neuronal discharge with delivery of a food pellet. In short, firing rate of the individual cell was transformed to parameter controlling an auditory/visual feedback using a mathematical formula. The feedback was provided to the monkey so that the subject was aware of the state of the cell's firing rate at each moment in time. Modulating the firing rate beyond a fixed threshold was reinforced using reward pellets. Fetz and colleagues showed that after several training sessions, the monkey were able to volitionally modulate the firing rate of individual cells by up to 500 percents beyond the rates before reinforcement, without intervening movements.

This observation that subjects can volitionally control firing rates of individual cells in their brain using a (neuro)feedback, paved the way for the emergence of the Brain-Machine Interfaces (BMI) as a scientific field of study. Figure 2.1 summarizes the main idea behind a closed-loop motor BMI.

First the activity of multiple brain cells in a single or multiple motor-related areas of the brain is recorded using a multielectrode array device. After some preprocessing steps(similar to those that I recruited in the Chapter 3), the signal is passed to a *decoding algorithm*, that transforms the recorded brain activity into kinematic and kinetic variables such as joint angle and velocity [72, 146]. Decoded kinematic parameters are then used to drive the

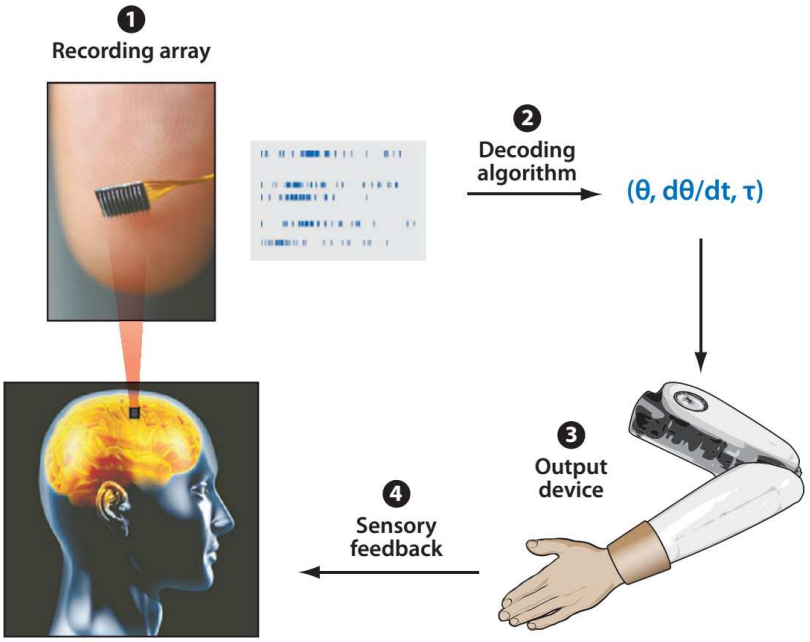

Figure 2.1: **Basic components of a Brain-Machine Interface. 1)** a recording array, implanted through or on top the cortex and records the activity of a population of cells on multiple channels. **2)** a decoding algorithm (often one sort of regression) that translates the brain activity into motor commands **3)** an output device controlled by the translated motor commands **4)** and sensory feedback often in forms of auditory or visual feedback .Adapted from [118]

prosthetic device through a desired trajectory and the subject receives information regarding this movement via visual feedback.

2.2.2 Challenges

While BMIs have provided an unprecedented opportunity to explore brain's ability to directly control artificial machines, they are still far from being clinically viable. A recent human study of tetraplegic patient has shown the capability of an advanced BMI to control 4 degrees of freedom (DOF) for a reach to grasp task [123]. More recently, Andrew Schwartz's group reported successful control of 7 DOF using two 96-channel implanted arrays in the motor cortex of one patient suffering from tetraplegia [53]. Although this is quite an achievement for the scientific community, there is a long way to go for approaching a natural hand control. Human arm has 7 DOFs and the whole hand has been modeled using 27 DOFs or even higher [111]. Thus in order to restore an able-bodied level control of the prosthetic, higher DOFs are required. Whether current approaches of transforming activity of ensembles of neurons to individual degrees of freedom will enable generalized control of more degrees of freedom is yet to be studied [102, 118, 151].

This in fact is the main challenge of the current implementation of BMIs. Recent progress in control and robotic engineering provides simultaneous control of many degrees of freedom for a robotic arm that in turn enables very dexterous reach and grasp actions. One may expect that this dexterous control of robotic arm gets translated in cortically driven neuroprosthetics as well. In my opinion, part of the limitation is rooted in the 'majority' approach to the decoding problem in BMI. It has become a common practice to decode the trajectory of the prosthetic arm on a moment-by-moment basis from the recorded neural data [20, 44, 214, 222]. An alternative 'minority' approach promoted by Richard Andersen at

Caltech is to decode movement goals from the brain activity and delegate the problem of finding the optimal trajectory to the robotics [10, 166, 189].

2.3 Temporal Organization of Action

Since the discovery of the so called *memory cells* [96], Joaquin Fuster has dedicated his career to do research on the prefrontal cortex. In the fourth and latest edition of his popular book *The Prefrontal Cortex* [95], he introduced a framework to understand and interpret the role of the prefrontal cortex in the *Temporal Organization of action*. His model is based on the following three propositions:

1. Frontal cortex is dedicated to representation and production of action.

2. There exists a causal relation between the neural substrate of action representation and production.

3. That neural substrate is organized hierarchically, with the lowest compartment being primary motor cortex responsible for the production of elementary action and dorsolateral prefrontal cortex (in primates) sitting at the top representing abstract and complex plans.

The proposed model disputes the modular view (rooted from sensory and motor physiology) for the function of frontal lobe and instead emphasizes on the network view that supports widely distributed *cognitive networks* across many different brain areas. While emphasizing the role of prefrontal cortex in the top-down control of action, the framework does not support an initiation role for the prefrontal cortex or any other brain area but rather advocates a theory of parallel and circular perception-action cycles with no true origin, neither

cortical nor subcortical. In other words, in this model the prefrontal cortex is not considered a *central executive* unit but a *principal conductor of an orchestra* would be a better analogy[1]. It is the continuous flow of information between the organism and the environment that enables goal-directed behavior and the prefrontal cortex is the *supreme temporal integrator* in that cycle. In the functional hierarchy of the frontal cortex or we should call it the *action cortex*, primary motor cortex is located at the lower stage of representing and producing action with the premotor areas sitting on top of that below the supplementary motor areas. Lateral prefrontal areas are at the top of this hierarchy. Whereas in the primary motor cortex there is a somatotopy, premotor and prefrontal cortices represent actions in a more global level, by goal and trajectory. A schematic block-diagram of this hierarchy is shown in Figure 2.2.

Goal-directed behavior should be distinguished from habits in the sense that goal-directed actions are educated choice that the organism make in order to satisfy and end through an interaction with the environment. This type of action is routinely considered deliberate since it is motivated by a *deliberation* of choices and their corresponding risks and values. There are two basic principles that one should bare in mind in order to interpret the temporal dynamics of neural representation in the prefrontal cortex during execution of a goal-directed action. First is that any goal-directed action is structured sequentially based on the goal of the action and the relations between its *component actions*. And second, that the structure of the action is determined by an on-line interaction between the organism and the environment, with prefrontal cortex playing the role of an orchestra conductor controlling temporal integration and sequencing of the actions.

[1]The analogy is mine, Fuster might have use a different.

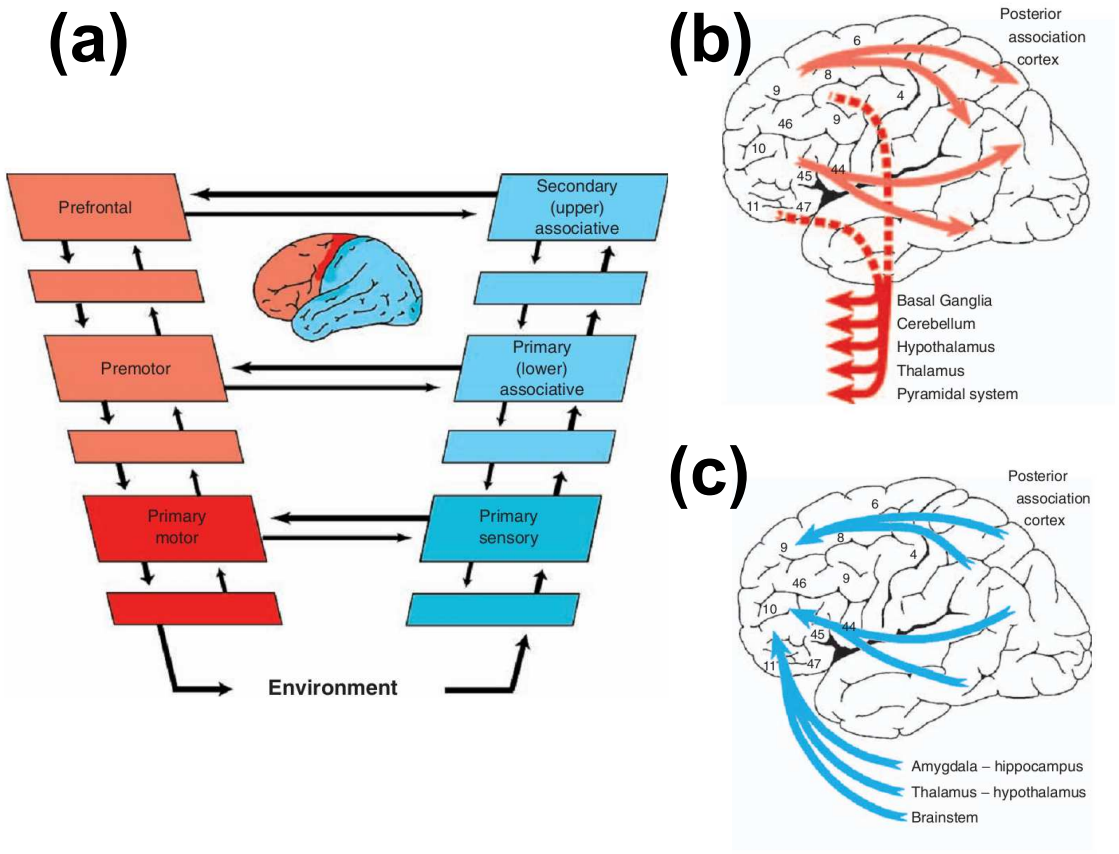

Figure 2.2: **Schematic of the top-down control of a goal-directed action (a)** Any goal-directed behavior is mediated through an interactive neural control with the prefrontal cortex as the top of the hierarchy. Different brain areas are specialized to translate the motor plans (schema) into muscle movements or relay the movement related sensory information from the environment required for online monitoring of the task execution. **(b,c)** Afferent(red) and efferent(blue) of the prefrontal cortex involved in the monitoring and execution of goal-directed tasks.

Fuster's framework utilizes more than 50 years of electrophysiology and imaging studies of the frontal lobe. Under the umbrella of this general framework, we will review some relevant literature in more details and use those as a basis and motivation to design an experiment that helps elucidate the mechanism of prefrontal cortex function in more details.

2.4 Delayed Reaction

In an episode of the Tom and Jerry© show, Jerry is sneaking in the room to run away with some cheese while Tom is leisurely laying down on a pillow with his back to the cheese. He notices some noise and turns his head to the other side that he glances at Jerry. Noticing that, Jerry runs towards the wall and jumps into one of the three holes in the wall before Tom can react. Not surprisingly, after Jerry escapes into the hole, Tom will move towards the hole where Jerry is hiding and a series of pursuit starts.

Inspired by observing a similar scene in 1913 William Hunter wrote a PhD dissertation on *The delayed reaction in animals and children* [132]. The phenomenon that he studied is a very typical mammalian behavior in which the determining stimulus is absent at the moment of response. More specifically he asked two questions: "1) *How long after the determining stimulus has disappeared can an animal wait and still react correctly?* 2) *Does the animal give any behavior cues as to its method of solving the problem? If so, what are they?*" He then postulates that some *images* or *ideas* are the driving force for the reaction in the absence of determining stimuli.

In a quest to answer the above mentioned question, he designed an experiment very similar to the case of Tom and Jerry skit, with a subtle difference where he used three lights inside the holes to cue the animals of the location of the food. A picture of rat version of the

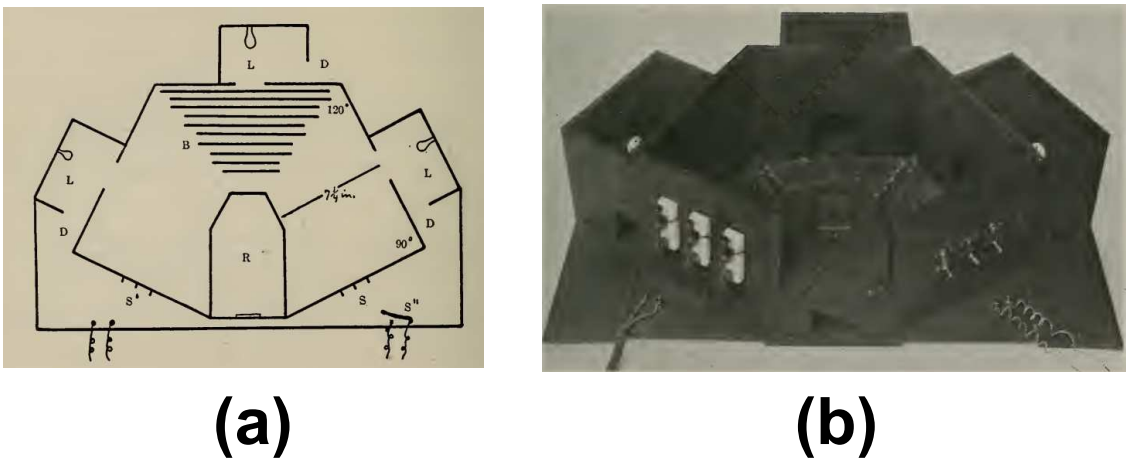

Figure 2.3: **Experimental apparatus used in Hunter experiment a)** Schematic of the design and **b)** the apparatus used in the rat version of the study.

experimental apparatus is shown in Figure 2.3. He repeated variants of the this experiment for dogs, raccoon and children.

The animal is initially located in the area R(release) of the cage and one of three targets (area L) is lighted while the animal is still in area R. After a few seconds the light in target is turned off and the animal is released after 5 seconds and is free to move to the target. The behavior of the animal is monitored throughout the session and correct visits are rewarded. A careful detailed record is kept of the animal orientation before and after the release. The animal should go to the lighted box and come back to the entrance area in order to get rewarded. The maximum length of the delay period for different animal subjects is shown in Table 2.1.

Only four out of the 14 animals reached a maximum delay greater than 1 second. Raccoons performed a bit better (one of them reached a maximum of 25 seconds of delay versus the maximum of 10 seconds in rat) and one of the dogs could perform at 68% with delays of up to 5 minutes (although the second dog subject could not exceed 10 seconds depicting very high subject variability). Above all, human children could keep a memory of up to 25

Subject ID	Maximal Delay	Correct Responses (%)
2	1 sec	64
4	1 sec	52
5	did not learn association	N/A
6	did not learn association	N/A
7	3 secs	56
9	10 secs	72
10	1 sec	76
11	1 sec	64
12	1 sec	72
13	4 secs	88
14	3 secs	80
15	1 sec	86
16	1 sec	50
17	1 sec	37

Table 2.1: Distribution of reaction times across different rats.

minutes.

With regards to the second question that Hunter was looking after, he observed animals using three different startegies:

1. Orienting head or whole body towards the target

2. No orientation cues used by the animal

3. Animal moves to get closer to the target location inside the release area

Hunter concluded that the animals use the *ideas* in a similar fashion to humans to direct their action toward the goal. He also pointed out that these ideas could be ideas of objects (representing stimulus aspects of the situation) or ideas of movement and its sensory consequences. The methods he used at the time were not developed enough to help dissociate the sensory aspects of the memory from their motor aspects. He mentions that "*An experimental technique to isolate and control the movement factor would be extremely*

difficult if not impossible to devise. I doubt that whether experimental technique can ever control this movement factor."

To my knowledge, this is the very first study that investigated the delayed reaction behavior systematically which inspired a corpus of ongoing research in cognitive neuroscience. Many of the concerns he brought up (such as the subjects' use of body orientation in directing behavior) are valid question need to be addressed in any subsequent study.

In his work, Hunter was more interested in the behavioral aspects of the delayed task and the across species comparison. He did not posit any mechanism for the formation and maintenance of the *ideas* that he believed were the key to delayed reaction. Time needed to pass by so that other investigators will build up on his contributions and investigate the mechanisms by which the animals performed the task.

Almost 20 years had to pass so that Jacobsen would publish the results of his work [135]. The work later became one of the classical papers of neuroscience (reprinted by the Society for Neuroscience in their archive of classics). At the time there was a controversy on whether the frontal lobe of the animal cortex exerts a functional role in the animal's behavior as some lesioning studies had shown *" no symptoms indicative of affection or impairment of the special sensory or motor faculties "*. Reviewing the fuzzy literature about the realm of frontal cortex function, Jacobsen described a series of experiments designed to answer the question of the exclusive role of the frontal areas of the cortex in the production of the behavior: Do frontal areas mediate a behavior that the animal is incapable of expressing when the frontal cortex is impaired?

In one experiment that is relevant to the subject matter of this discussion, he tested primates for their delay responses where differential cues determined whether a right or left box is rewarded. However the cues were concealed from the subject and the subject had to

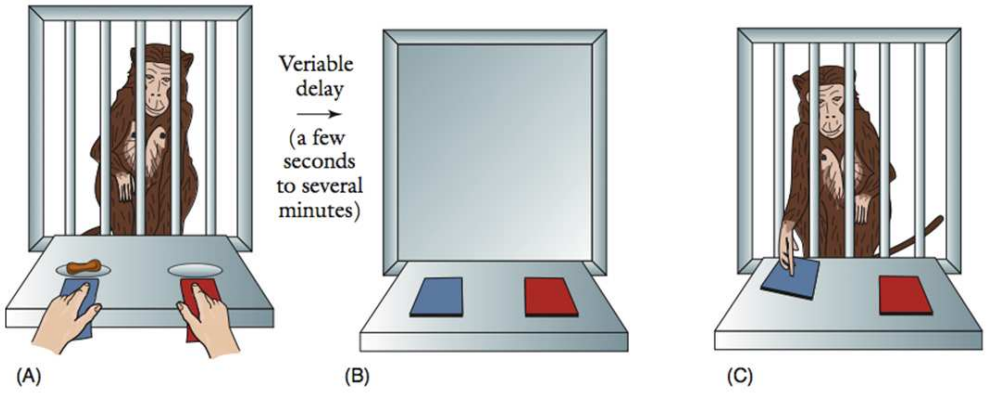

Figure 2.4: **The experimental design Jacobsen used to study the PFC** where differential cues determined whether a right or left box is rewarded. However the cues were concealed from the subject and the subject had to use a memory trace to decide about the target location. Adapted from Banich and Compton [19]

use a memory trace to decide about the target location. A cartoon summarizing experimental design is shown in Figure 2.4.

Basically the subject observes the experimenter hiding the food under either of the food ports but shortly before the subject can act and reach for the food, the experimenter puts an opaque the subject and the food ports. After a variable delay the subject the door is removed and the subject is allowed to reach for the food and the subject will be rewarded only if reaches for the correct target.

This piece of the experiment is very similar and in fact inspired by Hunter's work. The novelty in Jacobsen's experiment was linking brain activity to the subject's behavior in delayed responses. Subjects were trained to perform the task with higher than 80% accuracy and after they reached the final stage, different parts of their frontal cortex were surgically removed in different subjects and their postoperative performance was measured.

Unilateral removal of frontal association area did not affect the monkey performance in the delayed reaction task, however when it was removed simultaneously from both hemispheres, the performance was impaired permanently. Lesions to the temporal and parietal

areas left the delayed reaction task intact. Lesions to motor and premotor areas impaired the motor movement, to the extent that the subject was not able to open the food port door and after pointing to the door, the experimenter had to open the door for them. However, the accuracy of the performance was not affected.

Jacobsen's study was a major breakthrough for the cognitive neuroscience research. For the first time, the now called dorsolateral prefrontal cortex (dlPFC) was shown to be critical to the execution of delayed response tasks. More importantly, Jacobsen showed that the dlPFC is exclusively required for the performance of the task. Thus he concluded that the machinery required to perform the delayed reactions is localized in this area. However, it was still early to discover the cellular details of this machinery. Technology needed to advance and another 40 years had to pass.

It was in 1971 that Joaquin Fuster used the newly invented electrodes to record brain activity of dlPFC in primates while performing a delayed reaction task at a cellular level [96]. Fuster began by reviewing Hunter and Jacobsen's investigations and postulated that if the so called prefrontal cortex has a role in the performance of delayed reaction tasks, one should observe a modulation in the temporal dynamics of single cells' firing throughout the execution of the task. The experimental design Fuster used was very similar to that of Jacobsen's in which one of the visible targets was baited and shown to the subject and the subject's field of view was blocked for a delay period. The subject would be rewarded only if reached to the baited target after the delay period. Single unit activities were recorded in the prefrontal cortex and MD neucleus of thalamus using chronic implants. Delay periods were varied between 15 seconds and 60 seconds. Both baseline and task related activities were recorded in prefrontal (110 single cells) and MD thalamus (57 single cells). Most of the cells (both in MD and PFC) showed higher levels of modulation (with different magnitudes)

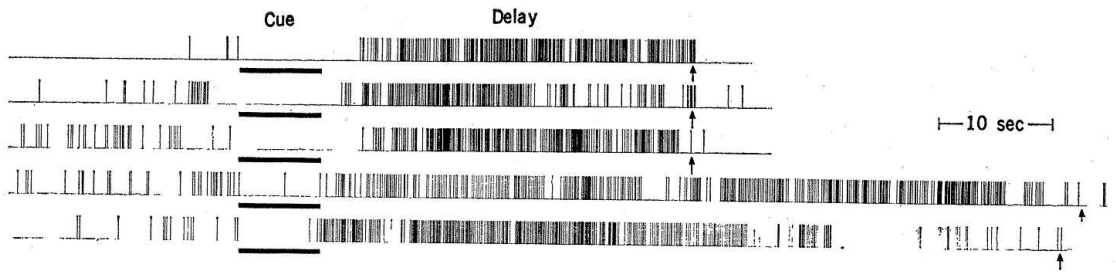

Figure 2.5: **Raster plot of a sample cell recorded in primate dlPFC**, across different trials during a delay period. Adapted from Fuster's seminal study [96].

during the task execution compared to the baseline. Some cells were only active during the cue presentation, some during the delay period and some in both. Figure 2.5 shows one such unit with sustained activity during delay periods of five consecutive presentations of the cue.

Fuster did not observe any unit with differential responses to the two positions of the rewards and thus concluded that whatever the functional role of these cells is, it is not coding the information about the test cues. He also suggested that the activation of MD cells in thalamus might be indicative of shifting attention to specific stimuli, required to guide an action.

The discovery of cells in primate prefrontal cortex with sustained activity modulation during delay periods, that were later called *memory cells* was a great breakthrough in the study of delayed reactions. However as Xiao Wang mentioned in a review article [233], the behavioral responses were manually controlled and these made some concerns about functional interpretation of the sustained activities measured during the delay period. The one study published in 1989 by the late neuroscientist Patricia Goldman fulfilled this drawback [94].

In order to enforce accurate temporal control on the behavior of the monkey Goldman and colleagues had to deviate from the original experimental design that Hunter, Jacobsen and Fuster used. They trained the monkey to perform delayed oculomotor tasks and examined the spatial memory properties of the cells in the prefrontal cortex. The subjects were trained

to fixate on a central spot on the screen in front of them and maintain their gaze during a brief presentation of a peripheral cue followed by a delay period (of up to 6 seconds). Upon the extinction of the fixation marker, the subject was required to make a saccade toward the peripheral target in order to receive a reward. Peripheral targets were presented randomly in one out of eight uniformly distributed locations separated by 45 degrees. Incorporation of eight peripheral targets, extended the investigation of the mnemonic processes from a right-left paradigm to a multi-object test.

A total number of 228 neurons were recorded in the dlPFC area, 170 of which showed modulated activity during at least one phase of the task with 87 cells active only during the delay period. About 79% of these 87 cells showed *directional* responses, meaning that the modulated delay activity response was repeatedly observed in certain directions. One sample of such cell having a preferred direction of 270° is shown in Figure 2.6.

The overall conclusion of the study was that dlPFC in primates maintain information regarding the spatial location of the visual cues during delay periods and different neurons were shown to encode different target locations, consistently repeated across multiple presentation of the same cue. That being said, Goldman and colleagues introduced the concept of *memory map* in the primate dorsolateral prefrontal cortex.

Even though the original delayed reaction task was designed for and tested in rodents, but majority of the neurophysiology investigation was performed in primates. However with the advent of microelectrode arrays, performing electrophysiology in rodents became much more appealing and some investigators tapped into examination of the neural correlates of delayed reaction tasks in rodents. I will conclude the review of primate neurophysiology work at this point and in the next section we will review some rodent experiments.

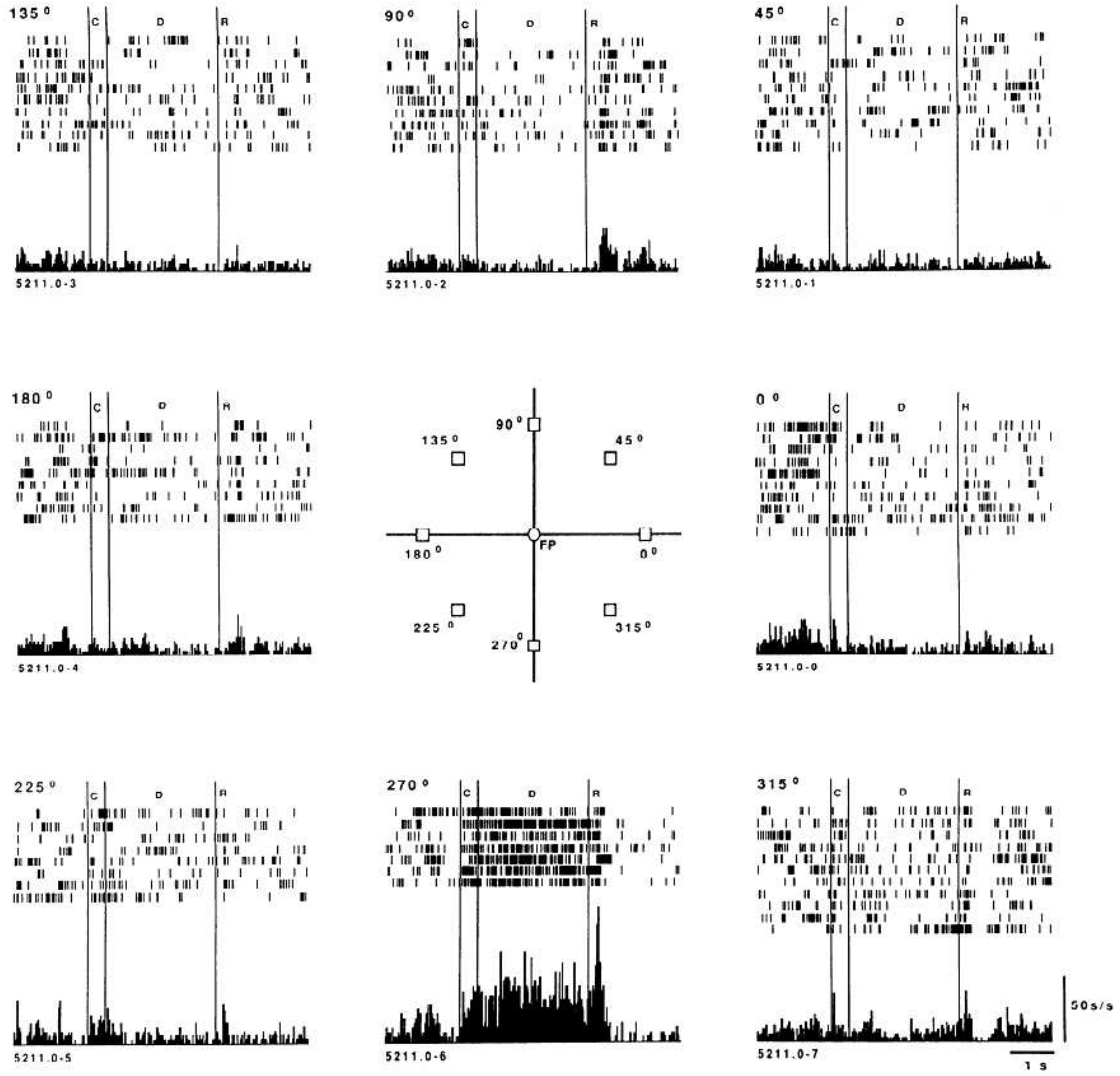

Figure 2.6: **A memory cell observed in dlPFC of a monkey performing an oculomotor task**, with orientational tuning. Raster plots of the cell's spiking across multiple trials the average firing rate are plotted for different orientations. Adapted from [94].

2.5 Neurophysiology of Delayed Reactions in rodents

I mentioned earlier that the original delayed reaction task was designed for rodents. However the ease of recording electrophysiological data from primates, probably paved the way for most of the neurophysiology of frontal cortex to be carried out in primates, limiting the rats solely for lesioning studies of PFC impairment. But the game has changed in the last decade with more investigators developing interest in rodent electrophysiology.

There is a long-lasting debate whether rats have prefrontal cortex. Although there are apparent anatomical differences between primate and rodent prefrontal cortex, attempts have been made to find functional similarities between the two. A very popular hypothesis is that rodent prelimbic area (PrL) in medial prefrontal cortex (mPFC) is later developed as dorsolateral prefrontal cortex (dlPFC) in primates and the two areas share some functional properties [213].

For about a century, different maze designs have been used to test cognitive aspects of rodent performance in laboratory [80, 238]. This appeal of the maze design, made it a number one choice for those interested to perform delayed reaction experiments. However as we will discuss, the choice of maze might not be the most appropriate choice for the study of delayed reactions. In this section we will review some recent studies of rodent delayed response experiments and discuss their strengths and shortcomings. This will make a foundation to start introducing our own experimental design.

Min Whan Jung has been studying value-based action selection in different frontal areas for years. In a recent article published in *Neuron* [220], Jung and colleagues presented some data on the distinct role of rodent orbitofrontal and medial prefrontl cortex in decision making. Neural signals were recorded from prelimbic and infralimibic areas (total of 751

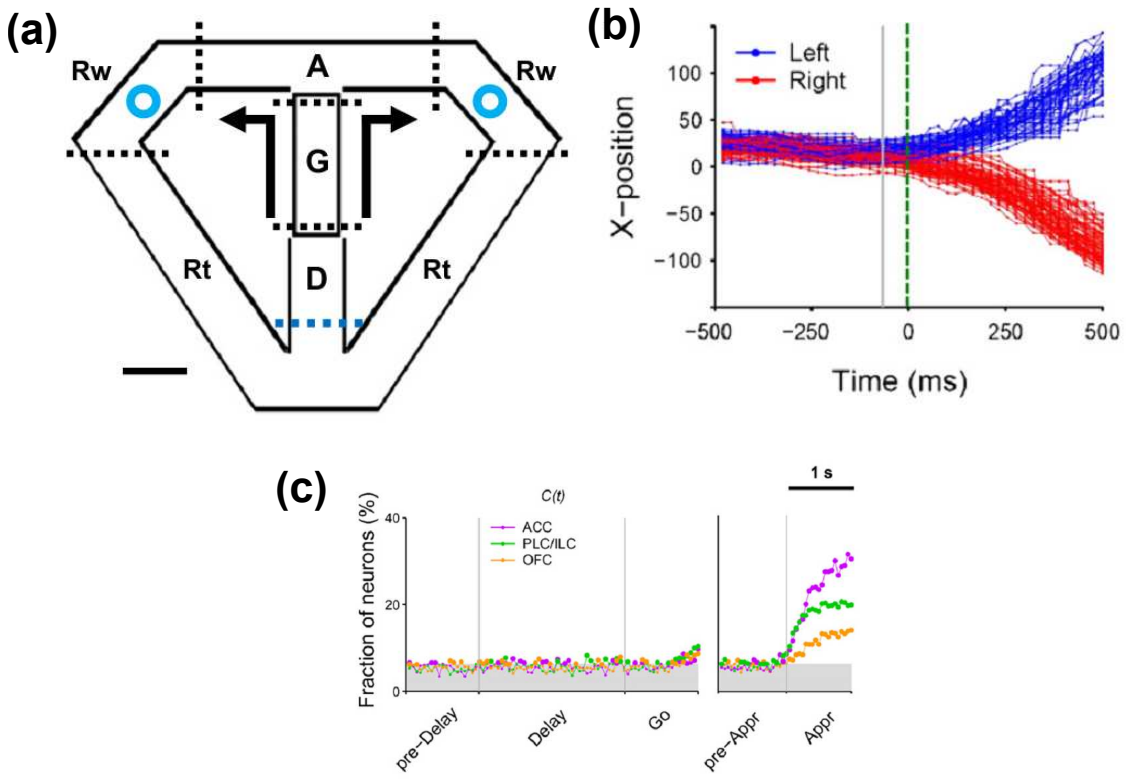

Figure 2.7: **Rodent two-armed bandit task (a)** Schematic of the task design that shows the distinct epochs: delay (D), go (G), approach (A), reward (Rw), and return (Rt) **(b)** Body posture of the subject shows two distinct trajectories **(c)** Percentage of selective neurons recorded from different parts of the prefrontal cortex. Adapted from [220]

neurons), as well as the lateral orbitofrontal cortex (a total of 1148 single neurons) while the subjects performed a dynamic two-armed bandit task.

Behavioral task was divided into a few stages based on the spatial location of the rat in the maze. A schematic of the maze design is shown in Figure 2.7. Note the delay (D), go (G), approach (A), reward (Rw), and return (Rt) epochs of the task.

Surprisingly, (as some of the results shown in Figure 2.7 suggest) neural signals representing upcoming choice were not found in the rat mPFC and OFC. This was unexpected if one considers the preparatory activity observed in the primate dlPFC. The authors suggested that this different response pattern might be due to different experimental designs used in primates and rodents. Whereas in primate experiments the subjects were sitting in front

of a screen and required to gaze towards the target, the rats "*navigated toward a branching point before committing their goal choices*". The authors also suggested that if the rats were allowed to make a choice without a need to navigate, the choice signals might have appeared earlier in the mPFC. The findings of this study supported the encoding of action values in the mPFC.

In another popular study, Gyuri Buzsaki and colleagues used a T-maze design and studied the temporal dynamics of the prelimbic area of mPFC in a working memory task required odor-place matching [92]. A schematic of the task design is shown in Figure 2.8. The task required the subject to associate an odor (cheese or chocolate) presented in the start box of the maze with a T-maze arm (left or right correspondingly). Correct visits to the left and right arm were correspondingly rewarded with cheese and chocolate .

A total of 633 single units were recorded from the prelimbic area across different subjects. Many of the cells showed location specific modulations during different epoch of the task. One example response is shown in Figure 2.8. The differential firings however, were only active during a very short *life-time*.

The authors suggested that environmental stimuli and motor behavior cannot account for the observed activity and thus there is need for an *internally generated* signal to guide the subsequent action. Then the authors used a cross-correlation technique and inferred functionally connected networks of spiking neurons which they believed is representing the *internal signal*. This can be regarded as an empirical evidence for the Hebbian idea of cell assembly [41, 115, 119].

Besides the very interesting finding of functionally distinct networks of interacting cells, this study suffers from the same drawback that Jung et al. mentioned in their own study design [220]. Since the sensory and motor components of the task are not decoupled in

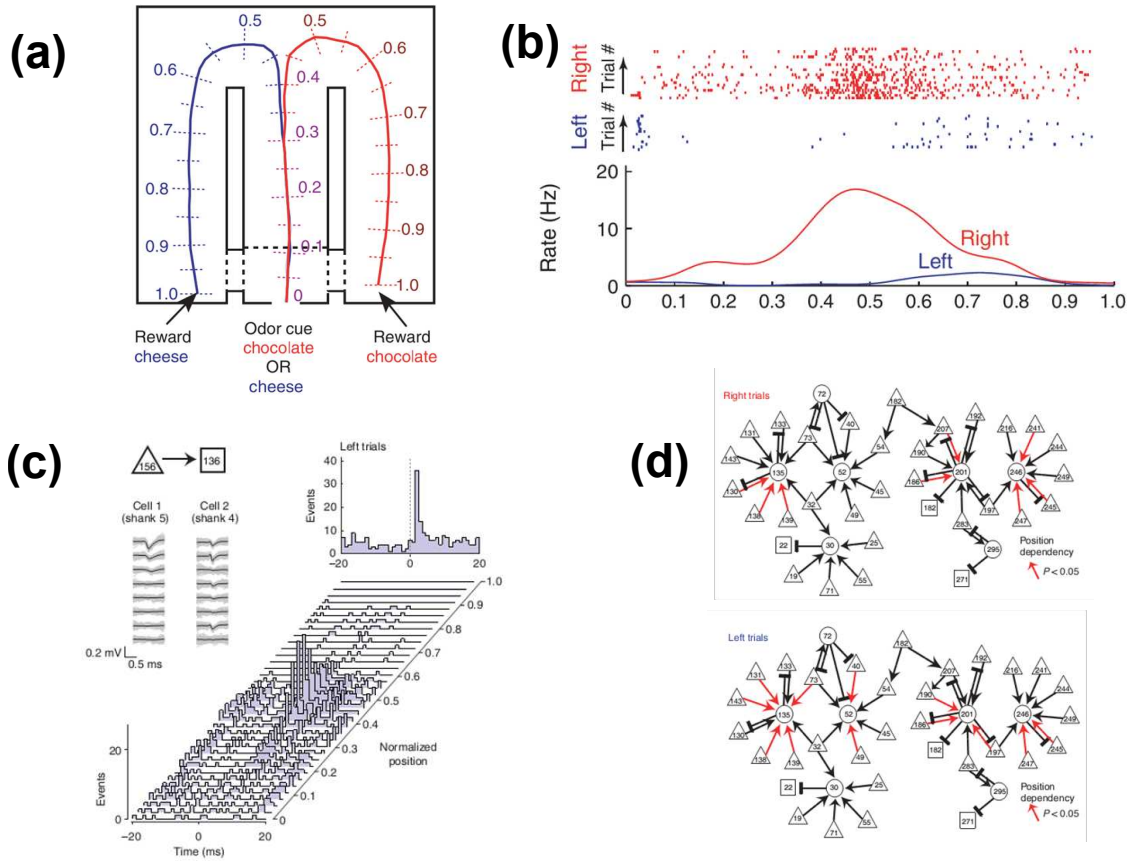

Figure 2.8: **T-Maze design to study short-term plasticity in the prefrontal circuit** **(a)** A forced two-choice task using a T-maze. **(b)** Average estimation of firing rate and across trial raster plots for a sample PFC cell selective for the targets. **(c)** Correlation between the firing rate of a sample couple of cells as a function of the travelled distance in the maze, depicting very transient dependency between the two cells. **(d)** Separate networks inferred using a correlation analysis between the firing rates of the two cells for different motor targets. Adapted from [92]

the T-maze task design, any conclusion about the temporal evolution of the PFC response and the content of the encoded signal, will be susceptible of having confounds of sensory or motor influences. Buzsaki and Jung findings along with some other electrophysiology of the mPFC in rodents [141, 145, 167], show a selective modulation of neural response during the delay period and thus suggest a functional similarity between the rodent mPFC and primate dlPFC.

Most of these rodent studies neglect the overt movement during the so called delay period that was accounted for in Goldman's study [94] by enforcing the subject to fixate and start the movement after a Go cue. The question has been risen among the scientific community and a few investigators [58, 85, 103] have suggested that the selective activity observed in rodent mPFC might have sensorimotor confounds and after all, rodent mPFC might have a different role rather the maintanance of the short-term (working) memory in delayed reaction tasks.

Gisquest-Verrier and Delatour [103] questioned the role of rat mPFC in short-term memory storage. They used a delayed version of a win-shift task in a radial arm maze. PrL lesioned rats performed the task at the same level of the control subjects, even in trials with delay periods of up to 5 minutes. The conclusion of the authors was that the PrL circuit is not necessary (and thus not directly involved) in holding specific information over a 5 min time period.

This controversial opinions on the role of mPFC in the delayed reactions on one hand and the lack of experimental designs that provide very precise control over the temporal dynamics of rodent behavior, motivates the design of the experiment that will be described in the following chapter of this proposal. The design helps to decouple the sensory and motor elements of the task both in temporal domain and behavioral domain. This is crucially

needed to study the temporal dynamics of neural reponses. But before moving to the next chapter we will briefly review two very recent studies investigating the role of different cortical and subcortical areas in a delayed reaction task. The design of these two experiments are very similar to what we propose. Given that the both area studied by Berke et al. [99] and Brody et al. [83] are monosynaptically connected to mPFC, comparison between the patterns of activity of the two areas (Striatum and secondary motor area correspondingly) and those of the prefrotnal cortex will shine some light on the puzzling question of the neural response structures in a delayed reaction task in rodents.

2.6 The role of basal ganglia

Basal ganglia which consist of four nuclei, play an important role in voluntary movements [137]. Patients with Parkinsons and Huntington disease, all of which have characteristics of motor disturbances, were shown to have pathological changes in these areas using post-mortem histology. These disorders were either slowness or paucity of movement (in Parkinsonian patients) or unwanted movements (in Huntington's victims). Animal models of basal ganglia function have shown their involvement in a number of behavior including (and not limited to) **1)** motivation toward goals [18], **2)** selection of specific actions [208], **3)** timing of action initiation [155], **4)** evaluation of the results [198] and **5)** learning new skills [142].

Given the substantial drawbacks of of maze task when investigating temporal evolution of neural activity, Berke et al. [99] used an operant conditioned instructed delay reaction task where the timing of key events could be closely monitored throughout each trial. A schematic of the task is shown in Figure 2.9. Rats were put in operant boxes with five nosepoke holes. Illumination of a center hole determined initiation of each trial and the

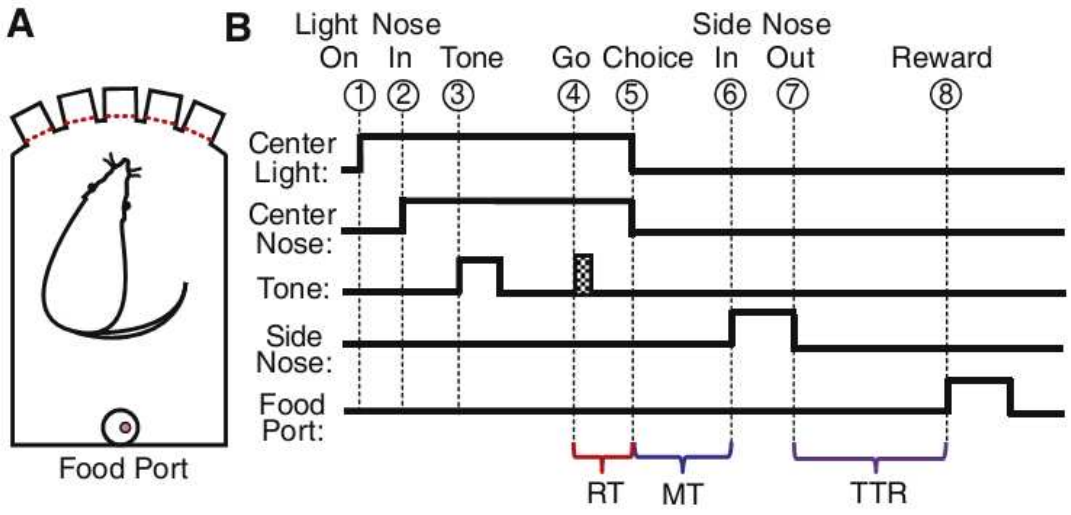

Figure 2.9: **A 5-hole nosepoke design used to study the selective role of basal ganglia in a reaction task**, adapted from [99].

rat had to poke inside that hole and maintain their nose inside until a go cue is presented. Immidiately after the rat pokes inside the center nosepoke a tone is played that is either a pure 1 KHz tone or a 4 KHz tone. The rat has to turn right for trials with a 1 KHz tone and to left for 4 KHz tone trials, but the movement should not start until a go cue (a white auditory noise) is presented.

Berke et al. then implanted the subjects with movable tetrodes and simultaneously recorded activity of multiple single cell. A total of 437 distinct cells were recorded in different brain regions (striatum: 239, M1: 73, GP: 25) and differentiated the putative cell types based on the shapes of the action potentials of each cell. As shown in Figure 2.10 , many cells showed selective response modulation during two epochs of the task: choice and reward. However, changes in firing rates of clusters of cells were observed before the movement onset both in M1 and striatal cells (with an average of -55 msec and -117 msec before the movement onset in M1 and striatum respectively).

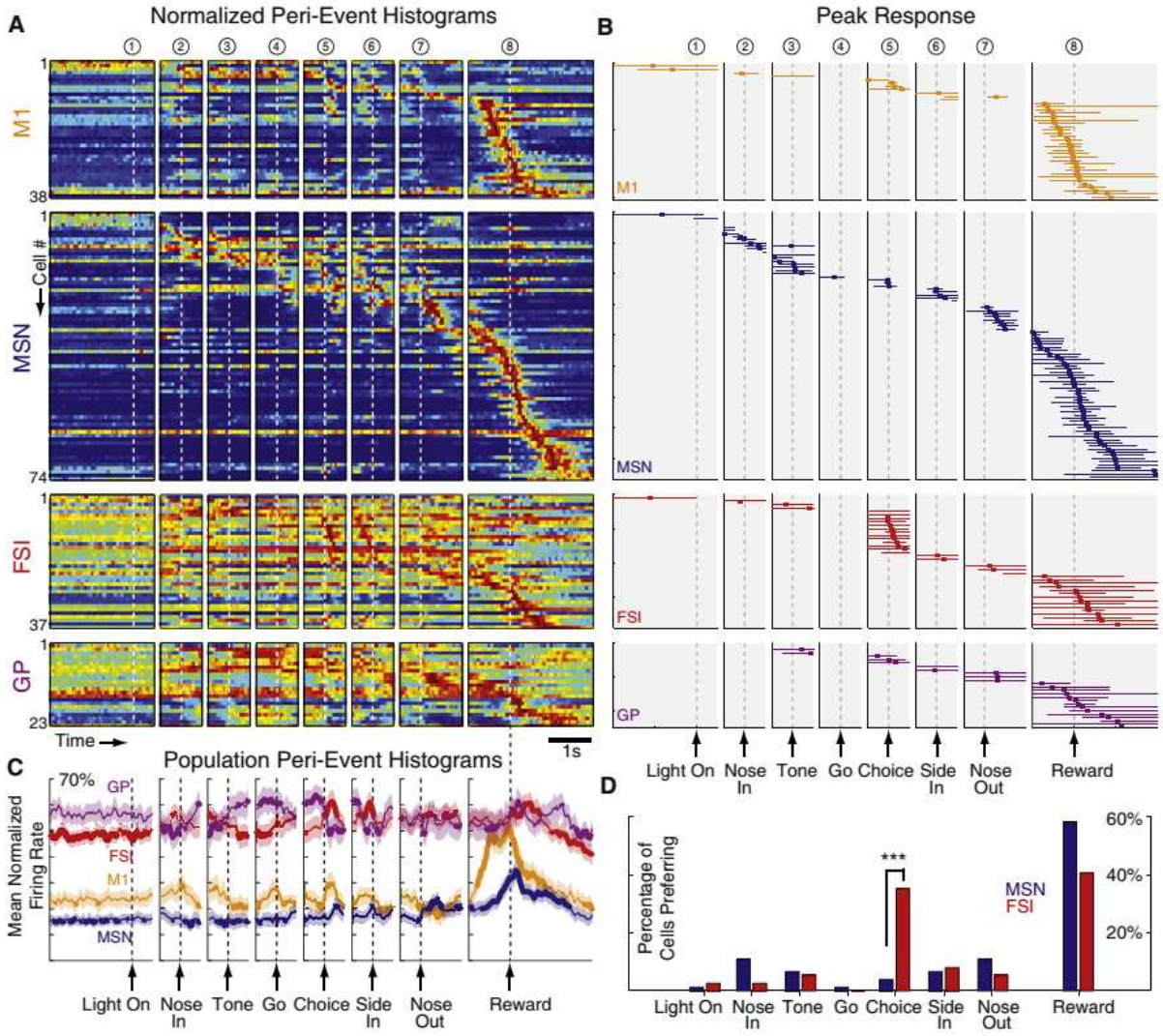

Figure 2.10: **PETH for cells recorded in different brain areas during the execution of the a delayed response task A)** PETH for cells recorded from M1, MSN and FSI cells of the striatum and GP cells. **B)** Peaks responses for the same cells and instances of selectivity. **C)** Across population average PETH for the signals recorded from different brain area. **D)** Percentage of cells with target selective responses during different task epochs. Adapted from [99]

Any voluntary action can be distinguished in three different stages of preparation, selection and execution, performed sequentially through time [100]. The authors suggest that based on the experimental results of the study, basal ganglia is more involved during the execution of a voluntary task rather than preparation and selection.

2.7 On the functional role of secondary motor areas

Premotor areas receive most of their afferents from the prefrontal cortex and send efferent projections to the primary motor cortex [36]. Although the neural correlates of premotor cortex activity has been extensively studied in primates [4, 8, 49], the functional properties of this area is still unclear in rodents.

Brody et al. [83] used a very similar experimental design to that of Berke et al. [99] to study the temporal dynamics of secondary motor area in rats. Again, the use of this experimental design enabled high temporal control over the behavioral events. The only major deviation from Berke et al. [99] design was in the type of the instruction cue. Whereas Berke et al. [99] used single tone auditory cues of different frequency to instruct for the orientation of the movement, tone pip of a constant frequency were used as the instruction cue and the click rate, determined the orientation of the movement (20 clicks/sec for left and 100 clicks/sec for right).

Upon completely acquiring the task, the subjects were implanted in their secondary motor area (M2) with microwires and the activity of multiple single cells were recorded simultaneously. A total of 242 cells were recorded in five subjects. The majority of the cells recorded depicted a prospective encoding for the orientation of the future movement. The population became significantly active about 850 msec before the Go cue. Figure 2.11 shows

the development of choice selective activity through time.

The overall conclusion of this work is the finding of an area in rodent frontal cortex (M2) responsible for preparation and planning of orienting movements.

Later in this proposal I will get back to Berke et al. and Brody et al. experiments and try to describe my preliminary results in accordance with the results of these studies.

2.8 Chapter Summary

In this chapter I reviewed some studies related to the subject matter of this proposal. Starting with Fuster's framework for prefrontal cortex function, I reviewed the historical evolution of delayed response tasks. Bill Hunter's dissertation on the delayed responses in animal and children from 1913 was reviewed. To my knowledge this document is the first scientific investigation of a delayed reaction. Constructing a foundation for such investigations, Jacobsen conducts his seminal research in 1935 and found the prefrontal cortex areas to be responsible for the execution of such tasks. He discovers that lesions to prefrontal xortex in primates impairs the subject to perform a delayed reaction task.

Fuster is the first neuroscientist to record neural correlates of a working memory task in primates. He finds the first evidence of cells in the dorsolateral area of the primate cortex to have elevated responses selective of a goal. Patricia Goldman later uses a very structured experimental design to have better control on the events during an experiment while recording from cell in dorsolateral prefrontal cortex of non-human primates. While the results of her discovery verifies those of Fuster's, the findings also suggest a model of tuning for the cells in the prefornal cortex activity during a delay period.

Some early rodent studies of delayed responses were also reviewed. Majority of delayed

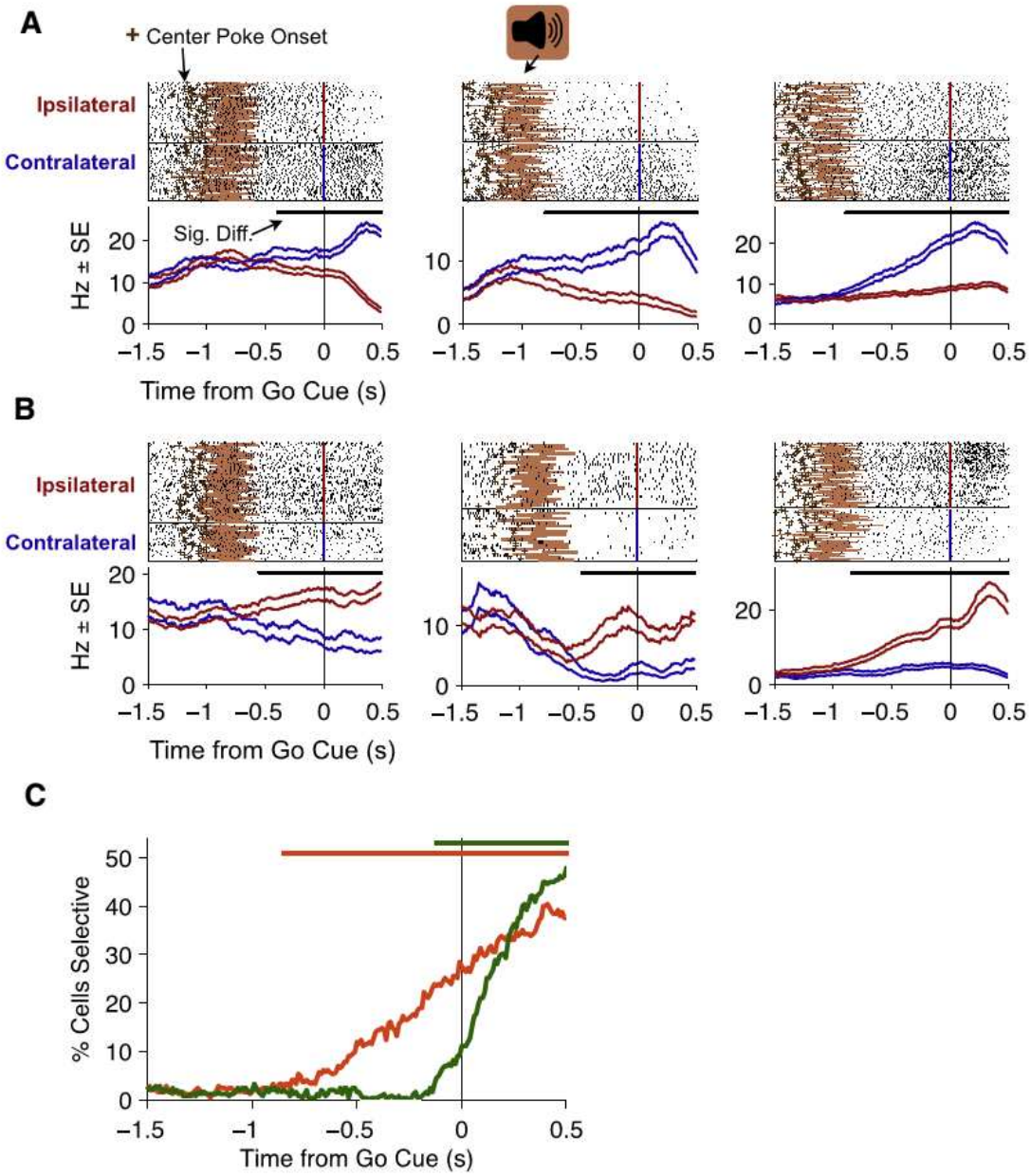

Figure 2.11: **Population response in the rat premotor area during a delayed response task A,B)** Six sample neurons showing contralateral and ipsilateral preferences in their firing rates **C)** Percentage of target selective cells. Adapted from [83]

response investigation was performed using different types of navigation mazes. Experiments from Jung and Buzsaki were reviwed both of which suggested a similar function between primate dlPFC and rodent mPFC. However other pieces of literature discount the role of rodent mPFC in the maintanance of short-term memory and investigate the confounds of sensorimotor contributions in the observed responses so far. Studies from McNaughton and Delatour were reviwed in this regard. Lastly, some very recent studies were reviewed which investigated the role of the rodent basal ganglia system and premotor areas in voluntary movements.

In the next chapter we will use what we have learned so far from the literature reviewed and design an experimental design to help answer some of the concerns about the study of rodent mPFC during delayed response tasks.

Chapter 3

Methods

If no experiences could, in principle, count for or against a proposition, then it is not only unknowable. It is devoid of content.
— Rebecca Goldstein, *Betraying Spinoza - The Renegade Jew Who Gave Us Modernity*

3.1 Delayed Choice Task

In this section, I will describe a framework of operant conditioning for rodents which have been used to test a few cognitive tasks [21,34,83,99,165]. In this framework, the subjects are required to fixate inside a nosepoke hole and maintain their snout inside until the presentation of a go cue. During the delay period the subjects are presented with a range of instruction cues that will guide them to select the appropriate action. The experimental design enforces the subject to minimize its overt movement over a brief interval and thus minimize the sensorimotor confounds on the neural responses observed during critical moments of decision making and motor preparation. A schematic flowchart of the task is shown in Figure 3.1.

The task uses a five-hole nosepoke design that is conventionally used for 5-choice serial reaction time task studies [21]. The operant conditioning box (Coulbourn H10-11R-TC) consists of a five-hole nosepoke wall (Coulbourn H21-06R) on the left side and a food delivery trough on the opposite side (Coulbourn H14-01R). The center nosepoke hole is considered as a 'fixation' hole and the four other holes (two on each side of the fixation hole) are motor target

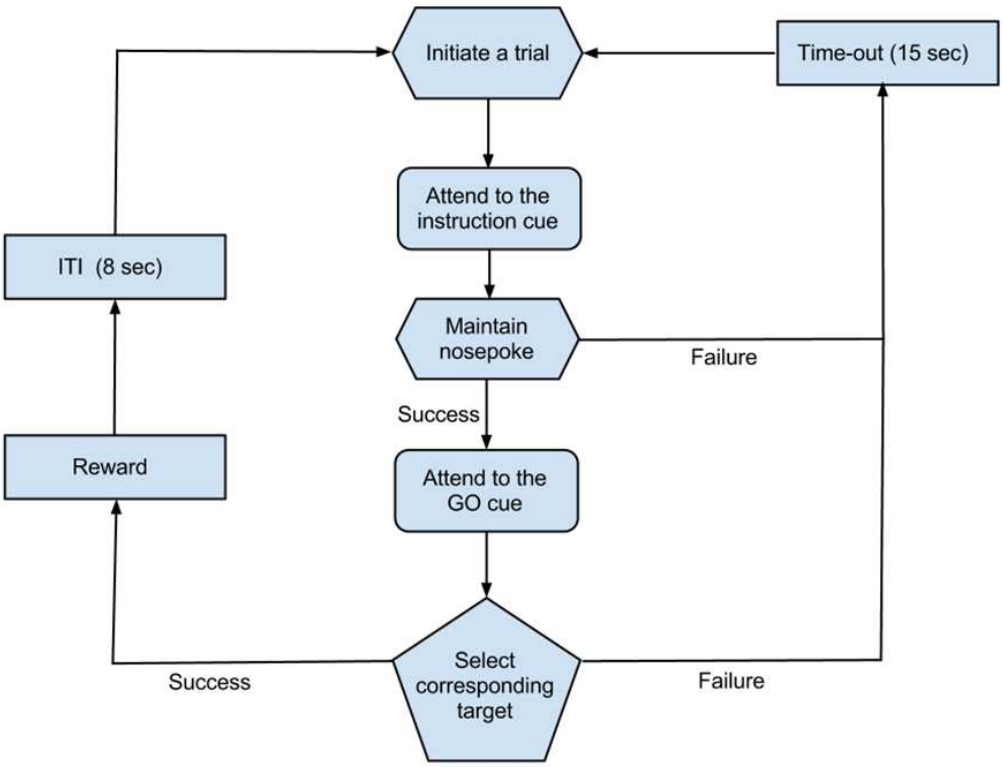

Figure 3.1: **Flowchart of a sample trial showing the sequence of actions and events during a trial.** The subject initiates a trial on their own by poking their nose inside the fixation hole. Briefly after the nosepoke, an instruction cue (a single frequency tone) is played followed by a delay period. The subject is required to maintain their nose inside the fixation hole until the presentation of the Go cue. Any premature retraction will cause the trial to be aborted and the subject is penalized by a time-out. After a delay period of random length, a Go Cue (auditory white noise) is presented and the subject is free to move towards the instructed target. Successful trials are rewarded by a 45mg food pellet while failed trials are timed out for 15 seconds.

holes. Each hole is equipped with an (tri-color) LED and an infrared beam emitter-detector package to detect entrance and retraction from the fixation hole. A programmable tone generator (Coulbourn A12-33) is used to generate single frequency tones with millisecond precision and is connected to a speaker mounted inside the operant box. The tone generator and nosepokes are controlled through the Habitest Linc system (Coulbourn H02-01) in the Graphic State software. The software provides millisecond timescale monitoring of behavioral events and control of cues and responses.

Time course of task events is shown in Figure 3.2. A flashing light in the fixation hole signals the subject to start a trial at their own will. Immediately after the subject poke inside the fixation hole, the light turns off and the instruction cue is played. Instruction cue is followed by a silent delay period during which the subject should still maintain their snout inside the nosepoke hole. Length of the delay period is randomly chosen between 1.3-1.8 seconds based on a uniform density during each trial. [1] Termination of the delay period is announced to the subject by a Go cue which is an auditory white noise. The subject is allowed to retract from the fixation hole and initiate the movement anytime after the Go cue.

Rats have been shown [114, 142] to be capable of discriminating single frequency tones of quarter octave distance. One trials with either a 5 KHz instruction cue the subject should turn right to be rewarded, while the 14.2 KHz instruction cues instructed a left choice.

All correct visits to the target holes were rewarded with a 45mg food pellet delivered in a food port on the opposite wall of the cage.

Erroneous trials were timed out for 15 seconds and the subject was required to wait until

[1] In this experiment I am more interested to study the sensorimotor contribution to mPFC response in the delayed reaction task and thus to rule out any temporal prediction by the subject (the subject anticipating a go cue) we suggest to choose the delay period length randomly.

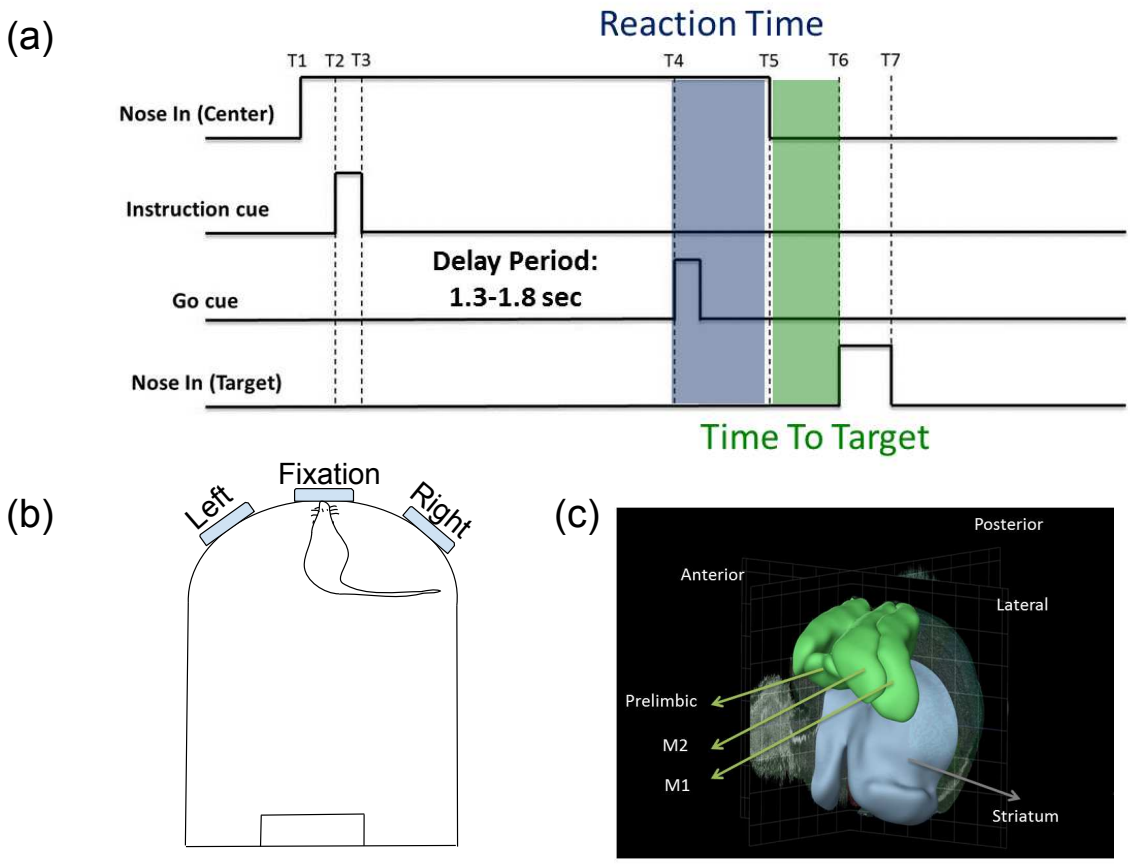

Figure 3.2: **Proposed study to investigate the role of the rat mPFC in an instructed delayed response task (a)** Time-course of the proposed task, showing the relative timing of the instruction cue, Go cue and the delay period. Subject's entrance into the fixation and target holes are monitored with millisecond precision **(b)** Schematic of the operant conditioning box with the fixation hole and the two target holes **(c)** A 3-D anatomical view of the target area in the mPFC, the prelimbic cortex (PrL). Also the primary motor cortex (M1), premotor cortex (M2) and the striatum are shown.

the fixation hole light starts flashing. There are three types of error the subject can commit. Premature retraction errors occur when the subject retracts from the fixation hole before the Go cue. Commission errors occur when the subject visits a target hole that was not instructed (e.g. visiting the right target hole when was instructed to go left). Omission errors occur when the subject does not visit any hole before the trial times out.

The subjects were trained in a sequence of protocols in order to reach 85% of performance. Details of subject training are described in the next section.

3.2 Behavioral training

All animals were housed on a 12:12 hour reverse light/dark cycle. The experiments were carried out during the dark phase. All animal subjects were housed in Michigan State University ULAR facility in the basement of Trout building. The subjects were carried to the lab in their home cage and kept in a dark behavioral training room were all the experiments were carried out. All animal procedures were approved by the Michigan State University Institutional Animal Care and Use Committee (IACUC) under the animal use forms of 07/07-102-00, 05/10-054-00 and 06/13-120-00.

3.2.1 Early habituation

The subject is gradually food restricted to 5 gr per 100 gr of the subjects normal weight (e.g. over the course of 3 days). It should maintain an 85-90% of their ad libitum weight. The subject is habituated to handling by the experimenter starting from the first day of food deprivation. The subject is then place in the operant conditioning box and food pellets are provided in the pellet trough to encourage the subject to explore the cage and get familiar

with the reward delivery location.

3.2.2 Subject Training

The task suggested here needs precise coordination between perception of an auditory cue, self-inhibition and movement execution. Thus the subject needs to be gradually trained step-by-step in order to perform the final task. At each stage, the subject needs to maintain above 75% behavioral performance for more than three consecutive training sessions before it is allowed to enter the next stage of training. After reaching the final stage of training, the subject should be kept for an entire week to ensure the performance is maintained at a desirable level. The subject will then be ready for further electrophysiology recordings or lesioning experiments.

3.2.2.1 Start

At this stage the subject needs to become familiar with the nosepoke holes, food delivery trough and association between correct nose poke holes and rewards. To do this, one out of four targets is selected on a random schedule. The Go cue (white auditory noise) is played and a red flashing LED (0.3 sec pulse duration) goes off inside the hole. Upon visiting the target hole, the subject is rewarded by delivering one food pellet (45mg) on the opposite side of the cage. Erroneous visits should not be punished at this stage. The trial should timeout after 30 seconds and a new trial should start immediately.

3.2.2.2 Target Selection

This stage is very similar to Stage 1. The only difference is punishing erroneous visits of the non-target holes in each trial. If the subject pokes inside an incorrect hole, the flashing LED

in the correct hole should turn off followed by 3 seconds of black-out and then a new trial starts without any reward delivery.

3.2.2.3 Nosepoke

The subject should have learned during the previous stage to associate flashing light holes with reward. At this stage they learn to poke inside the fixation hole to initiate a trial. The session starts with the fixation hole flashing yellow light. Once the subject pokes inside the fixation hole, one out of the four target holes should be selected randomly and the red LED turns on flashing. The subject should be rewarded upon visiting the correct hole. Incorrect visits should be penalized by 5 seconds of timeout.

3.2.2.4 Delay

After the subject learns the strategy of poking inside the fixation hole to initiate a trial, they should learn to maintain their nose inside that same hole until they are cued with a Go cue. At this stage, they gradually learn to wait for an average period chosen by the experimenter (e.g. 500 msec). The subject is required to maintain their nose inside the hole for a random delay period with an average of 500msec, and immediately after the termination of the delay period they are cued with the Go Cue. After the Go Cue presentation one out of four possible targets is randomly selected and the LED light associated with that target starts flashing. Upon visiting the correct target hole, the subject is rewarded. Premature retractions (before the Go Cue) and incorrect visits are penalized by a timeout.

3.2.2.5 Two Cues (w/ visual aid)

To rule out any effect of anticipating the delay period, the length of the delay period should be randomly chosen between 1.3-1.8 seconds based on a uniform density during each trial. The instruction cues are introduced at this stage. Instruction cues consist of single frequency tones, pulsed in triplet (150 msec pulse duration with 100 msec interpulse interval). The triplet are known to help the rats distinguish the pitch of the auditory stimulus34,35. Instruction cues are presented immediately after the subject enters the fixation hole. Ultimately four distinct auditory cues are presented to the subject where each pair of the tones instructs a specific motor target (Table 1). However, only two out of four instruction cues, corresponding to different motor targets are introduced at this stage. After the Go Cue the LEDs inside the target hole will be flashing. This provides an assistive cue for the subject. Later, when the subject learns to associate the auditory cue with the target hole the assistive cue is removed.

3.2.2.6 Two Cues

Ultimately the subjects should plan for moving towards the target hole merely based on the auditory cue. Earlier in the training protocol we used visual cues (flashing LEDs inside the target holes) as a conditioning stimulus to assist the subject to associate tones with targets. Gradually the assistance should be removed and the subject should learn to only use the auditory cue to select the target. Here we remove the assistive visual cue for the target holes. All the other parameters of the task remain similar to the previous stage.

3.3 Reaction Time Analysis

Reaction time (RT) which is also called response time or latency, is defined as the time between a stimulus and response to that stimulus [80, 86, 106, 133, 217]. Reaction times are considered to be modeled as a stochastic process; their value changes from one realization to another even under same conditions. Distribution of reaction times is best modeled as an ex-Gaussian distribution, which is convolution of an exponential function with a Gaussian function [77, 144]. The ex-Gaussian distribution can be written as:

$$f(x) = \frac{1}{\tau} exp(\frac{\mu}{\tau} + \frac{\sigma^2}{2\tau^2} - \frac{x}{\tau})\Phi(\frac{x - \mu - \frac{\sigma^2}{\tau}}{\sigma}) \tag{3.1}$$

This distribution has three parameters, μ and σ for the mean and standard deviation of the Gaussian segment and τ representing the decay constant of the exponential distribution. The parameters along with a sample RT distribution are shown in Figure 3.3.

The bimodal distribution of the reaction time, is often attributed to two different processes: fast and slow responses with different neuronal mechanisms arising each one [121,211]. To estimate the parameters of the distribution, I used a maximum-likelihood (ML) approach where determined the parameters such that the likelihood of the observed data is maximized. Here, likelihood is defined as

$$L(\boldsymbol{\theta}|\chi) = \prod_{i=1}^{N} f(x_i|\theta) \tag{3.2}$$

Here, $\boldsymbol{\theta} = [\mu, \sigma, \tau]$ is a vector of the parameters, χ is the observations of the reaction time and x_i are the samples. Since both exponential and Gaussian distributions are expressed in forms of exponential functions, it is easier to perform the optimization on the log of the

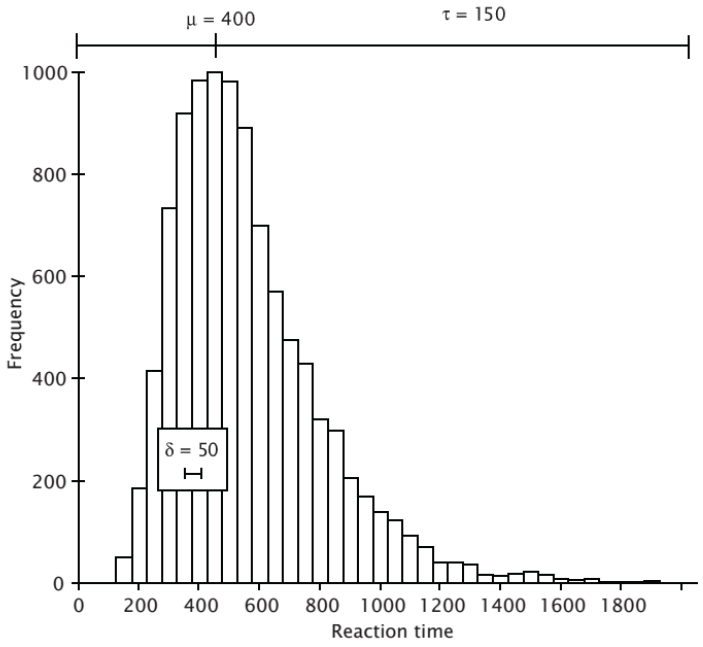

Figure 3.3: **A simulated ex-Gaussian distribution**, showing the characteristic shape of proposed model for reaction time distribution, illustrating different distribution variables μ, σ and δ. Adapted from [237].

likelihood function. Thus the problem of maximum likelihood can be re-formulated as a minimum log-likelihood problem:

$$\log L(\boldsymbol{\theta}|\chi) = -\sum_{i=1}^{N} \ln f(x_i|\theta) \tag{3.3}$$

I used the MATLAB optimization toolbox (Simplex method) to solve for the minimum log-likelihood problem.

3.4 Reversible inactivation

The ability to stereotaxically target certain brain areas and manipulate their activity, provides many opportunities to study the role of certain brain area and their relation to organism's behavior [45]. Ablation and permanent extraction of the tissue are the have been

widely used for that purpose. This can be easily done by aspirating the brain tissue. However, lesioning the brain tissue is not reversible and thus it would be hard to design control experiments to establish a causal relation between the role of the lesioned tissue and any behavioral/functional impairment.

One other way is to use pharmacological agents that bind to certain receptors and can selectively activate or inactivate specific types of ion channels or receptors. These pharmacological agents can be either *agonist* or *antagonists*. While agonists can activate their targets, antagonists inhibit the biological activity. **Muscimol** is a popular GABA agonist drug that increases the effects of inhibition and thus is widely used to inhibit neural circuitry during *in vivo* electrophysiology experiments both in mPFC and other brain areas [7, 83, 99, 134, 209, 243].

In the next phase of this experiment I will examine the effect of reversible inactivation of the mPFC on the subject's performance. Subjects would be trained on the task and upon accomplishment, muscimol will be delivered to the target area using a bilatral chronically implanted guide cannulae. 1μL of a baclofen-muscimol cocktail ($GABA_B$-$GABA_A$ agonists, respectively) should be injected at each side using a Hamilton microsyringe. Control injections of saline will be used to rule out any confound of the injection prodecure on the subject's performance.

Given the results so far and the selective modulation of the PFC cells, we expect that by temporarily inactivating the prelimbic circuits, the performance of the subject will be impaired and thus there would be a significant decrease in the performance between the muscimol and saline treated session. However the extent of this impairment has to be shown.

3.5 Electrophysiology

The neuron doctrine is the fundamental premise of modern neuroscience, which states that individual neurons are the basic building blocks of the brain responsible for sensing the environment and producing actions to affect the environment [107, 137, 172]. Since the early introduction of the concept, the ultimate goal of the neuroscience has been dedicated to understand how the activity of these cells gives rise to mind: our ability to perceive, act and memorize [59, 60, 229].

In short, neurons are believed to function collectively through generating brief electrical potentials called *action potential* or *spikes*. Action potential is a short-lasting change in the cell's membrane potential caused by input dendritic currents moving the membrane potential closer to a threshold (typically considered to be around -55 mV). Consequently the action potential from a neuron will get propagated through the axon and may activated its downstream neurons. A neuron that emits spikes is said to 'fire'. Action potential of an individual cell can be measured intracellularly using a technique called 'patch clamp'. Figure 3.4 shows a sample of such recording, illustrating the underlying mechanism of action potential generation which is basically changes in the conductance of Sodium and Potassium channels [137].

Although recording the intracellular potential is the gold standard for measuring a single neuron activity, its application in limited due to practical issues. In practice, neurophysiologists measure extracellular potentials recorded at the tip of a metal electrode penetrated inside the brain tissue (with respect to a reference electrode) and use that as a proxy for multiple single cell activity [39]. In fact, by placing more than one electrode inside the brain tissue one can record the activity of multiple single neurons at a time. Figure 3.5 shows

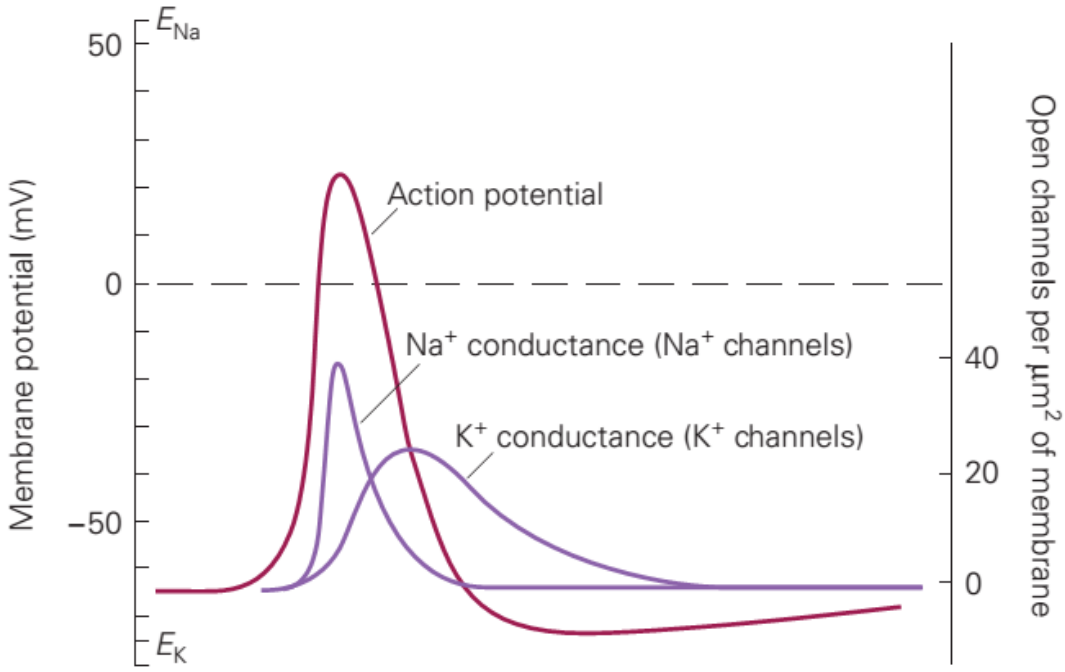

Figure 3.4: **Opening of voltage-gated channels and the generation of action potential**. As described by Hodgkin and Huxley [125], during an action potential conductances of Na^+ and K^+ changes and this ultimately attributes to generation of an action potential. Adapted from [137].

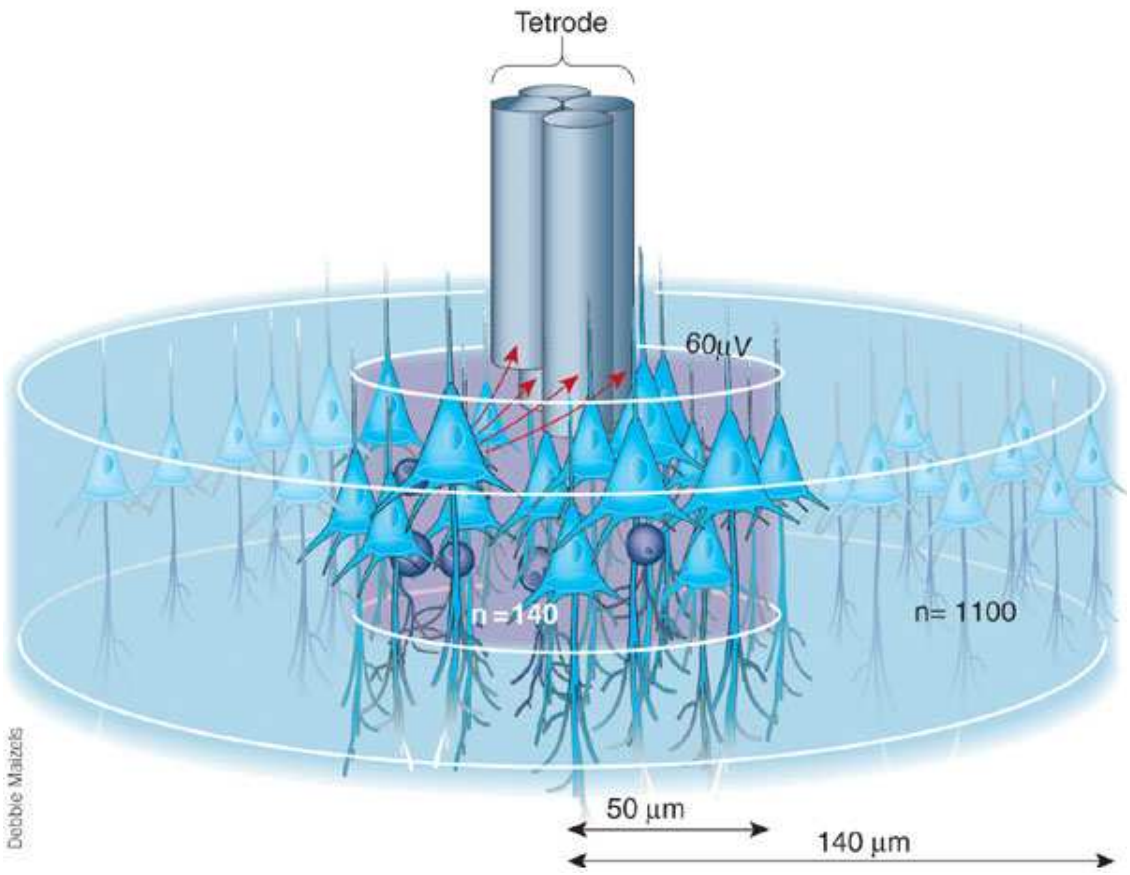

Figure 3.5: **Recording unit activity using a multisite electrode**. Schematic showing how multisite electrodes (here a tetrode for example), will be placed in the vicinity of a neuronal population to pick up the extracellular activity. If the sites are close to each other, one can use triangularization of the action potentials to better isolate single units. Adapted from [39].

a schematic of an extracellular electrophysiology recording of brain activity. As apparent in the figure, electrodes are located in the vicinity of multiple cells and consequently will pick up activity from more than one cell, unlike the intracellular recording where the voltage traces show activity of a single cell. Thus the extracellular recorded signal needs to be processed to isolate the activity of single cells. This procedure is called 'spike sorting' and will be described later in this chapter.

In recent years, the advent of multielectrode arrays (MEA) has enabled very large-scale recording of multitude cells at a time in awake behaving animals [25, 39, 170, 206]. Several

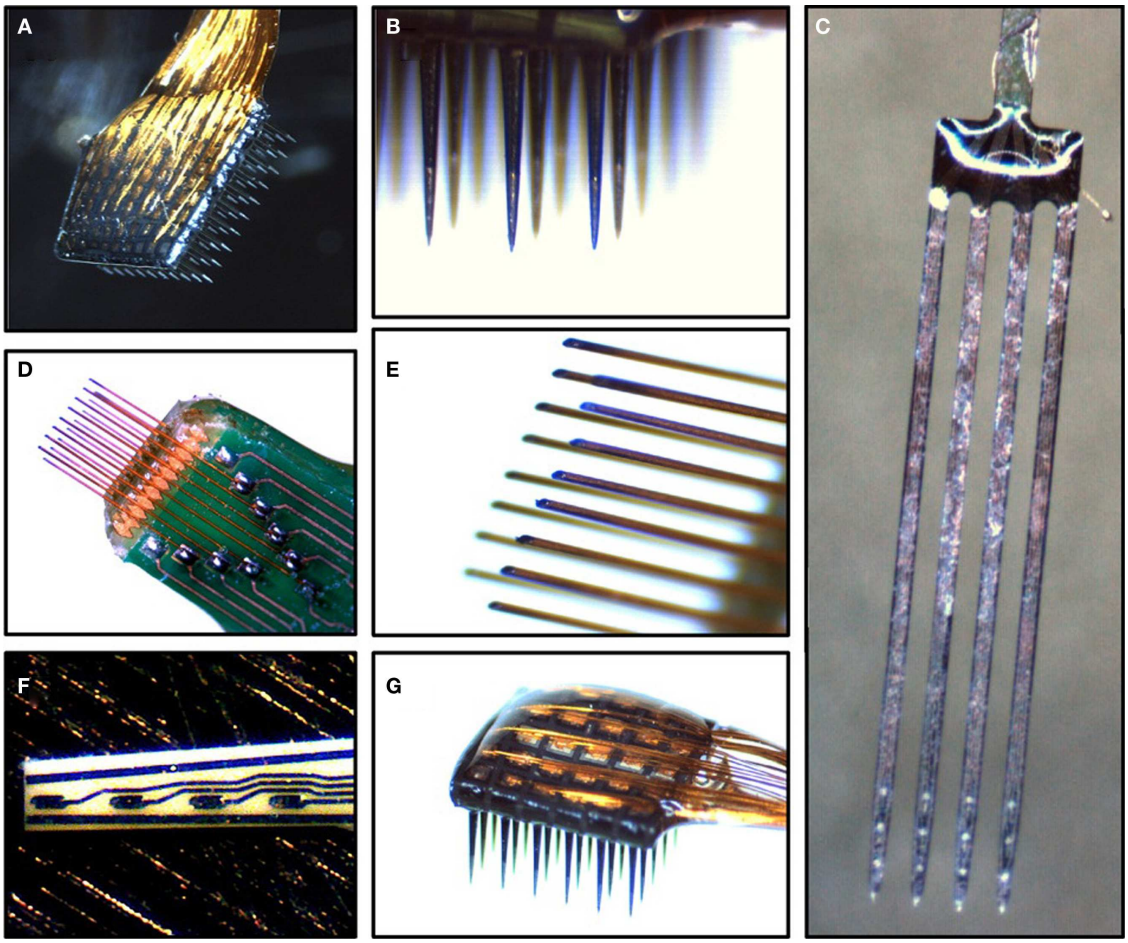

Figure 3.6: **Examples of different multielectrode array designs A)** Cyberkinetics 100 channel silicon array **B)** recording sites of the Cyberkinetics array **C)** Neuronexus Michigan probe, another silicon-based MEA **D)** Tucker-Davis microwire MEA **E)** a close-up view of the TDT microwire array **F)** Moxon's ceramic-based MEA **G)** Cybekinetics 36 channel probe .Adapted from [236].

different MEA designs have already being commercialized and ready to use for research purposes. These include but not limited to the Michigan probes from NeuroNexus®, Utah probes from Blackrock microsystems® and the microwire arrays from Tucker-Davis Technologies ®. Figure 3.6 shows pictures of these different probe designs.

Among these different probe designs, each one comes with their pros and cons and the choice of the optimal design is dependent on the application [236]. Geometrical design, number of electrodes, sturdiness of the device and tissue response of a few parameters to

consider [170, 192, 236]. During the pilot studies for this experiment I used two kinds of probes: Michigan probes and TDT microwire arrays. While the planar design of the Michigan probes, provided more localized recording of neighboring cells, device integrity and longevity of the recorded signals made me to choose TDT microwire arrays. Similar observations was reported in other labs through personal conversations and documented in the Ward study [236]. I used a 4x8 microwire array that enabled targeting two different regions: mPFC and M2. Only the mPFC data is used for this dissertation, while the M2 data is reserved for further investigations. This left me a total of 16 recording channels per subject spanning a good area of the prelimbic cortex in the AnteroPosterior (A-P) axis. The data used for this dissertation is from the subjects with a neural yield of more than 70%, meaning that at least one unit was detected on each channel.

3.5.1 Surgery

Once the subject is implanted with the recording device, we allow up to a week of post-operation recovery period before putting the subject back on food deprivation protocol. It is important to monitor the weight of the animal and both food and water intake on a daily basis. In case needed, special food supplements should be provided to compensate for the weight loss.

3.5.2 Data Preprocessing

After the subject is ready for recording, we tether them to the data acquisition system (TDT RZ2 system) using a high impedance headstage. Full band signal (no frequency filtering) is recorded from 32 channels at the rate of 25KHz/channels. The data is then digitized in

16-bit format and stored on the hard disk in a TDT specific format. A modified version of the ActiveX controller provided by TDT is used to import the data into MATLAB. All the subsequent analyses is performed in MATLAB unless mentioned otherwise.

Wide-band neural signal picked up at the tip of penetrating electrodes is a superimposition of electrical current contributions from all active processes in a brain tissue surrounding the electrode [42]. It has become a tradition among neurophysiologists to use a lowpass butterworth filter to extract LFP (cut-off frequency of 200 Hz) and a bandpass filter (cutoff frequency between 500-5000 Hz) to extract spiking information. Although the butterworth filtering is easy to implement, the simplicity comes at the price of introducing distortion in temporal domain [244]. Our lab has previously shown the merit of using wavelets for neural data preconditioning, preserving the spike SNR [6,178,181]. Here I adopted the same techniques and used the Symlet wavelet family to separate the lower frequency content of the recorded extracellular potential from the higher frequency signal carrying information about individual cells' activity. Lower frequency, slowly-varying local field potentials (LFP) and higher frequency extracellular potential carrying action potential information of a few neighboring cells. In Figure 3.7 I have shown a trace of the recorded data of a single channel recorded from layer V, prelimbic area in subject PFC2.

Black trace is showing the wide-band extracellular data (no filtering), amplified and sampled at 25KHz. Red trace is the slowly-varying LFP and the blue is the higher frequency content. High amplitude events are the spikes from presumably individual cells (called '*units*' from now on), two examples of which are shown in the figure inset.

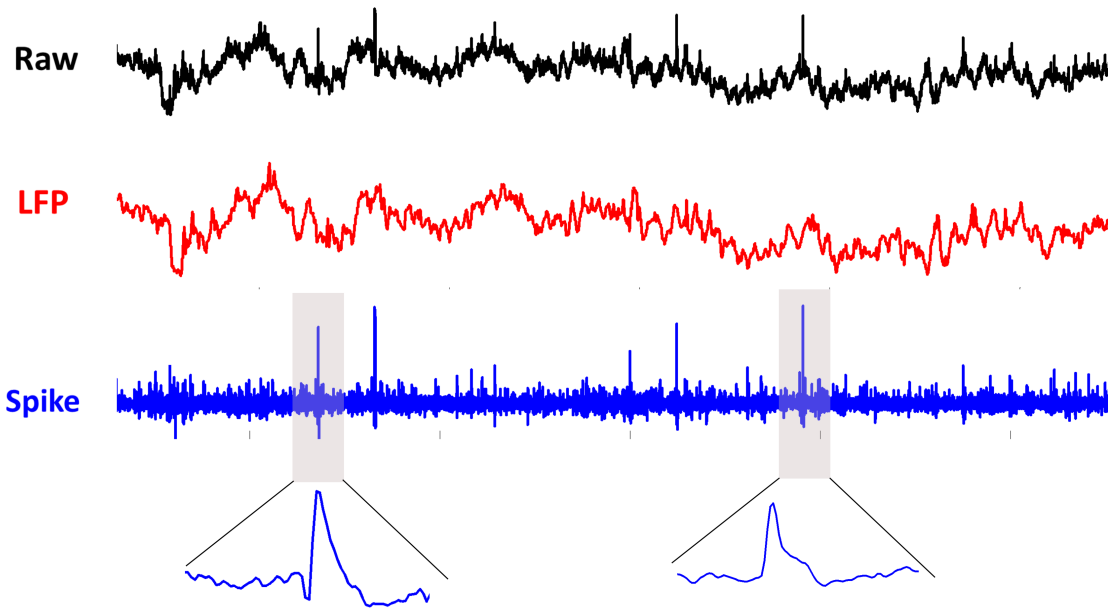

Figure 3.7: **Separating LFPs from the high frequency signal** An example of the trace of an extracellular potential recorded on a single channel (**Black**). Using Symlet wavelets, the signal is decomposed into lower and higher frequencies. The lower frequency (**red**) is called LFP and shows slow oscillations where the higher frequency (**blue**) carries information about action potentials

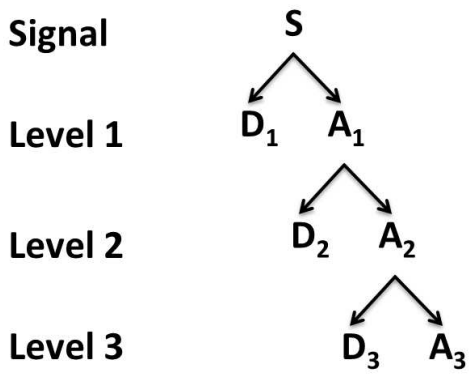

Figure 3.8: **Three level wavelet tree decomposition**, showing approximations and details for each level.

3.5.2.1 Symlet Wavelet

Wavelet analysis is a relatively modern signal processing tool first introduced in the late 80s for seismology applications [152, 153]. The analysis consists of an atomic decomposition of a signal successively into different frequency bands, given some orthonormal basis function. The packet is a set of shifted and dilated versions of a scaling function $\varphi(n)$ and a bandpass wavelet function $\psi(n)$. In short, DWT of a discrete signal $x(t)$ is calculated using a cascade of filters, also called a '*filter bank*'. At each level, the signal is simultaneously decomposed into low-frequency and high-frequency components, by convolving the signal in high-pass and low-pass filter. The procedure also known as 'wavelet tree decomposition' is illustrated in Figure 3.8.

The basis functions at each step can be obtained from the mother wavelet and scaling functions using the following formula:

$$\psi_{jk}(n) = 2^{-j/2}\psi(2^{-j}n - k) \quad ; \quad \text{j=1,2,...,L , k=1,2,...,N} \tag{3.4}$$

$$\varphi_{jk}(n) = 2^{-j/2}\varphi(2^{-j}n - k) \quad ; \quad \text{j=1,2,...,L , k=1,2,...,N} \tag{3.5}$$

$$\psi(\frac{n}{2}) = \sqrt{2}\sum_{k} h(k)\psi(n-k) \tag{3.6}$$

$$\varphi(\frac{n}{2}) = \sqrt{2}\sum_{k} g(k)\varphi(n-k) \tag{3.7}$$

In the formula, $h(k)$ and $g(k)$ are impulse responses of the previously mentioned low-pass and high-pass filter which can also be expressed as the following dot product:

$$h(k) = \left\langle \frac{1}{\sqrt{2}}\varphi(\frac{n}{2}), \varphi(n-k) \right\rangle \tag{3.8}$$

$$g(k) = \left\langle \frac{1}{\sqrt{2}}\psi(\frac{n}{2}), \varphi(n-k) \right\rangle \tag{3.9}$$

I performed the above procedure in MATLAB, using the `wavedec` command in the Wavelet Toolbox. A trivial question to ask is the choice of wavelet basis where one may argue that the choice of these basis may affect the SNR. Given that most wavelets share common properties such as symmetry and biorthogonality, this may not be a straightforward question. Oweiss and Anderson [180] have quantitatively compared the effect of different wavelet basis of a large dictionary of basis such as Haar, Daubechies, Symlet, coiflet, etc [50, 63–65, 152]. The conclusion was that *'symlets seem to be the closest match in waveform shape to the neural spike waveforms'* [177]. In the same study, Oweiss and Anderson evaluated the effect of the symlet wavelet order on the waveform SNR and identified the 4^{th}

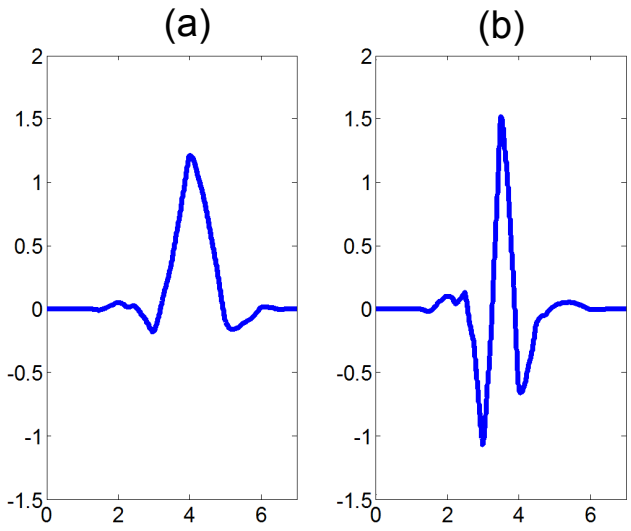

Figure 3.9: **Basis functions for the Symlet wavelet**. **a)** Scaling function and **b)** wavelet function

order to be the optimal. Following this advice, I have adopted a 4^{th} order symlet wavelet for filtering out LFPs from the higher frequency contents of the extracellular signal. Scaling and basis function of the wavelet are plotted in Figure 3.9.

Once the signal is decompsed to different band components using the wavelet decomposition tree method, coefficient thresholding is used to separate different band content. To extract the low-frequency LFP signal, all the 'detail' coefficients are set to zero, and to obtain the higher frequency signal, the approximation will be zeroed out. In each case, the signal is reconstructed with zeroed out coefficients. Thresholding and reconstruction procedures are performed using MATLAB wavelet Toolbox via `wthcoef` and `waverec` commands respectively.

3.5.3 Spike Detection and Sorting

As illustrated in Figure 3.7, higher frequencies of the extracellular potential recorded on a single channel probe, contain spiking information of individual cells. Similar to the intracel-

lular action potential shown in Figure 3.4, extracellular spikes are reflected as very shown as very brief (shorter than 1 msec) changes in the recorded potential, the prominent feature of which is an amplitude modulation. Thus exact timing of a spike can be determined using a threshold crossing method [147, 178]. Thus a first step in preprocessing spiking data is to detect these 'putative' spikes through a process called 'spike detection'. Assuming that the neurons' activity can be distinguished from the background noise biological noise via the height of the event, a threshold is adaptively determined using the background noise level for each channel. Threshold detection is not the only spike detection algorithm but the most common approach due to its simplicity, accuracy and ease of hardware/software implementation. The threshold is conventionally [73, 147, 177, 178, 196] determined using the following formula:

$$Thresh = 4 \times \sigma_n \quad ; \quad \sigma_n = median \frac{|x|}{0.6745} \tag{3.10}$$

Here x is the band-passed (using wavelet) signal and σ_n is an estimate of the background biological noise. The rationale of using the median instead of the standard deviation (which some groups use) is that the standard deviation is affected by the large amplitude spikes and thus may lead to a large threshold where the median is robust against such large deviations and thus the interference from spikes are diminished or minimal.

As mentioned in an earlier section of this chapter, extracellular electrophysiology enables recording the activity of potentially more than one cell using a single channel electrode. Thus one required preprocessing step to analyzing single cell data is to cluster the detected action potentials into coherent clusters. Grouping of detected events is mainly performed using their shape, with the assumption that different neurons in the vicinity of the electrode tip may fire

action potentials of different shapes given their type or the proximity to the electrode may affect their shape either via the amplitude or the width of the spike [22,42,105]. There is no physiological evidence to illustrate that spikes clustered together in a same group belong to the same neuron. In fact these could come from different similar cells located in relatively similar three dimensional distances from the recording electrode tip. Thus it is common to call these 'putative' neurons a *'unit'* to emphasize this uncertainty. I will observe this nomenclature throughout the text of this dissertation.

Two general approaches have been proposed for the problem of spike sorting: 1) is a pattern recognition approach that relies on the features extracted from single detected events and 2) a Blind Source Separation (BSS) approach that operates on the raw data [178,179]. Each approach has its own advantages and disadvantages and here I pick to adopt a pattern recognition approach one the grounds of its simplicity and ease of implementation in MATLAB.

In the pattern recognition approach to spike sorting, each detected event is considered as a vector data point. However prior to feature extraction, these events are required to be aligned with respect to a common reference point. 'Alignment' of spikes are done using different techniques references such as the maximum peak, minimum peak, energy etc. Here I use the maximum peak to align the detected events. After the spikes are aligned, *'d'* discriminative features are extracted from each spike so each event will be represented as a single point in a d-dimensional space. Finally, a clustering algorithm partitions the d-dimensional space into P distinct clusters. Figure 3.10 illustrates these steps.

Principal Component Analysis is an increasingly popular feature extraction used for spike feature extraction as well [215]. In this method, individual events are stacked into rows of a matrix S. Then the matrix is zero-meaned and a transformation W is calculated such that

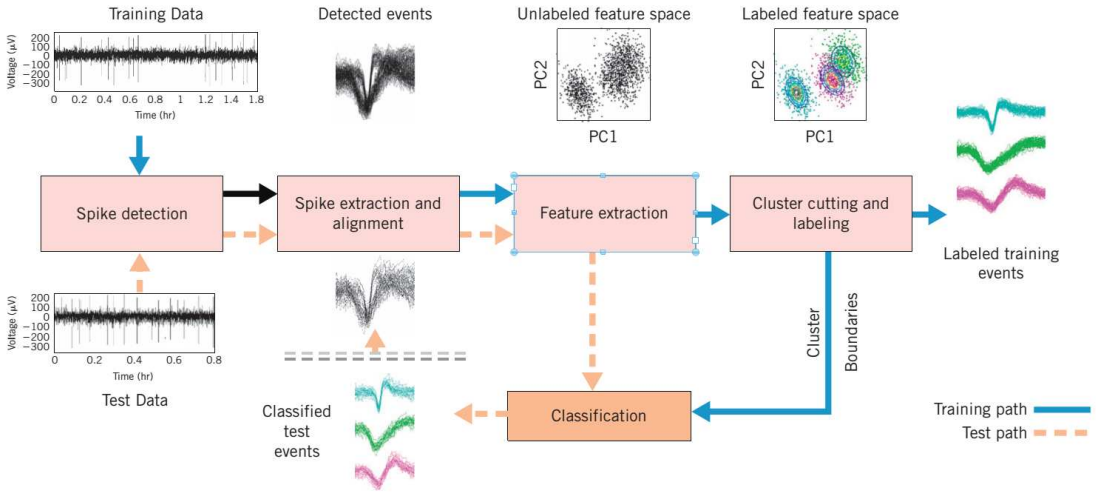

Figure 3.10: **Pattern recognition approach to spike sorting** Using a thresholding method, spike events are detected and discriminative features are extracted. Then a clustering algorithm is applied to use the extracted features to group the events together and determine the boundary decisions based on the training data. Decision boundaries are later used on the test data to separate different groups of extracellular action potential waveforms. Adapted from [178]

each row vector is mapped into new vectors of principal component scores $t_{k(i)}$, in a way that successive variables of t inherit the maximum variability:

$$t_{k(i)} = S_i \odot W_k \tag{3.11}$$

Finding the appropriate weight matrix W is done via an algorithm known in 'linear algebra' as *Singular Value Decomposition* (SVD). Once the feature matrix is formed, a clustering algorithm such as Expectation Maximization (EM) [68], Fuzzy C-mean (FCM) [184], etc is used to cluster the data into a pre-determined number of distinct clusters. Here I used the FCM algorithm based on its simplicity of implementation and speed of execution.

Once the spike sorting is done, I use a number of quality metrics to asses isolation of each classified cluster.

- Initially, the clusters' waveform are visually inspected for any physiologically unacceptable shape. These can be motion artifacts induced by movements of the head, chewing artifact induced by the Electromyography (EMG) signals from jaw muscles or background EM noise. These contaminated clusters are removed and excluded from further analysis.

- Furthermore, stability of the spike waveform is inspected throughout the recording session. For this purpose I developed a *'temporal evolution'* graph illustrating the features of the detected spikes of each cluster through time. Non-stable clusters are also excluded from further analysis.

- Once a neuron fires an action potential, it goes through a so called 'refractory period' during which it will not fire any spikes. This delay period is considered to be in a range of 1 millisecond. Thus a clean isolated unit should not contain spikes happening within 1 millisecond of each other. To asses this sanity test, one may form a histogram of interspike intervals, ISIH, and ensure that there are no events happening withing the refractory period. If the cluster shows violation of the refractory period, one may go back and redo the clustering step.

I developed a MATLAB based spike sorting package called EZsort that contains implementations of different algorithms mentioned above and tools to do sanity inspection. The software is provided in two different 'Basic' and 'Advanced' versions. Details of the package is described in the next section.

3.5.3.1 EZsort

There are a number of commercial software solutions available for spike sorting. The list includes SpikeSort 3D from NeuralynX, OpenSorter from TDT, OfflineSorter from Plexon etc. Also exists a number of open-source solutions developed with different objectives in consideration [31, 116, 143, 196, 207, 241] . Here I developed a MATLAB -based spike sorting Graphical User Interface (GUI) with all the above mentioned options. The software is called EZsort, on the grounds that the User Interface is very simple and all processing capabilities are reachable from the main window. Since the process of spike sorting is to some extent subjective, it is important to provide as much visual aid as possible. To this end, the software is equipped panels showing ISI distribution, Peak Distribution, Temporal Evolution of the peak, Principal Components and the waveforms. A user can select to merge clusters together, split a cluster into subclusters, remove a cluster or remove an entire channel. An additional 'outlier removal' tool will help removing events that are far from the center of the cluster (beyond 4 times standard deviation of the cluster). A screen-shot of the EZsort GUI is shown in Figure 3.11 .

3.6 Single Unit Analysis

Once spike sorting is performed and single 'units' are identified, activity of each unit can be represented as a binary series of time bins where 1 represents occurrence of an action potential. The obtained time series is conventionally called a spiketrain. Since the refractory period of a neuron is considered to be around 1 millisecond and thus no two spikes from a single unit can happen withing one millisecond, it is reasonable to downsample the data into 1 millisecond bins. In this section I will describe the methods I used for single unit analysis.

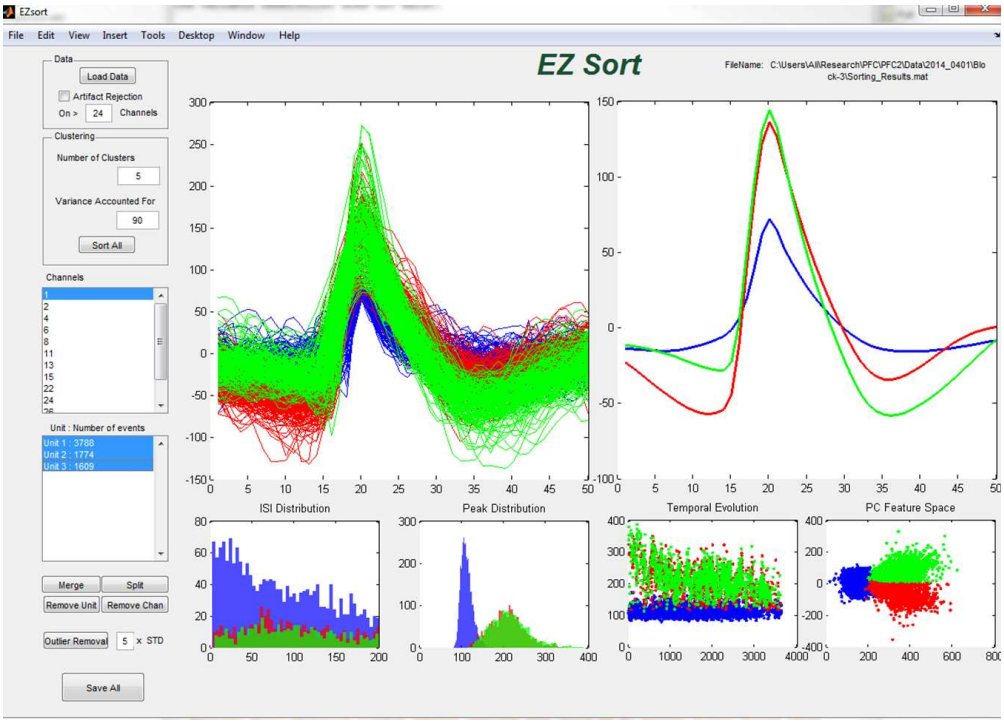

Figure 3.11: **Snapshot of the EZsort software**, developed for the purpose of this dissertation using the GUIDE toolbox in MATLAB

In short, the goal of this analysis is to establish a functional relation between a neural time series (spiketrain) and some behavioral element of the task. This functional relationship is often referred to as a *'neural code'* [66, 163]. Spiketrains are discrete-time binary processes, mathematically best modeled as point processes [66, 87, 205].

Another way to describe a single neuron's activity is to use a measure known as *firing rate*. Firing rate denoted as $r(t)$ is the probability density for the occurrence of a spike. Due to limited amount of observational data, we can not analytically determine the firing rate of a cell. However different methods of estimating the firing rate have been suggested in the literature. Figure 3.13 shows a few estimate of a firing rate from a single spiketrain. Local likelihood methods can be used to estimate the PETH in terms of a mathematical function if needed [122, 150].

Spiketrain is represented using the a sum of shifted Dirac functions with spikes occurring

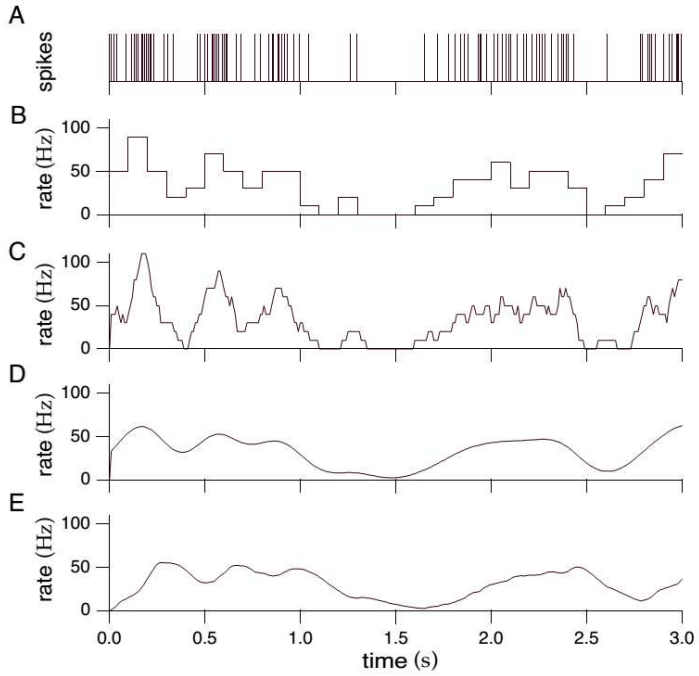

Figure 3.12: **Firing rate estimation** using different kernels. **A)** Raster plot of a spiking neuron, each marker shows on spike sampled at 1 msec bins. **B)** Discrete-time firing rate estimated using Δ=100 msec bins. **C)** Discrete-time firing rate using sliding windows of Δ=100 **D)** Continuous-time estimation of firing rate using a Gaussian kernel of σ=100 msec **E)** Firing rate estimated using an α function where $1/\alpha$=100 msec.Adapted from [66]

at times t_i:

$$\rho(t) = \sum_{i=1}^{n} \delta(t - t_i) \tag{3.12}$$

Firing rate is thus calculated through convolving this spiketrain with a Gaussian kernel $h(t) = a \exp(-\frac{t^2}{2\sigma^2})$. Parameter a is selected such that the units of the calculated firing rate is spike per second. Thus the firing rate can be calculated using the following formula:

$$r(t) = \int_0^T d\tau h(\tau)\rho(t - \tau) = \sum_{i=1}^{n} h(t - t_i) \tag{3.13}$$

Throughout this dissertation, whenever a firing rate is required I use a Gaussian window with a standard deviation of $\sigma_n = 50msec$, unless mentioned otherwise.

3.6.1 Peri-Event Time Histogram (PETH)

Peri-Event Time Histogram (PETH) is a histogram of the times that a neuron has fired a spike. This histogram is often the first step to analysis of a functional relationship between a stimulus or a task event and the firing rate of a cell. Prior to calculating a PETH, often the spiketrain is binned into larger (overlapping) bin of size Δ. Regular values for Δ are 25,50,100 msec, however the conclusions from the analysis should not be dependent on the bin size. Then spike timing of the binned data is aligned to the onset of the behavioral event. The stimulus (or event) is repeated for a total number of N times. Number of spikes for occurred during each bin is counted, k_i spikes within bin i. The histogram value is calculated as $\frac{k_i}{N \times \Delta}$ in units of spikes per second. Figure 3.13 shows a sample PETH of a neuron in the LIP area of a non-human primate's brain, in response to a visual stimulus. The histogram shows a clear modulation with respect to the stimulus and also can illustrate the delay in

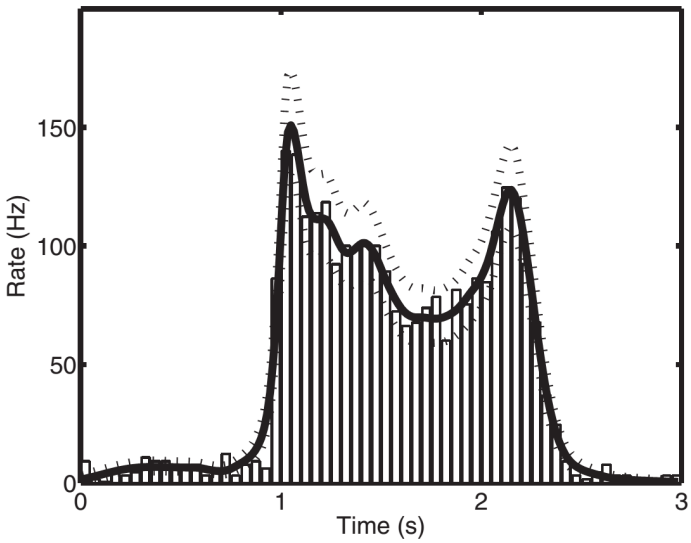

Figure 3.13: **A sample Peri-Event Time Histogram (PETH)**, of a neuron in the LIP area of a non-human primates brain, in response to a visual stimulus. Adapted from [163]

the neuron's response to the stimulus.

3.6.1.1 Statistical significance of a PETH

Often, once a PETH is constructed using the above mentioned algorithms, a comparison is required between PETHs corresponding to different conditions of the experiment. The problem of neural encoding then becomes whether the cell is encoding a certain feature of the stimulus or a certain condition of the task. A trivial question to be asked is whether the neuron is selective for any condition of the stimulus. This would be a classical hypothesis testing problem, discussed vastly in statistics and signal detection theory [193, 204]. A more delicate question is to determine the exact timing of the different modulations in neuron's response to task conditions.

Here, in order to determine whether a unit is response-selective, at any point during the trial, I divided correctly performed trials into contralateral-choice and ipsilateral-choice groups. At each time point, I used a two-sample Kolmogorov-Smirnov test [109, 240] to assess

whether the firing rate is selective for contra versus ipsi trials. Kolmogorov-Smirnov is a non-parametric test, often used to determine whether two underlying probability distributions differ from one another. The test was performed in MATLAB using the `kstest2` command and a $p-value$ of 0.05 was used for the significance level. For each unit, ipsi and contra trials were randomly shuffled 1000 times and the test was repeated for cross-validation. Individual time-bins were labeled as random if less than 5% of the shuffled tests resulted in significant differences between the two groups. A cell is considered to be significantly encoding one of the conditions if its firing rate is selective for one of the conditions for at least 50 msec. A selectivity index is used to determine whether a unit is selective for contra versus ipsi choice, using the following formula:

$$SI(t) = \frac{PETH_{contra}(t) - PETH_{ipsi}(t)}{PETH_{contra}(t) + PETH_{ipsi}(t)} \tag{3.14}$$

An index of +1 will indicate a preference to the contralateral choice while -1 is indicative of ipsilateral. The absolute value of the index will show the magnitude of selectivity, the closer to zero indicates less selectivity for the unit.

3.7 Spectral Analysis

Oscillation is a fundamental property of many natural systems, speech [67], climate [101,186], and seismic data [246] just to name a few. Oscillation is also abundant in biological systems including 'rhythms of the brain' [40, 71, 138]. Thus, to better understand the underlying dynamic of these characterizing the oscillatory behavior of the system is essential. Such oscillatory behavior is better characterized in 'frequency domain' rather than 'time domain'.

Frequency domain and time domains are related through the fourier transform [174].

$$X(f) = \int_{-\infty}^{\infty} x(t) e^{-\jmath 2\pi f t} dt \tag{3.15}$$

$X(f)$ calculated via the above formula is a continuous version of the frequency representation of signal $x(t)$. Attention to the limits of the integral shows that in order to extract the exact frequency information of a signal one need to a) observe the signal for its entirety and b) have continuous representation of the signal. In reality, however a signal is sampled at (often) fix frequency and is observed only for a brief period of time.

Thus, only an an estimation of the true frequency content of a signal is feasible for real signals. A discrete-time formulation of Fourier transform can be for a discrete-time signal $x(k)$ sampled at Δ intervals for N samples ($k = 0, 1, 2, \ldots, N-1$) can be obtained using the following:

$$\hat{X}(f) = \Delta \sum_{k=0}^{N-1} x(k) e^{-\jmath 2\pi k f \Delta} \tag{3.16}$$

Although the Fourier transform provides very useful information regarding the the frequency content of a signal, there are two major drawbacks of using a frequency domain representation for the biological signal. First, there is an inherent assumption of stationarity in Fourier transform that the nature of biological signals violate. Secondly, since in calculating the Fourier transform of a signal, temporal information is discarded due to the sinusoid kernel used, changes in frequency content of the signal cannot be displayed using this method. The need to represent the temporal changes in frequency content of the brain signals justifies the use of a time-frequency analysis method. Below we will discuss a number of popular time-frequency analysis techniques and justify the use of a wavelet approach in

this dissertation.

3.7.1 Introduction to time-frequency analysis

Number of different time-frequency analysis techniques have been introduced, developed and tailored for different applications [30, 51]. As mentioned earlier, all these techniques deal with simultaneous representation of time and frequency information of a time-series and are suitable for short-lived non-stationary signal whose statistics are subject to change in time. Short-Time Fourier Transform (STFT) [174], wavelet transform [128, 152], hilbert transform [113] and multitaper methods [164, 190] are among the popular methods of time-frequency analysis in neuroscience [52].

Detailed descriptions of these techniques is outside the scope of this dissertation. Here I will briefly elaborate of the limitations of each and justify the use of a wavelet approach for the current application.

A major drawback of STFT method is the fixed time and frequency resolution, imposed by the specific tiling of time-frequency space recruited in this method. In fact, the width of the window determines the resolution of the transform and dictates the way the signal is represented. A wide window provides good frequency resolution at the price of poor temporal resolution and correspondingly a narrow window sacrifices frequency resolution for a good temporal resolution. This is a major drawback that indeed motivated the development of filterbanks and wavelets.

The multitaper method was originally developed to address the issue of bias and variance in spectral estimation [13, 224, 225]. Though the multitaper method is beneficial in analyzing noisy data with limited number of realizations, it suffers from over-smoothing lower frequencies of the time-series and thus make it difficult to isolate discrete-time events. This becomes

a challenge in some neuroscience applications where oscillations of interest are low-frequency (delta or theta oscillations).

On the other hand, wavelet transforms provide a compromise between temporal and frequency resolutions by using different window widths for different frequency ranges of interests. Thus, I used a wavelet based approach to analyze the time-frequency features of the neural signal. Among different wavelet approaches, I chose to use Morlet wavelets for the reasons I will describe in the next section.

3.7.2 Morlet wavelets

The problem with Fourier transform is that the lack of temporal localization of frequency content. This is due to the sinusoid kernel used in the transformation. The amplitude of a sinusoid wave is constantly fluctuating between two peak from negative infinity to positive infinity. Thus multiplying this kernel with the time-series and summing over the product will smear any temporal information. It seems a logical next step to use a windowed sinusoid and use one or a few cycles of the sinusoid as the kernel. This is known as boxcar temporal weighting. The main issue with boxcar windowing is the edge artifacts, since it weights all the data points in the box-car equally. A good solution is to use a Gaussian taper to window the sine wave. The Gaussian taper will eliminate the sharp edge and also provides a control over the desired precision between temporal and frequency resolution. A sine wave windowed by a Gaussian taper is called a *Morlet* or *Gabor* wavelet first introduced by Dennis Gabor [98] in 1946. Jean Morlet later formulated this as a wavelet basis and showed applications of the

transform in seismology [110]. The kernel can be formulated as following:

$$G_e(t) = \frac{1}{\sqrt{2\pi}\sigma} e^{-\frac{t^2}{2\sigma^2}} sin(2\pi f t) \tag{3.17}$$

$$G_o(t) = \frac{1}{\sqrt{2\pi}\sigma} e^{-\frac{t^2}{2\sigma^2}} cos(2\pi f t) \tag{3.18}$$

The transformation can be written in two odd or even versions based on the core kernel used. Using a cosine function will result in an odd transformation and a sine kernel will yield to an even Morlet wavelet. These two wavelet basis are shown in Figure 3.14.

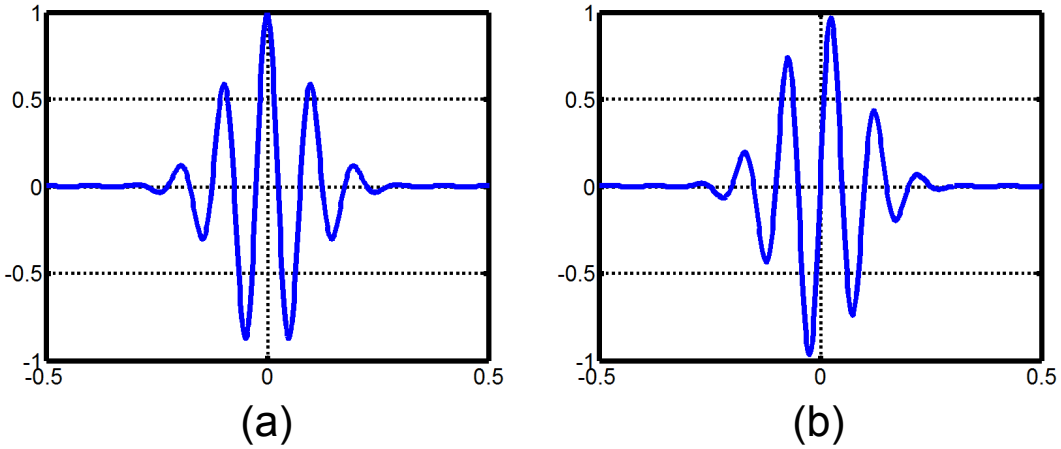

Figure 3.14: **Morlet wavelet functions**,**(a)** Even **(b)** Odd.

To make a Morlet wavelet, one should construct a sinusoid wave at a desired frequency, and multiply that with the time-series on a point-to-point fashion. Frequency of the sine wave is also the wavelet frequency and is considered called the *peak* or *center* frequency. Standard deviation of the Gaussian kernel is calculated using the following formula:

$$\sigma = \frac{n}{2\pi f} \tag{3.19}$$

where f is the peak frequency and n is the number of wavelet cycles. The parameter n controls the trade-off between temporal and frequency resolution. The larger the parameter n is selected, the frequency resolution will be finer, at the expense of temporal resolution. A wavelet decomposition method involves a many different wavelets of different frequencies.

As seen by the differences between the odd and even wavelet basis, the phase offset between the wavelet and the data affects the results of the convolution. Furthermore, Morlet transform is practically equivalent to band-pass filtering and thus provides no explicit information regarding the power and phase of the transform. In order to resolve these limitations a different formulation for the Morlet wavelet is suggested. In this new *complex Morlet wavelet*, time-series is convolved with wavelets that have both real and imaginary parts. This provides both power and phase information and also the result of the convolution would not be dependent on the phase offset between the wavelet and the time-series.

A complex Morlet wavelet can be formulated very similar to the Morlet wavelet with the difference that the real sine wave is replaced with a complex sine wave:

$$G(t) = \frac{1}{(\sigma\sqrt{\pi})^{\frac{1}{2}}} e^{-\frac{t^2}{2\sigma^2}} e^{\jmath 2\pi f t} \tag{3.20}$$

Using Euler's formula this can be decomposed into real cosine and imaginary sine components. Similar to the Morlet wavelet, f here is the peak frequency. Once the complex wavelet basis is convolved with the time-series, the result will be a complex number. The magnitude of this number will indicate the power of the signal at any point in time and the phase of the number is an estimate of the phase of the signal at each point.

3.8 Decoding population activity

Studying the activity of individual neurons and their functional relationship with stimuli or actions has provided tremendous amount of information abut the mechanics of nervous system during the past decades. The approach as mentioned and also pursued in this dissertation is to study single-cell responses average across several repetitions of stimuli or behavior. However, the brain uses information from a large population of cells to gather information and make decisions in a single-trial. Thus, one trending approach in neuroscience, promoted by the advent of microelectrode arrays [28, 61, 139, 206] is to study collective activity of a number of units in a single trial.

There are two major approaches to processing single-trial information being carried by a population of neurons. The first uses *decoding* algorithms to predict a given stimulus or behavior from the observed pattern of population activity, and the other incorporates concepts from *information theory* to calculate the amount of information that the population response carries about the stimulus or a certain behavior. Decoding is primarily concerned with reconstruction of the stimulus or prediction of a behavior, the more accurate we can reconstruct an input from a given population response the population carries more information. It is important to distinguish between two types of decoding: continuous decoding and discrete decoding. In continuous decoding, a neural response is used to regress over a continuous variable (such as an arm kinematics or spatial location of an animal in a maze), whereas in discrete decoding accumulated population responses are used to predict a discrete behavioral variable such as a discrete movement or gaze direction or deflection of specific whisker pads in an anesthetized rat. On the other hand, information theory approaches use *bits* to quantify the amount of information transfer between the input and output of

a system. The information theory approach has been extensively discussed in the literature [5, 26, 66, 178, 212]. Here I use a decoding approach to study population encoding mechanism of the mPFC neurons. Following is a description of two known decoding schemes I implemented for this dissertation.

3.8.1 Bayesian decoding

Decoding is the prediction of which stimulus or behavior evokes a particular neural response in a given trial. In a Bayesian framework, encoding and decoding are two sides of a same problem. Let $\boldsymbol{r}$ represents response of a population of N neurons, $\boldsymbol{r} = (r_1, r_2, \ldots, r_N)$, and let s represents a stimulus or a behavior parameter. Then using Bayes theorem, we obtain:

$$P(s|\boldsymbol{r}) = \frac{P(\boldsymbol{r}|s) \cdot P(s)}{P(\boldsymbol{r})} \tag{3.21}$$

where

$$P(\boldsymbol{r}) = \sum_s P(\boldsymbol{r}|s) \cdot P(s) \tag{3.22}$$

And $P(s)$ is the probability that the stimulus s is presented, which is often called the 'prior probability'. $P(s|\boldsymbol{r})$ is called a posterior probability and shows the odds of observing the response $\boldsymbol{r}$, had the stimulus s was presented. The posterior probability can be calculated for all possible values of s and the one value that maximizes the posterior probability will be selected as the prediction of the decoder:

$$s^* = \arg\max_s \{P(s|\boldsymbol{r})\} \tag{3.23}$$

For the sake of comparison, I have implemented Bayesian decoding of neural responses in MATLAB. However, given the very high dimensionality of neuronal spiking data, to calculate an unbiased estimate of the probability densities, large amounts od data is required that is typically not practical for awake behaving subjects. To overcome this limitation, model based estimation of probability densities have been suggested [37, 185, 191, 239]. An alternative approach is to use machine learning algorithms where there is no explicit requirement for calculating the probability densities. These are discussed in the next section.

3.8.2 Machine Learning approaches to decoding

An area of study concerned with learning rules and making inference from data is called Machine Learning. These algorithms are optimized to represent the observed data in a robust, generalizable fashion such that the inferences are valid for the unseen data [27]. *Representation* and *generalization* are the two most important aspects of any machine learning approach and are dealt with in independent steps. Often some form of transform is used to represent certain features of the data, this procedure if called *feature extraction* and is very dependent on the type of the data and the required analysis. Once features are extracted different methods of regression are used to partition the data and explore orders within the dataset. Below I will describe the approach I used for extracting features from the population of spiketrains and local field potentials. Next I will elaborate on the regression technique I used to partition the data.

3.8.2.1 Feature extraction

Similar to the single-unit analysis, here I used a Gaussian kernel to convert the binary spiketrain into a continuous-valued time-series. However, unlike that analysis, the kernel

used here is causal (one-sided), since the decoding analysis is supposed to determine the predictability of the neural response up to time t, and thus should not be affected by the spikes happening after time t. Assume that $\boldsymbol{R}^{1:T}$ is the observed population response during a single trial, through time T, smoothened with a causal Gaussian kernel. Response matrix will have a dimension of $N_u \times T$, where N_u is the number of sorted units and T is the number of timebins. This sample response matrix is then projected onto a 'Template' matrix, M. This template matrix is obtained using SVD analysis and contains the first 50 modes of a previously analyzed training dataset and ensures the largest variability among the projected features. This step is performed due to the very high dimension of the neural data and in fact will reduce the dimension of the data to a set of features that maximizes the variance. Given the limited size of the observed data, this step if required to guarantee the generalizability of the decoding algorithm, otherwise the algorithm will suffer the curse of overfitting to the observed sample [27].

To extract features from local field potentials, a very similar approach is adopted. Using the time-frequency analysis described earlier in this chapter, the field potential is decomposed into different frequency components. The sample response matrix will then be of size $N_f \times T$ where N_f is the number of frequency components. The rest is very similar to the feature extraction procedure, where a template matrix is constructed using a training dataset and the sample response matrix is projected onto the reduced dimension space.

I also used a hybrid feature vector where features from spiketrain and LFP were calculated independently using the described method and augmented to construct a hybrid feature vector.

Ultimately, the extracted features are passed on to the regression algorithm to partition the data. Details of the regression algorithm used in this study, known as *support vector*

machines, is described in the following section.

3.8.2.2 Support Vector Machines

Support Vector Machine (SVM) is basically a binary linear classifier that takes a set of input data and predicts for each given data point which of the two possible classes it may belong to. To better understand the concept of Support Vector Machines (SVM), one should start with two-class linear classifiers. Similar to all classification problems, the data sample are represented by single (possibly multi-dimensional) points in a feature space. The problem is to find the best line that separates the data point belonging to different classes. Mathematically, we are interested to find the coefficients $\vec{w}$ of the following equation:

$$y = f(\vec{w} \cdot \vec{x} + b) = f(\sum_{j=1}^{N} w_j x_j + b) \tag{3.24}$$

In the above equation, b is just an offset value, N is the number of the features for each data point, $\vec{x}$ is the set of features representing eah data point, $\vec{w}$ is the linear classifier features and y is the output score assigned to each data point. The classifier coefficients ($\vec{w}$) should be selected such that the output score y be the indicator of the class labels for each data point. One useful convention is to define a dummy variable C_i for each data point such that the product of C_i and y_i always remains positive: $C_i y_i \geq 0$. This leads to choosing $C_i = +1$ for class 1 and $C_i = -1$ for class 2.

A training dataset will be used to determine the classifier coefficients. In case of a linear function, f is selected as a unity function. However, in general f can be any kernel function. One can imagine the linear classifier to be a hyperplane dividing the feature space into two partitions. This hyperplane is also called a *decision boundary*.

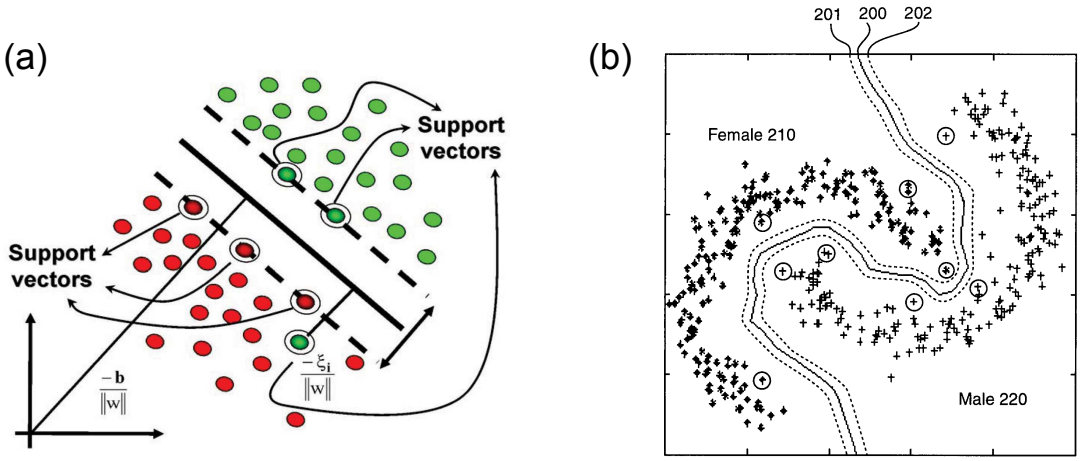

Figure 3.15: **About Support Vector Machines**,**(a)** An example of two linearly separable clusters, the decision boundary and support vectors **(b)** Two non-linearly separable clusters and the inferred decision boundary using SVM kernel trick.

SVMs, in their original definition and use, are nothing but a linear classifier that maximizes the *margin* of the decision boundary. The margin is defined as the distance between the decision boundary and the closest of the data points (known as support vectors). By definition the distance is defined by the following equation:

$$\frac{C_i y(x_i)}{\|\vec{w}\|} = \frac{C_i(f(\vec{w}\cdot\vec{x})+b)}{\|\vec{w}\|} \tag{3.25}$$

The maximum margin solution could thus be found using the following equation for $\vec{w}$ and b [27]:

$$\arg\max_{\vec{w},b}\left\{\frac{1}{\|\vec{w}\|} min_i C_i(f(\vec{w}\cdot\vec{x})+b)\right\} \tag{3.26}$$

We are interested to evaluate the performance of an SVM classifier [27, 75, 129, 131] in distinguishing the condition under which the neural response was observed. We train the classifier sequentially in time and the performance is assessed at each step (timebin) to

determine the temporal evolution of the neural response.

The data was always divided into a training (which comprised 70% of trials) and a test set. The training set was randomly chosen from across all successful trials and was used to compute the SVM parameters and the test set was used to evaluate the performance of the decoder. This was repeated for $n_{iter} = 50$ times to rule out any bias effect due to training and test set selection and 95% confidence intervals were computed.

In order to evaluate the information stored and passed to other processing areas through different mechanisms, we used different neural features as input features of our classifiers. In particular we used spike, LFP and hybrid features. Spike features were extracted by binning the spiketrain and calculating the spikecount in overlapping bins. On the other hand, LFP features were obtained using a short-time Fourier analysis in overlapping windows and the power of the signal in each window was selected as the input features [156,250]. In the hybrid mode, the features from spikes and LFPs were combined to boost up the performance. As a sanity check, we randomly labeled the trials to destroy any cue or target selective information. We expect an unbiased decoder not to significantly perform above chance level in this case.

A range of different bin widths were used and the maximum decoding performance for each was calculated. Also different channel counts (randomly chosen from available channels) were used and the maximum performance under each channel count was computed and cross-validated by $n_{iter} = 50$ iterations.

3.9 Inhibition using Opto genetics

Reversible inactivation using pharmacological intervention provides a useful tool to study the role of a specific brain area in certain behavior. But what if one is interested in detailed

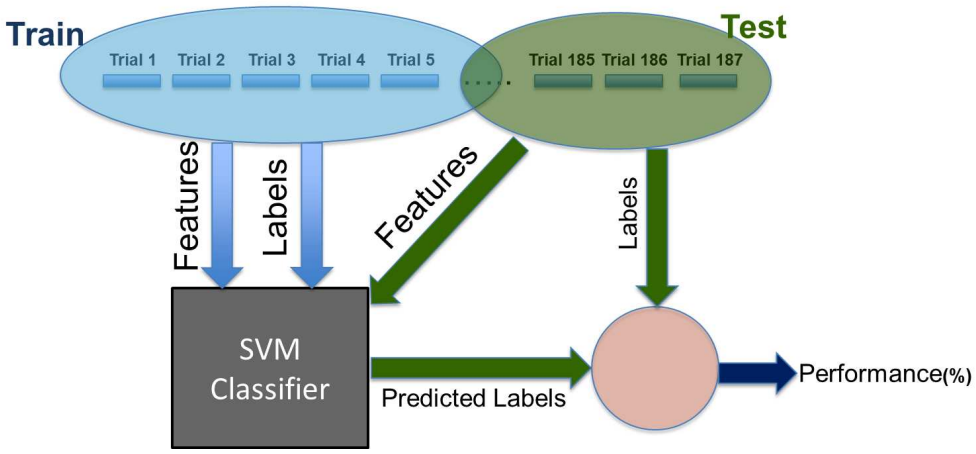

Figure 3.16: **One the use of SVM for single trial prediction**, Data is partitioned into train and test subsets. Features for each set is calculated. Features and labels of the train set are used to estimated parameters of the support vector machines. Then the same parameters are used to predict the labels for the test set trials. Performance of the SVM is determined by comparing the predicted and original labels for the test trials.

timing of the circuit recruitment in the action? Using pharmacological agents, there is no easy way of briefly activating or inactivating the brain circuits.

The advent of optogenetics, provided means of cell-type specific interrogation of neural circuits with millisecond precision [33, 158, 226]. Optogenetics recruits light activated ioc channels to either excite or inhibit the activity of individual cells of certain type. This is done through inserting[2] opsin genes into the cells of the brain.

Shown in Figure 3.17 are three popular such channels. Channelrhodopsins (ChR) are blue light-activated (470 nm) cation channels that enables the flow of inward (excitatory) currents. Halorhodopsins (NpHR) are inhibitory chloride pumps, while the other inhibitory channel category (bactereorhodopsins and proteorhodopsins BR/PR) are proton pumps. Both inhibitory type channels are most active at around amber light wavelength (590 nm).

To investigate the temporal dynamics of prelimbic circuit recruitment, I suggest to use

[2]Gene delivery can be done through different means. A popular way that has been used in our lab is to transfect the tissue using a viral vector (AAV or Lenti).

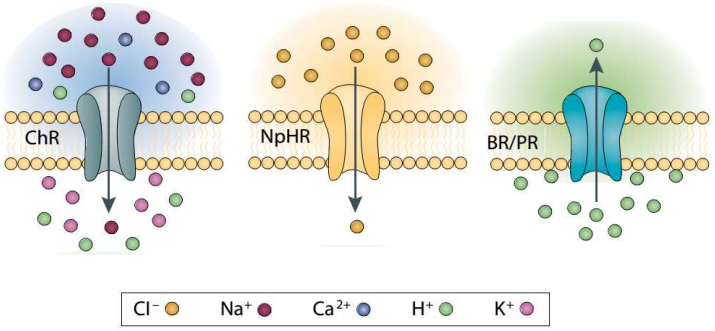

Figure 3.17: **Different categories of light-activated opsins** *Channelrhodopsin*, excitatory blue light-activated cation channel. *Halorhodopsin*, inhibitory chloride pump. *Bacteriorhodopsin*, inhibitory proton pump. Adapted from [247].

the optogenetics toolbox with either Halorhodopsins or Archrhodopsin. Using an amber laser or LED light source to silence the circuit only during certain epochs of the task. Figure 3.18 shows a design for such an experiment.

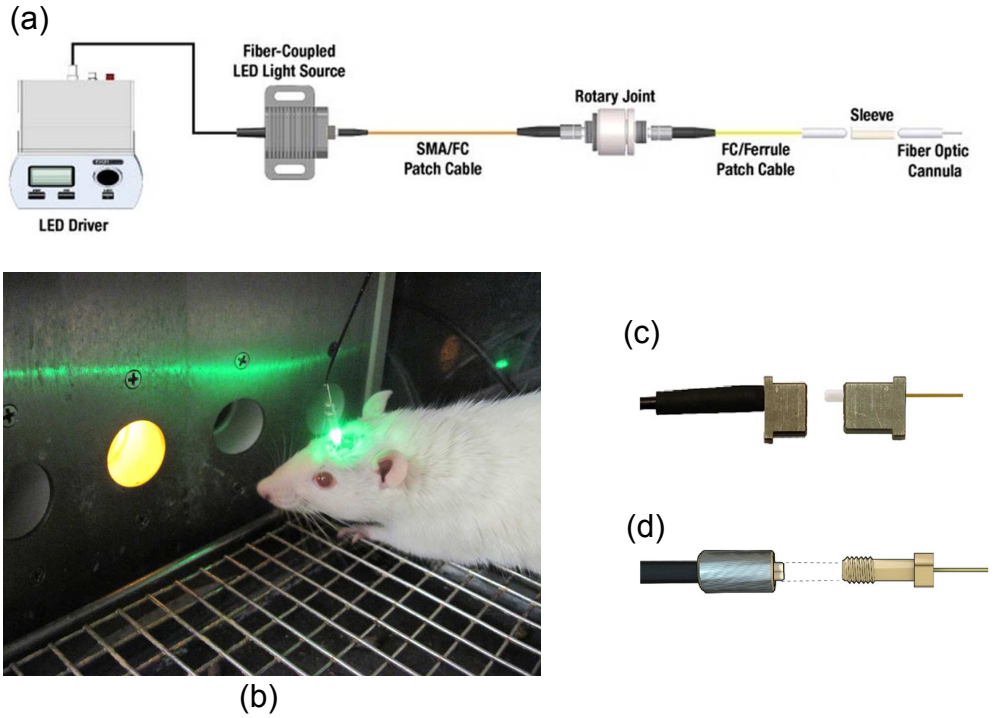

Figure 3.18: **Setup of an optogenetic experiment in awake behaving subjects a)** The optical source is connected through FC cables to a rotary joint. This is used to ensure that the cable is not twisted and tangled while the subject is freely moving in the cage **b)** Snapshot of the subject inside the cage with the fiber optic attached. Note: in our latest experiments we used a type of connector that blocks any light power leakage. This picture is for demonstration purposes only **c,d)** Two different optical cannula type with a magnetic or threaded designs

.

Chapter 4

Results

I have no data yet. It is a capital mistake to theorize before one has data. Insensibly one begins to twist facts to suit theories, instead of theories to suit facts.

— Sir Arthur Conan Doyle, *Sherlock Holmes*

4.1 Introduction

So far I have elaborated on the problem of cognitive neural prosthetic as a means of restoring motor function for the motor disabled patients. I have proposed exploring the potential of using motor related signal in the prefrontal cortex as sources of obtaining robust and stable driver signals for the prosthetic. I have selected rodents as the animal model for this experiment knowing the trade-off between cognitive complexity and low cost of performing experiments on the rodents. I have described the experimental design we used to investigate the role of rodent prefrontal cortex in execution of a delayed choice task. Different techniques such as reversible inactivation, electrophysiology and optogenetics have been used, details of which are described in the previous chapter. In this chapter I will describe the results of each experiment. I will leave interpretation of these results and their significance to the next chapter.

A total number of 24 adult female Sprague-Dawley rats were used for this project. This number does not include the subjects used for mastering the techniques and practices. Details

regarding each subject is described in the appendix. A total of 10 subjects were recruited for the reversible inactivation experiment, 8 were dedicated to the optogenetics experiment and the remaining cohort of 6 were assigned to the electrophysiology recordings. Number of animal subjects was chosen to satisfy the trade-off between the power of each test (number of recorded units for electrophysiology subjects were used instead of number of subjects) and the cost/duration of each experiment.

4.2 Behavioral Results

Subjects were food deprived to maintain 85% to 90% of their ad-libitum weight. Subjects' access to water was unlimited and each subject was caged individually in University Laboratory Animal Resources (ULAR) facility at Michigan State University Trout Food Science Building. Standard rat enrichment toys were provided in each cage. Subjects were also kept in a reverse 12-12 hour dark/light cycle (6 a.m to 6 p.m dark). All the experiments were performed during the dark cycle in dark acoustically isolated behavioral boxes. Each training/recording session lasts for 90 minutes and each subject receive 1-2 training sessions per day, 5 days a week. Over the weekends each subject received 12 grams of 'free food' [1].

All subjects were trained similarly until reached and maintained a pre-determined performance measure (overall success rate of above 75%). After meeting the criterion, they were assigned to different experiments and depending on the experiment were either implanted with a recording microelectrode array, chronically implanted with a bilateral cannula or injected with an opsin carrying virus and implanted with a fiber optic cannula.

[1]Per fellow graduate students' public belief, this is the most rewarding reinforcement that can drive any experiment

4.2.1 Task Acquisition

The task designed for this experiment is considered a rather complex task for the subjects. In order to accomplish the task correctly a number of different faculties should be involved. The subjects should **a)** maintain their snout inside a fixation hole until a Go cue. This requires an inhibitory control process in which prefrontal cortex is believed to be involved. **b)** the subject should attend to the sensory cue and **c)** associate the sensory cue with a target memory and **d)** plan for reaching to the correct target.

Thus it is essential to control different performance measures to ensure that the results obtained are not contaminated by the subject choosing an undesired strategy to accomplish the task because after all the subjects are not (presumably) aware of our intention as the experiment and the goals of the experiment and only seek the reward.

The first measure defined in this task is percentage of correct trials. Since the low and high pitch auditory cues are randomly assigned to right and left target memorys and the probability and amount of the two targets are equal, one expects no statistically significant difference between performance of the subject during trials in which right or left targets are instructed. Performance here is defined as the ratio of the trials where the instructed target is correctly reached. Performance of the subject is monitored on a daily basis. The subject may develop a bias towards a given target, if the bias is consistent a temporary reinforcement strategy is adopted to motivate the less visited target.

Figure 4.1 shows a distribution of performance across 24 sessions for the (n=3) subjects that received a microelectrode array implant for the two types of trial: *contralateral* trials where the subject is instructed to select the target contralateral to the implant side and *ipsilateral* trials where the subject is instructed to move to the same side with respect to

the implant. If the subject discards the instruction cue and randomly selects a target at each trial, the performance should theoretically be 50%. This is shown as the *chance level* in the graph. However as shown in Figure 4.1, the performance is significantly different from chance level ($p < 0.01, KS - test$). Also the performance of the contralateral trials is not significantly different from the ipsilateral trials($p > 0.5, KS - test$). This depicts that the subjects were attending to the instruction cue, maintaining some form of memory during the delay period and finally selecting a target memory given that instruction cue.

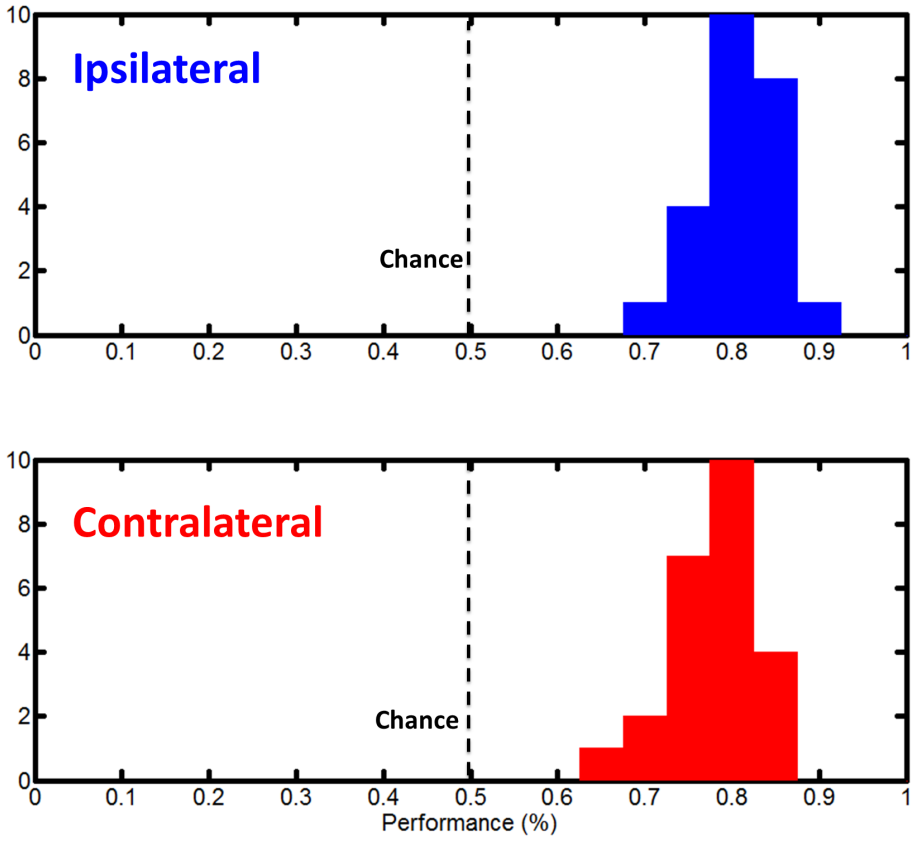

Figure 4.1: **Distribution of behavioral performances across subjects**, to ensure that the subjects have acquired the task and following the rules, performance for both ipsilateral (**top, blue**) and contralateral (**top, red**). If the subject is not attending to the rules, the performance should be around or below the chance level (50%).

The other behavioral parameter to monitor is the rate of errors of different types. In

this task four types of errors may occur: **a)** Premature retraction, **b)** incorrect responses, **c)** fouls and **d)** omission errors. Figure 4.2 shows the percentage of each error type, averaged across n=3 subjects from whom electrophysiology data was collected. The majority of errors (56% ± 4%) were due to incorrect responses that is committed when once instructed to a specific target, the opposite side is selected. Premature retractions contribute to other portion of errors where the subject retracts from the fixation beam prior to the Go cue. This constitutes 42% ± 6% of the errors. Omissions contributed to 2% ± .5% of the trials, where the subject dropped the trial after the go cue and did not reach for any of the targets within 3 seconds from the go cue. Fouls that are reaching to most distal targets in the cage did not happen in these well-trained subjects.

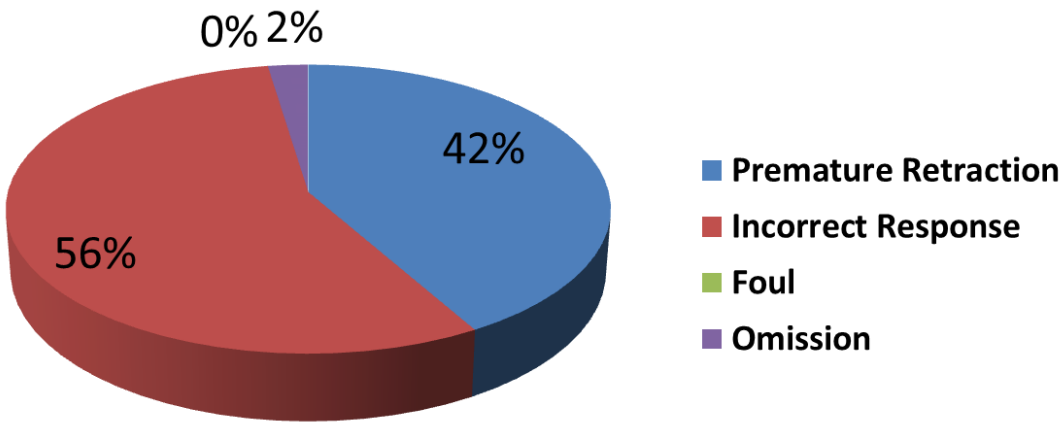

Figure 4.2: **Distribution of error types**, Incorrect responses where the subjects (n=6) selected the wrong direction contributes the most to the error types.

4.2.2 Response characteristics

Once the subject initiates a movement towards the target, a *ballistic* process is engaged. Prior to that a *controlled* cognitive process is recruited to perceive the cue, recall a target

memory associated with the instruction, maintain the target memory and waits for the Go cue. The boundary between the controlled process and the ballistic process can be conceived as the 'point of no return' after which the task is bound to execution [175]. Reaction time, the time elapsed between the onset of the go cue and the initiation of the overt movement can be indicative of cognitive processes involved in execution of the task, while the time to target is reflecting the ballistic movement. Figure 4.3 shows a distribution of the reaction times and the time to target for the chronically implanted subjects, pooled together across 24 sessions.

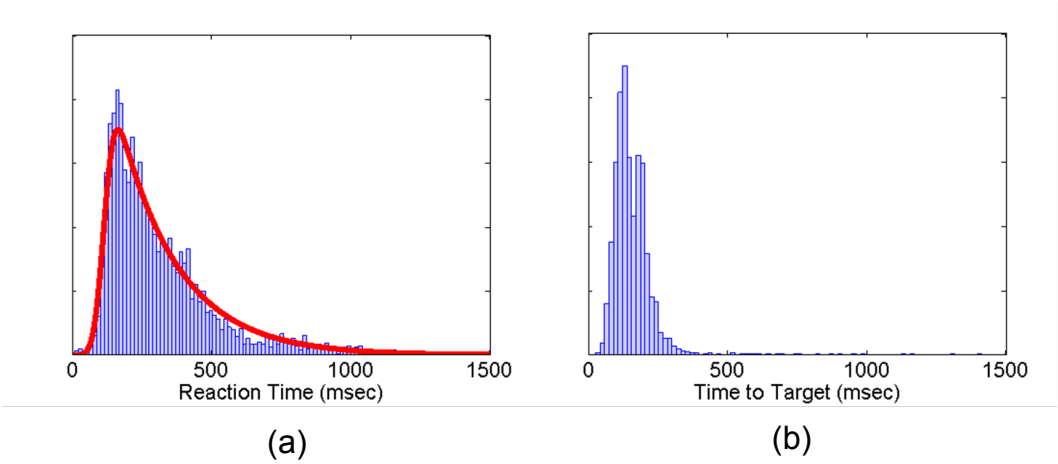

Figure 4.3: **Distribution of reaction time and time to target a)** Distribution for the reaction times, estimated parameters of an ex-Gaussian distribution: $\mu = 115$ msec, $\sigma = 30$msec, $\tau = 215$ msec^{-1}. **b)** Distribution of the time to target

Using the maximum-likelihood method explained earlier, an ex-Gaussian function estimate of the distribution was fitted to the observed data. The estimate has a an average of $\mu = 115msec$ and standard deviation of $\sigma = 30msec$ for the Gaussian segment and a decay constant of $\tau = 215msec^{-1}$ for the exponential part.

4.2.3 Perceptual discrimination

As mentioned earlier, two single frequency auditory tones were chosen as the sensory cues instructing the subject towards different target memories. A low pitch frequency tone (5KHz) was associated with the right target and a high pitch tone (14.2 KHz) was assigned to the left target. The frequencies were picked such that they are perceptually distinct. Evidences of rodent auditory discrimination studies suggest that rodents are capable of differentiating tones as low as 0.1 octave apart in their low threshold auditory range [114, 120]. The two frequencies selected here are 1.5 octave apart ensuring that they are perceptually distinct. To test that however, I designed an experiment results of which are illustrated in Figure 4.4.

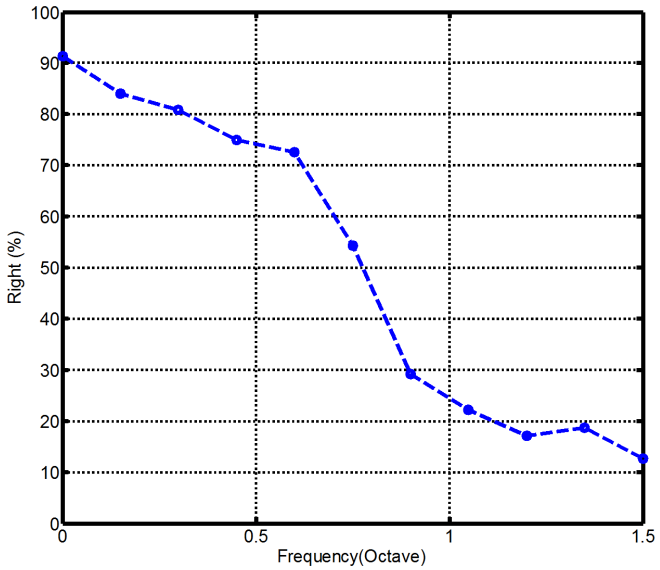

Figure 4.4: **Perceptual discrimination of the auditory tone** As the frequency of the instruction cue increases from the base frequency (5 KHz), the subject tends to be albe to better discriminate the two tones.

In this experiment a base frequency of $f_0 = 5KHz$ was selected. During each trial, a single tone frequency (f_1) tone was played as the instruction cue. f_1 was selected to be δ octave apart from f_0 where δ was selected from a uniform distribution between 0 and 1.5.

For $\delta < 0.75$ the subject had to select the right target after the delay period and for trials were $\delta > 0.75$, a left target was the correct answer.

In Figure 4.4, the y-axis shows the percentage of trials where the subject selected the right target. As we expect, this number is close to 100% illustrating that the subject can clearly associated low pitch tones to the right target. On the other hand, as the frequency get further from the base and δ approaches 1.5, percentage of the trials in which the subject selects a right target gets closer to zero. However, when close to the threshold (0.75), the ratio of the trials where the subject chooses a right target is close to 50%, that is the chance level. This suggests that for these *'fuzzy'* frequencies, which are perceptually hard to distinguish, the subject prefers to guess the correct target. This can be used as an additional evidence, along with behavioral performance results shown in Figure 4.1 that the subjects are attending to the task, have learned the associations between the instruction cue and the target memorys and basically are not just winging it!

4.2.4 Effect of delay period

Before delving into the problem of encoding mechanism of delayed choice in the prefrontal circuits, one question requires attention and that is the effect of delay length on the performance of the subject. The question is how long can a subject wait before wandering off the task. This problem has been studied for over a 100 years and has shown to be dependent on the subject species, age, sex and task requirements [15, 132, 162, 216]. Here I examined the effect of delay length in my experimental design using two modifications of the experiment.

In the first experiment, two cohorts of subjects were trained on two different tasks. Task number 1 is the regular experiment, where a single frequency instruction tone is followed by a delay period of length τ where τ varies from trial to trial and is pulled from a uniform

distribution between 1 and 1.5 seconds with millisecond precision. After the delay period a go cue (auditory white noise), instructs the animal to select the appropriate target. In the second version, no delay period and no go cue is present. This means that the onset of the instruction cue can be used as a go cue and as soon as the instruction is played, the subject is allowed to select the target. Figure 4.5 illustrates the behavioral measures for the two experiments.

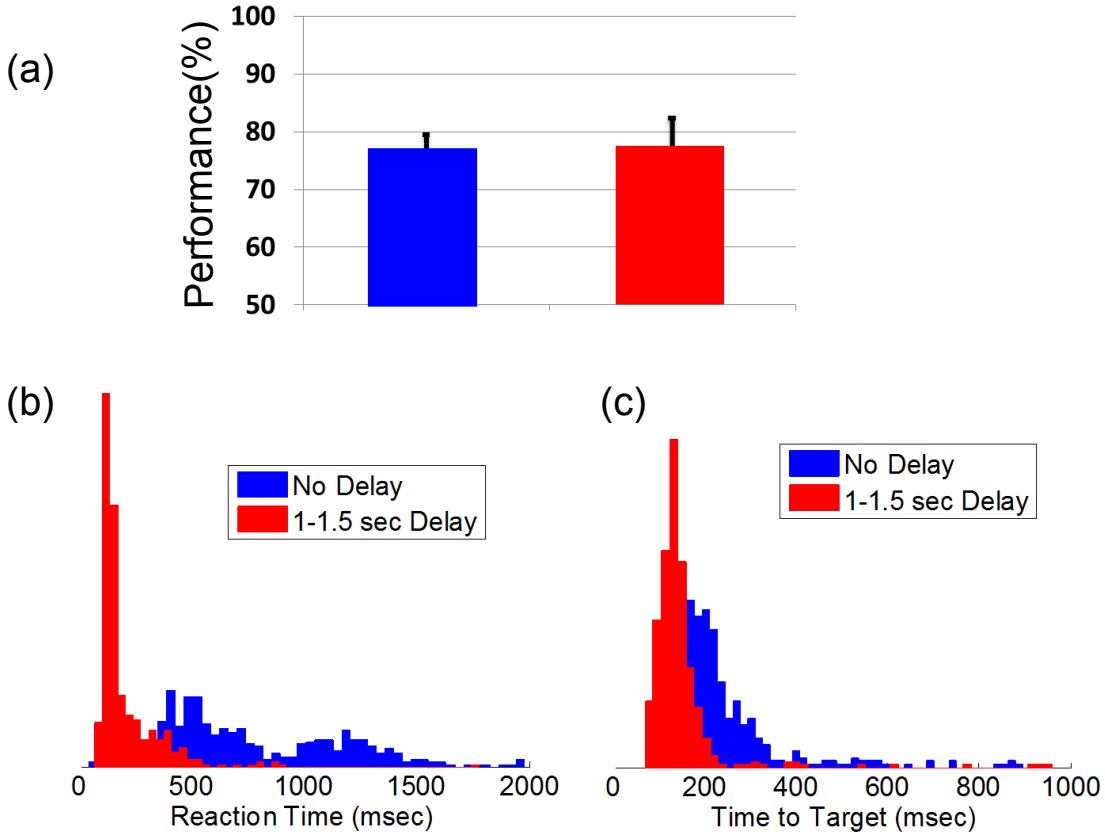

Figure 4.5: **Delayed vs. non-Delayed version of the task a)** Performance of the subjects is not significantly different for delayed versus the non-delayed versions of the task. **b,c)** However both distributions for the reaction time and the time to target are skewed to the right for the non-delayed version.

Depicted in Figure 4.5a, there is no significant ($p > 0.47 KS - test$) difference between average percentage of correct trials in two experiments. This suggests that the introduction of this delay period will not affect the memory requirements of the task and whatever memory

mechanism is involved is robust for the selected delay period length.

On the other hand, reaction times and times to target illustrate two very different distributions. While the reaction time distribution for the delayed version of the task is relatively narrow, the distribution is broad for the no-delay version. The same is true for the time to target distribution. This implies that the subject is using the delay period as a preparation epoch and thus the reaction to the go cue is much faster. The shorter execution time for the delayed version of the task suggests that kinematics of the task are also affected if a motor preparation window is provided to the subject and the preparation will yield to less motor variability [48].

In a different variation of the experiment, the length of delay period was varied randomly across trials pulled from a uniform distribution between 0 and 3 seconds with millisecond precision. The effect of the length of the delay period on percentage of correct trials and the rate of premature retraction is shown in Figure 4.6 .

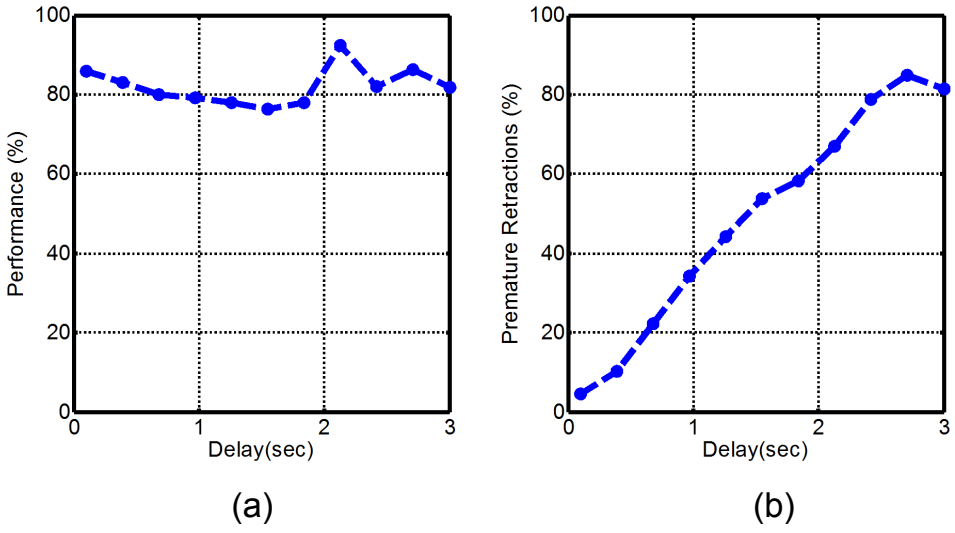

Figure 4.6: **Delay length effect**, **a)** the length of the delay period showed no significant effect on the choice performance. **b)** however, percentage of the premature retractions were increased linearly as a function of the delay length

As depicted in Figure 4.6a, the performance defined by the percentage of correct trials is

not affected by the length of delay period. However, Figure 4.6b that shows the percentage of premature retractions suggests that as the length of delay period increases, there is higher chance that the subject discards the task prematurely. In other words, if the subject shows enough patience and waits until the go cue, they will perform the task with same precision.

Length of the delay period also affects the response characteristics. As shown in Figure 4.7, there is a negative correlation ($r = -0.25, p < 0.01$) between the length of delay period and reaction time, meaning that the shorter the delay period, the more time it takes the subject to respond to the go cue. However, there exists no significant correlation between the delay period duration and the time to target ($r = -0.01, p > 0.42$).

All in all, results of these tests on the effects of the delay length period indicate that the delay length has little effect of the task performance, however the means of reaching the target (quantified by the reaction time or preparation time) are affected by that quantity.

4.3 Reversible Inactivation

Before investigating the detailed role of the prefrontal cortex in performing the delayed choice task, we have to test whether this area play a role at all. Knocking out a brain region and observe the effects of that on the subject's performance is an old established method for that. I decided to adopt a reversible inactivation method for that purpose. Muscimol which is a $GABA_A$ agonist and induces inactivation through inhibition increase, was diluted in ACSF until reached the concentration of 1mg/ml and injected unilaterally in the prefrontal cortex tissue through a chronically implanted bilateral cannula. Subjects were lightly anesthetized for the duration of injection using Isofluorane delivered through a gas mask and were immediately taken off the anesthesia and recovered upon the completion of

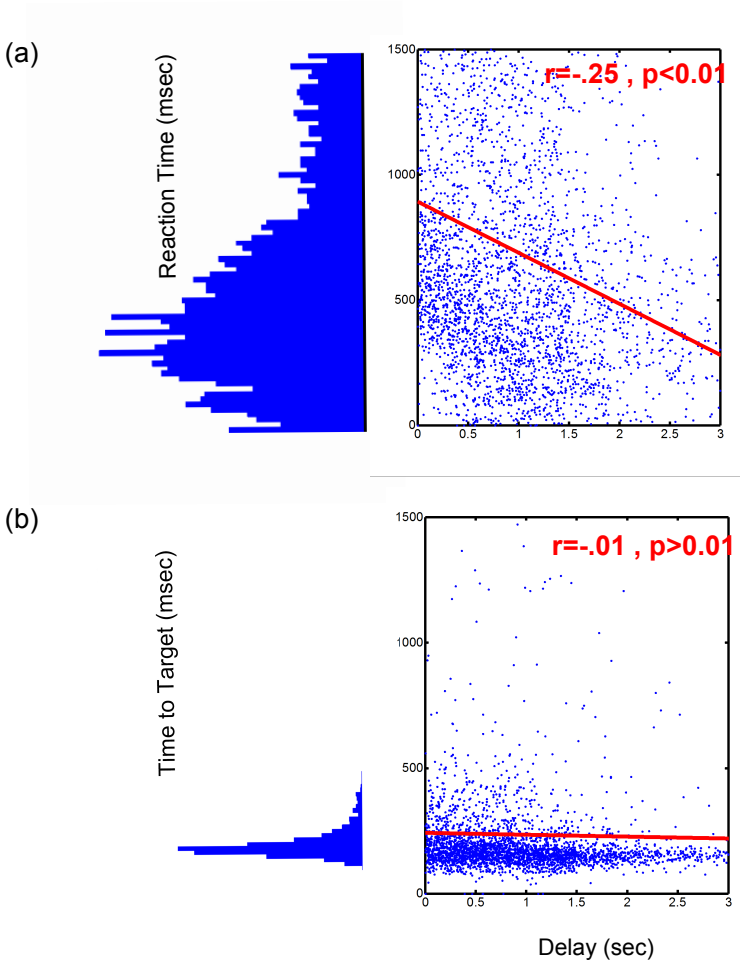

Figure 4.7: **Delay length effect on the task timing**, **a)** reaction time has a significant negative correlation with the length of the delay period **b)** no correlation is observed between the time to target and the delay period length.

the injection procedure. After 90 minutes of recovery period, the subjects were placed in the test boxes. Figure 4.8 shows the results of injecting $3.5\mu L$ of the 1mg/ml muscimol cocktail on the subjects' performance (n=3 subjects across n=21 sessions).

The graph in Figure 4.8 illustrates the performance of the subject under the influence of different injection conditions. For the experimental group $3\mu L$ of 1mg/ml muscimol was injected unilaterally, while for the sham injections the same volume of ACSF was injected. Control sessions had no injections and the subject were just anesthetized for the same period of the injection and were let recover for 90 minutes before the test. As evident by the results,

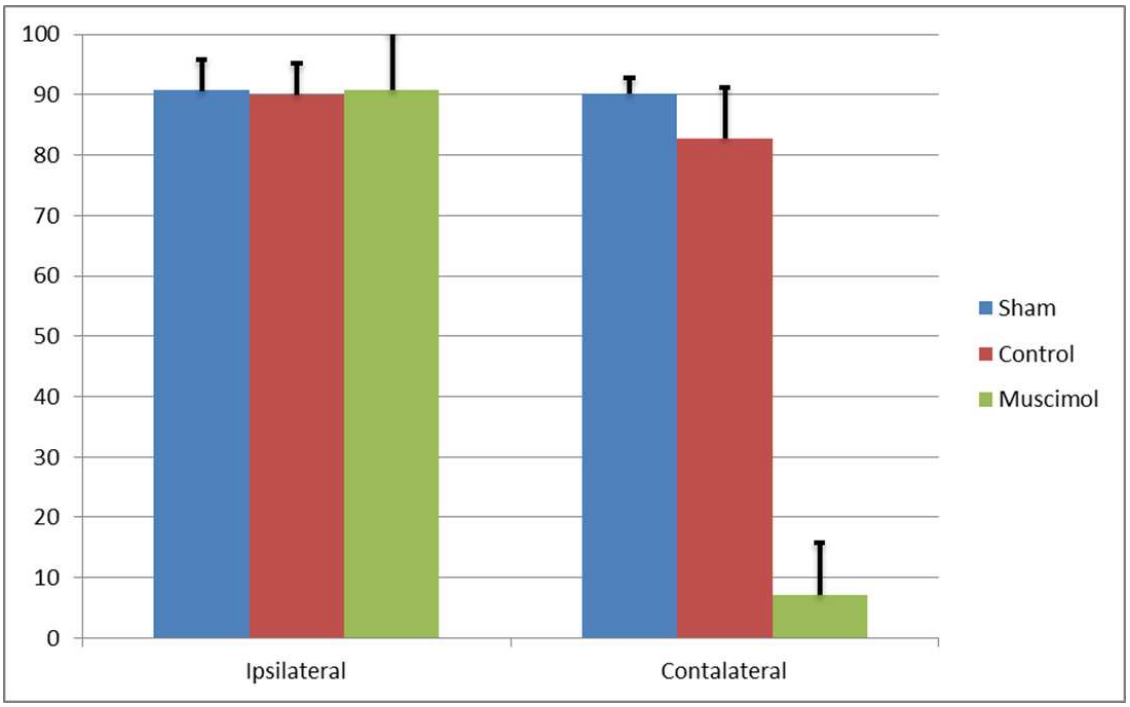

Figure 4.8: **Performance under the effect muscimol inactivation**, Lateralized suppression of the performance under 3μL of muscimol injection.

performance of the subject was affected only during those trials in which the subject was instructed to move contralateral to the injection side, i.e. if the drug was infused in the left hemisphere, the performance of subject was affected during trials with a right instruction cue. No significant drop in the contralateral performance was observed for the sham injection and control sessions.

The differential performance between the ipsilateral and contralateral trials is also dependent on the amount of diffused muscimol. Figure 4.9 shows the dosage curve for the muscimol effect.

As evident in Figure 4.9, the higher concentrations of the diffused Muscimol will result in larger differential performance between ipsilateral and contralateral trials. This hints that with an increase in the volume injected, larger area of the prefrontal cortex will be influenced by the drug and thus leads to stronger bias towards the ipsilateral choice.

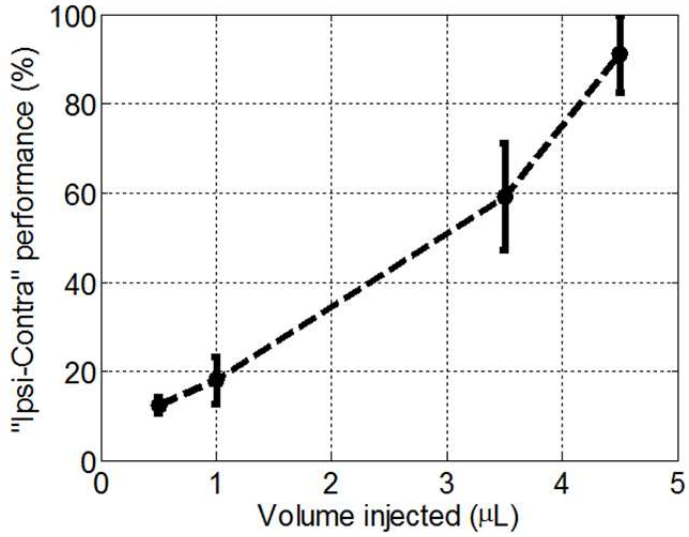

Figure 4.9: **Dosage curve for reversible inactivation**, the lateralized decline in performance is a function of the volume muscimol injected (n=6 subjects).

4.4 Electrophysiology

A cohort of subjects were implanted with microelectrode arrays after reaching the behavioral performance criterion and maintaining the performance level for a few consecutive sessions. Few days prior to the surgery the subjects were removed from the food deprivation protocol. Subjects were implanted with 16 channels of a microwire array in their layer V prelimbic cortex (+2.5-4mm AP, 0.6-0.9mm ML, -2.4mm DV). Individual ground and reference wires were soldered to different skull screws mounted posterior to the lambda point, on top of the cerebellum. This choice was due to the small amplitude of cerebellar LFP which elevate the quality of LFPs recorded in the PFC. Implanted probe was secured to the skull using dental cement. Subject was given analgesic and allowed to recover. Subject's health status, weight and food/water intake were constantly monitored. Upon recovery, almost after a week the subject was food deprived and tethered to the data acquisition system via a commutator. Full-band signals were amplified using a preamplifier, sampled at a rate of 25KHz/channel

and digitized using a 16-bit quantizer and recorded to file on a PC.

4.4.1 Histology

To verify the location of the implanted electrodes, post-mortem histology was performed upon completion of the experiment and collecting the required data. The subjects were trancardially perfused, the brain tissue was explanted and postfixed. Serial $50\mu m$ thick transverse sections were collected (through and perpendicular to probe locations). Sections were immunostained for NeuN and Neurofilament and counterstained with Hoechst for tissue response.

Figure 4.10 shows one such section. Electrode locations are evident in the image, and their relative coordinates can be verified, recording signals from the prelimbc area of the medial prefrontal cortex along the anterioposterior axis.

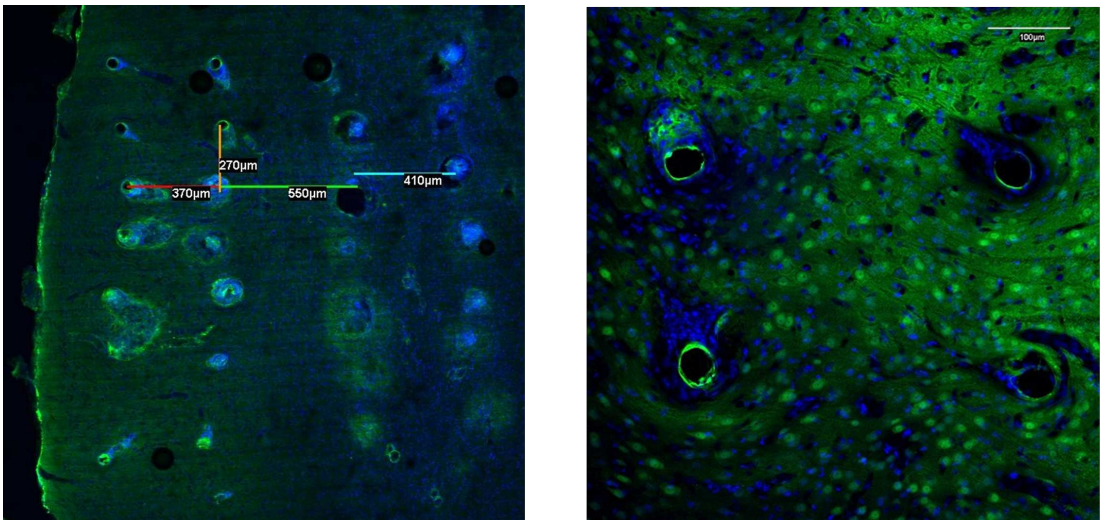

Figure 4.10: **Histological evaluation of the implanted brain tissue**, horizontal brain sections depicting the probe location (midline on the left, posterior at bottom).

4.4.2 Single Unit Analysis

Following the methods explained earlier, full-band extracellular potential was recorded for multiple channels simultaneously from an awake behaving subject inside a training box. Behavioral events were synchronized with the neural signal using an analog input to the data acquisition system and were sampled using the same sampling frequency and saved on the same machine. This provided sub-millisecond synchronization between the neural signals and behavioral events.

Using a wavelet method, lower frequencies of the extracellular potential signal containing LFPs were filtered out. Spike events were detected using a thresholding method. Manual spike sorting was performed using custom-designed MATLAB based software EZSort. Clusters were manually examined for inconsistencies and violation of the assumptions for a clean, well-isolated unit.

Spiketrains for each trial were constructed aligned to different behavioral epochs of the task. Due to variable delay period length from trial to trial, and the differences in reaction time and the interest to study the timing of neural response in a millisecond resolution, 3 different raster plots were constructed for each trial. For the first raster plot, neural events were aligned to the onset of the instruction cue. Instruction cue was presented for a fixed duration of 500msec followed a variable delay period of length 1-1.5 seconds. For the next raster plot, neural signals were aligned to the onset of the go cue. This event is a timemarker for the initiation of the reaction period. Signals prior to this point can be attributed to motor preparation. And last but not the least is an event aligned to the breaking out of the fixation nosepoke. This event marks the onset of the choice period is which the subject has chosen the target memory and is executing the motor plan. Corresponding to each event, a Peri-Event

Time Histogram (PETH) is constructed and used to investigate the encoding mechanism of a single unit. Figure 4.11 illustrates such a PETH for a sample unit, aligned to the choice event.

For every single unit, trials of similar instruction cue are grouped together and for every event at each timepoint, the firing rates each group of trials were examined to determine whether the unit is selective for any of the groups. A paired Kolmogorov-Smirnov test was used at each timebin to compare the firing rates of the contralateral versus ipsilateral trials. As mentioned, the algorithm operates on each timebin independently. The timebins in Figure 4.11 where the firing rate of the unit is significantly different ($KS-test, p < 0.01$) for the contralateral versus ipsilateral trials, are shown in red and period where the firing rates are different is depicted in red asterisks. Same procedure was repeated for all units recorded across all sessions (n=334 units across n=24 sessions). In Figure 4.12a, for each unit, epochs where the unit shows a selective response for the target memorys are shown in black.

The neural response in Figure 4.12 is aligned to the onset of the instruction cue that lasts for 500 msec, and the delay period that lasts for the minimum length of 1 second. In Figure 4.12a, units are sorted to indicate the first timebin that their response is selective for a target. Figure 4.12b indicates the percentage of population at each timepoint with selective response for the target. The plot illustrates a bump at the end of instruction period and a rather constant synfire chain like activity during the delay period.

Similar to the selectivity raster plot shown in Figure 4.12, two selectivity plots are constructed where the neural responses are aligned to the onset of the go cue and the onset of the movement. These plots are shown in Figure 4.13.

As Figure 4.13d depicts, the maximum population selectivity is achieved around the time

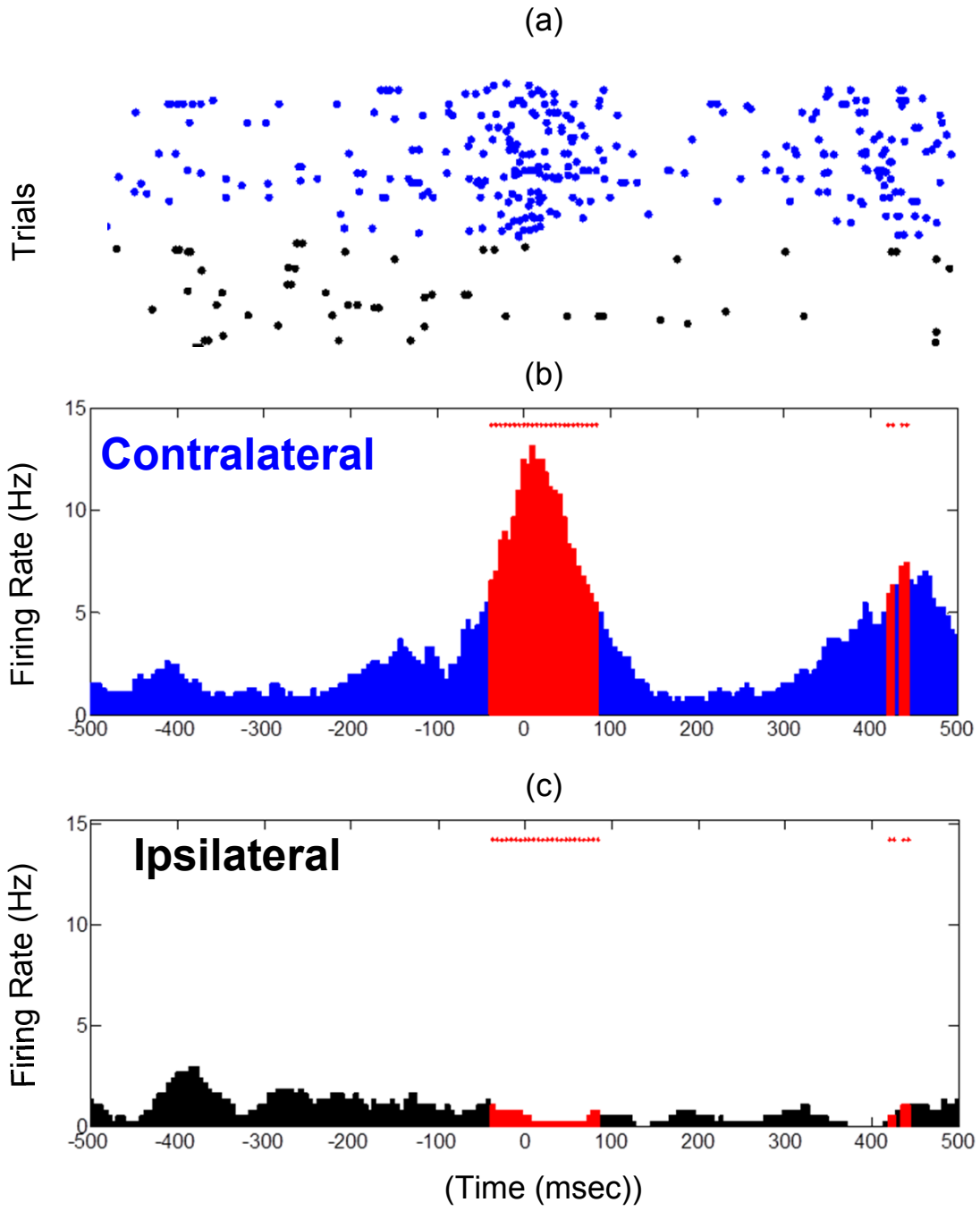

Figure 4.11: **PETH of a representative unit with contralateral prefrence**, **a)** raster plot of the spiking activity of the one cell for different trial, *blue* for the contralateral and *black* for the ipsilateral trials. **b,c)** binned PETH (overlapping windows) of the unit for both contralateral and ipsilateral trials. Bins with significant (KS-test $p < 0.01$) firing rates between the two trial conditions are shown in red.

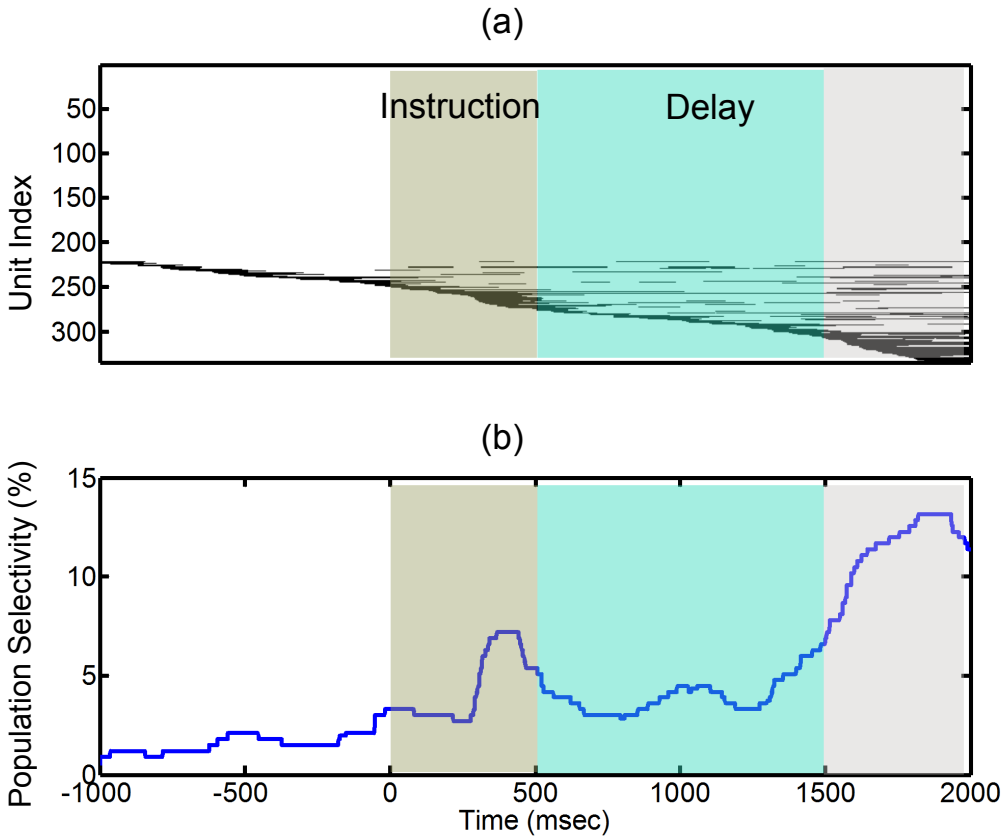

Figure 4.12: **Population selectivity during the delay period a)** Population selectivity for either of the target memorys. Units are sorted vertically based on the timing of their selectivity **b)** percentage of the units in the population with selective responses for either of the units. Shown in light brown is the instruction period between 0 and 500 msec. Shown in cyan is the delay period between 500 and 1500 msec and the shadede gray area is the variable length of the delay period.

where the subject is executing the task, i.e. the choice epoch.

4.4.3 Field Potentials

Using a complex Morlet wavelet, spectrogram was calculated for the LFPs recorded on different channels. A total of 60 wavelet were recruited for frequencies between 0.5-80 Hz in a logarithmically increasing steps. Number of cycles used for each wavelet was selected as a function of the peak frequency. Calculated spectrogram was normalized to a baseline

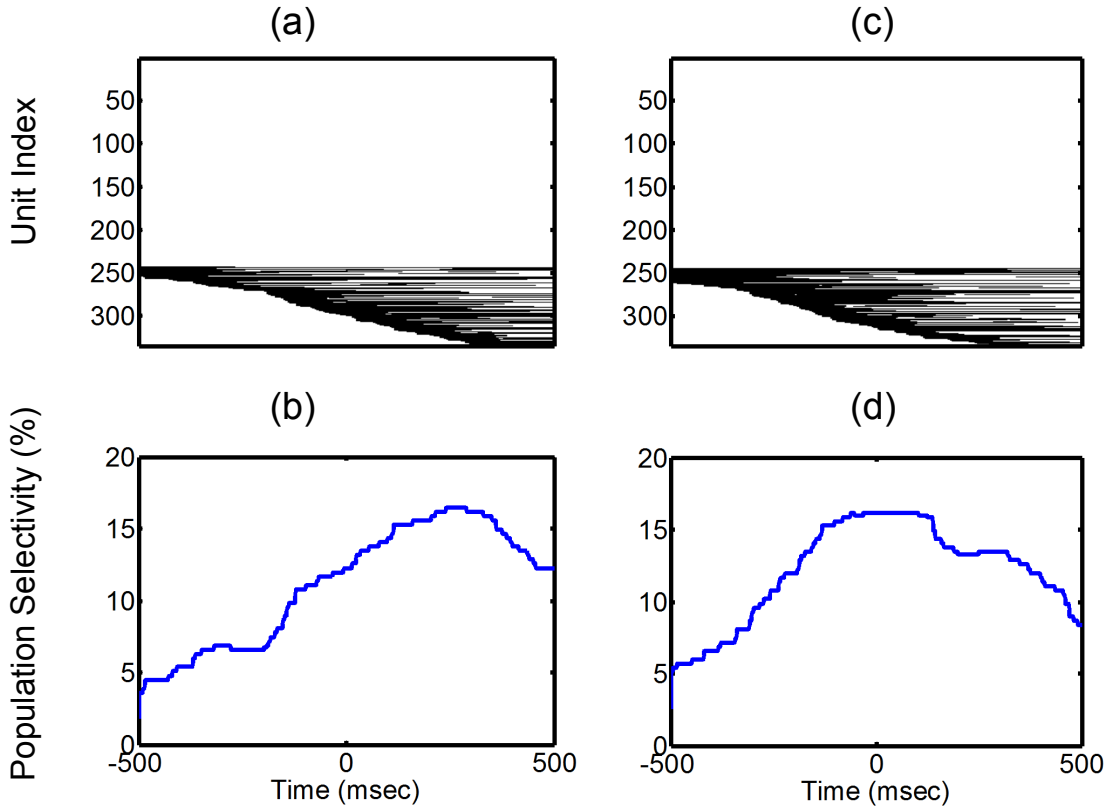

Figure 4.13: **Population selectivity during the reaction and choice epochs a,b)** individual units and percentage of the units selective for the target memory during the reaction epoch, t=0 is the onset of the go cue **c,d)** individual units and percentage of the units selective for the target memory during the choice epoch, t=0 is the moment of breaking out of the fixation beam and the start of the movement

spectrogram computed from the baseline activity recorded during the fixation period.

Shown in Figure 4.14 is the spectrogram for both the contralateral and ipsilateral trials, aligned to the onset of the instruction cue.

Figure 4.15 on the other hand illustrates an average of the spectrogram for the LFPs aligned to the movement onset.

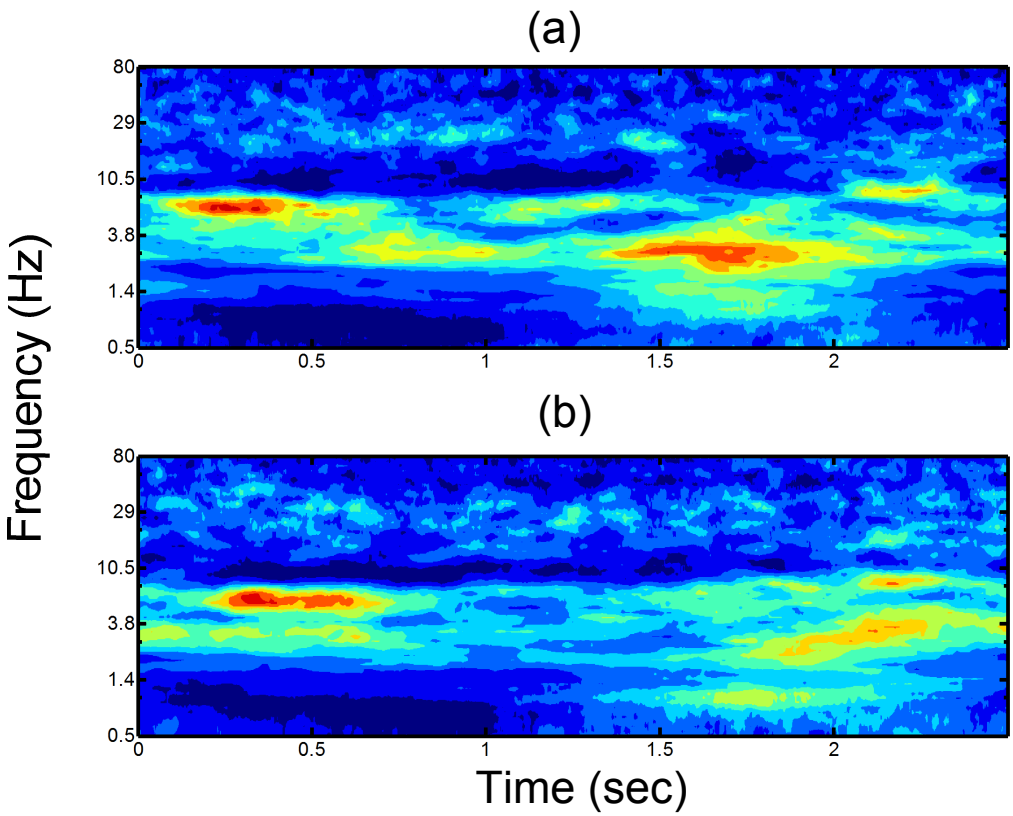

Figure 4.14: **Spectrogram during the delay period a)** for the contralateral trial and **b)** ipsilateral trials.

4.4.4 Ensemble Analysis

Decoding is a popular way of studying the mechanisms under which the neural circuits extract information in *single-trial* activity of neuronal population [202]. Information may be deciphered using different signal modalities and different signals may carry different information during different epochs of the task.

We used population spiking activity and LFPs as the input features of the classifier. Spiketrain were smoothed using causal Gaussian kernels (SD=50 msec) and spectral power density of LFPs were obtained using short-time-fourier transform and were used as input features to the classifier. Support Vector Machines (SVM) with linear kernels were recruited to perform the classification [131]. The data was divided into a train and test segments

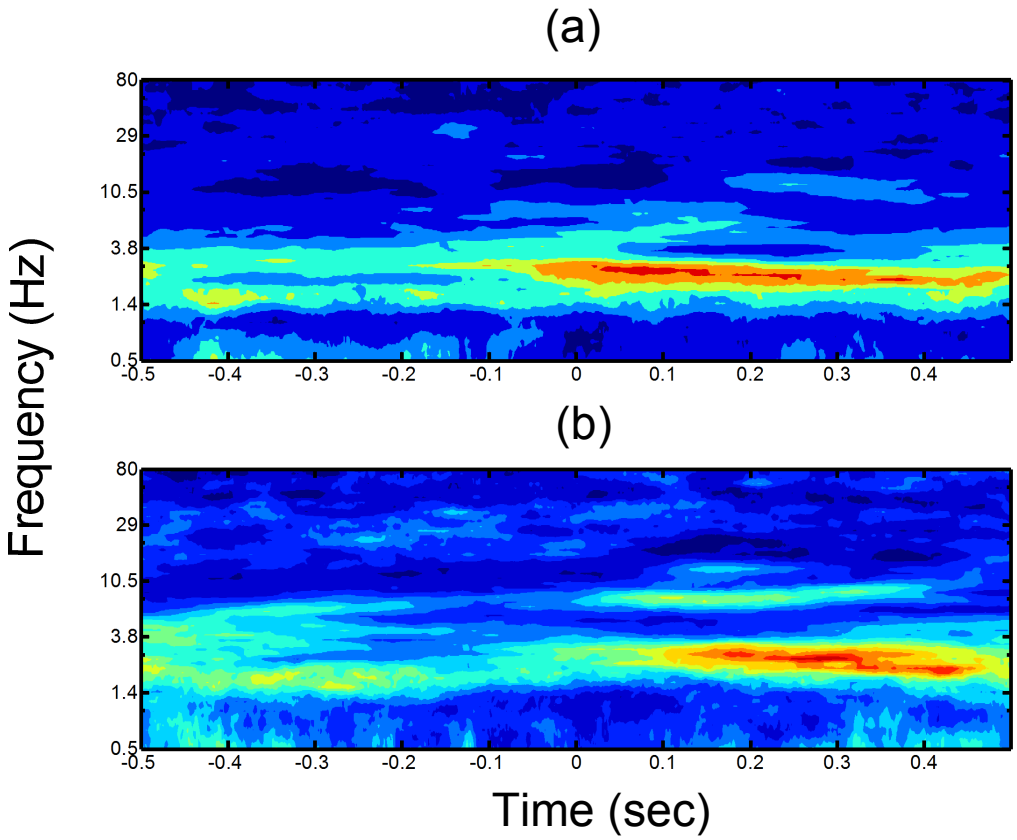

Figure 4.15: **Spectrogram during the choice epoch a** for the contralateral trial and **b)** ipsilateral trials.

(70% and 30% respectively). The train set was used to estimate the optimal coefficients of the SVM classifier. Using those coefficients, target memorys were predicted for single trials of the test set. The percentage of the correct predictions *in the test set* were considered as the accuracy of the decoding. Features were extracted for every time bin and thus the accuracy is a function of time and is a representative of the amount of information that can be extracted about the upcoming/ongoing motor decision from different modalities of the neural signals (Multiple single neurons vs. LFPs). To cross validate the decoding results, this process was repeated for 100 times and each time a different set of trials were chosen for training and test.

In Figure4.17a, the green trace shows the performance of the decoder when only features

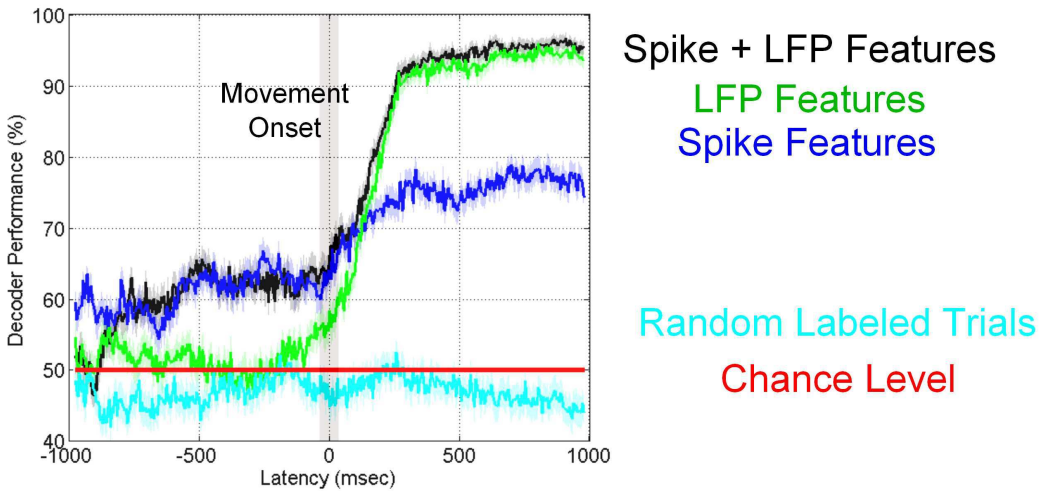

Figure 4.16: **Decoding of neural activity was performed to extract information about the encoding mechanisms of cell assemblies.** Different features of neuronal response were sequentially decoded across time using an SVM classifier. Black trace shows hybrid features of spikes and LFPs while in green and blue, only LFP and spike features were used respectively. Chance level is at 50%. To make sure that the performance of is not biased, we randomly labeled trials and run them through the decoder which as expected, resulted in chance level performance shown in cyan

from LFPs were used. The purpose of the decoder would here be to determine the target memory from the observed neural activity. Since there are only two possible targets (right and left), a random decoder would perform at 50% performance which we consider it as the chance level. As depicted in Figure4.17a, performance of the decoder using only the LFP features is not significantly different from the chance level before the start of the movement (time 0). However the performance reaches ¡90% after 200 msec from the start of the movement. This implies that LFP signal carries almost no information about the movement intention before the movement onset, but the information becomes immediately available after the action starts.

On the other hand, the blue line in Figure4.17a depicts the performance of the decoder using only population spiking activity. The performance is above chance level before the movement onset (although not by a large margin, only 60%) but after the start of the

movement the performance increases gradually to about 80%.

To benefit the most from all the available data we used hybrid features (where we combined features from both spikes and LFPs) as the input to the SVM classifiers. As expected the performance of this decoder is a combined performance of the two previously designed decoders.

As a sanity check, we randomly labeled trials used during the training of SVMs and used the derived SVM structure to classify the test set trials. Not unexpectedly the performance was not different from chance level. The performance is captured in the cyan trace of Figure4.17a.

To test the effect of bin size used to extract the features on the performance of the decoder, we performed the decoding for different bin size values ranging from 10 msec to 400 msec. The results of the maximum performance of the decoder for each bin size is shown in Figure4.17b. While the performance of the decoder is almost independent of the bin size when only LFP features are used, the performance of the spike decoder exhibits a clear bin size dependence. The performance is relatively constant for bin sizes of up to 100 msec but dramatically drops afterward. These results are not surprising due to the nature of these signals. According to temporal encoding theory of the neurons [66], information about external stimuli and internal states are encoded via precise spike timing, while the LFP signal is naturally a very slowly changing signal. According to these results we used time bin of 50 msec throughout this study unless stated otherwise.

Another issue is the number of channels used for decoding. Figure4.17c shows the maximum performance for each decoder when different the features were extracted from different number of channels. What can be immediately inferred from these results is the linear increase of the spike decoder performance with the number of channels used, while the LFP

decoder performance curve reaches a plateau soon. This can be seen in accordance with the previously developed theories on the role of cell assemblies in working memory [74, 78, 221].

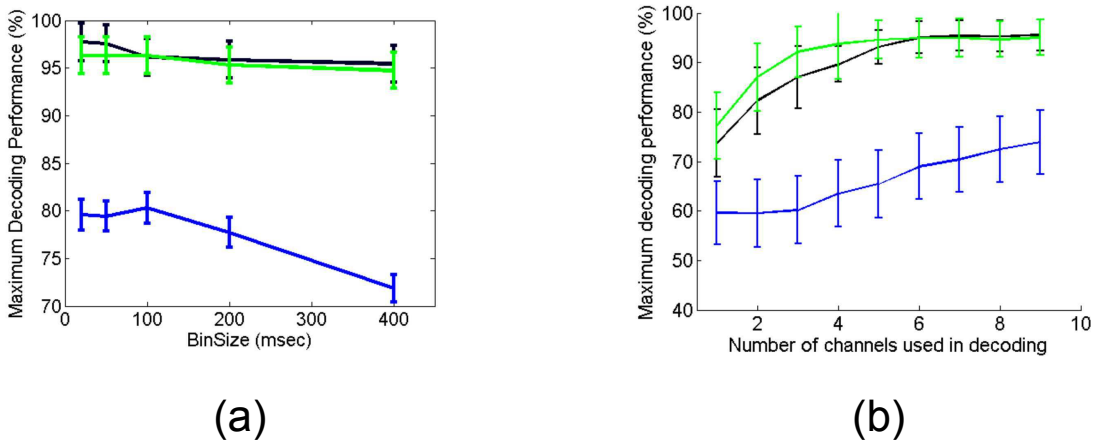

Figure 4.17: **Effect of binsize and channel count on decoding performance(a)** Dependence of the decoder performance on the bin size used to extract hybrid (black), LFP (green) and spike (blue) features. **(b)** Performance of the decoder increases with incorporating features from more channels

4.5 Optogenetic Inactivation

Using reversible inactivation, I have shown that knocking out the prefrontal cortex will affect the performance of the subject in a graded lateralized fashion. In other words, injection of the muscimol will cause a negative bias towards the contralateral trials (contralateral with respect to the injection site). This differential effect was shown to be a function of the amount of the drug delivered to the tissue, the more drug infused into the tissue the bolder the effect. Problem with the muscimol reversible inactivation is the very poor temporal resolution of the induced inactivation. Once injected, the drug will induce inactivation that will last up to 24 hours.

Introduction of optogenetics toolbox, enables fast millisecond precision control over the activity of trasfected cells. Here I used this technique to deliver and express ArchT, a proton

pump, in the membrane of excitatory pyramidal cells of the prefrontal cortex expressing CamKIIα.

4.5.1 Histology

To ensure that the expression of the ArchT in the tissue, post-mortem histology was performed. The channel was tagged with GFP that fluoresce green, when exposed to light in the blue to ultraviolet range. Brain tissue was perfused, explanted and 50μmcoronal sections were collected using a vibratome. Figure 4.18 illustrates a sample of the sections with ArchT expression in the prelimbic area. Subjects with poor expression of the channel were excluded from further analysis.

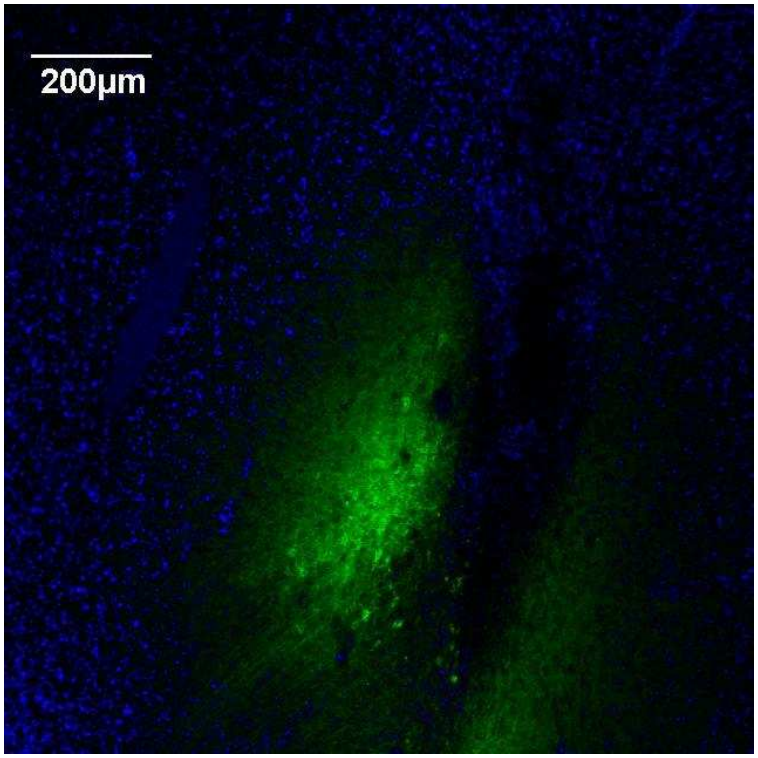

Figure 4.18: **Histological evaluation of ArchT expression**, a fluorescent image of a slice of brain infected with AAV-CaMKII-ArchT-GFP, a 50 μm coronal section at approximately +3mm from bregma. The transfection site is fluorescing in green.

4.5.2 Total suppression effect

Optogenetic constructs carrying the microbial channel ArchT provided by Ed Boyden at MIT, was delivered to the tissue packaged in an Adeno-Associated Virus in UNC vector core. The virus was injected unilaterally using a micropipette and $1.2\mu L$ of the virus was injected. Fiber optics were implanted chronically in the same tranfected area. Green laser system was used to deliver a green (520 nm) light of 120 mW/mm^2 power at the fiber tip. Figure 4.19 shows the behavioral performance obtained the optogenetic inhibition effect.

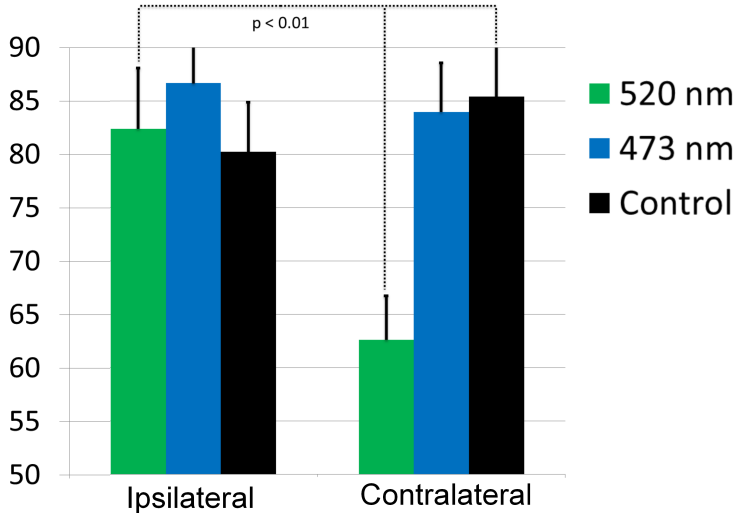

Figure 4.19: **Behavioral effects of optogenetic inhibition**, only trials with a target memory on the contralateral site with respect to inhibition using the green laser were affected by the optical inhibition.

Results depicted in Figure 4.19, illustrate a significant $(KS-test, p < 0.01)$ lateralized decrease in behavioral performance. Similar to results obtained for the reversible inactivation study, these results here show a negative bias towards the choice of the contralateral target. Two types of control experiments were performed. During the first experiment, the light was turned off during a subset of trials. No significant drop in the performance was observed for either type of the trials: neither ipsilateral nor contralateral. The second control, was designed to study whether the light has an effect on the choice of the subject or it is in fact

the suppression of the activity induced by the proton pump that is causing a bias in behavior. To this end, a blue laser ($473nm$) was used instead of the green laser. The wavelength of the blue laser is not supposed to activate the ArchT channels and thus is supposed not to have any neural activity suppression effect. Not to our surprise, the blue light showed no effect on the performance of the subject.

Chapter 5

Discussion

Memories can be distorted. They're just an interpretation, they're not a record, and they're irrelevant if you have the facts.

— Leonard Shelby, *Memento*

Amid the corpus of research conducted on the anatomy and physiology of prefrontal cortex, the functional significance of this part of the neocortex has remained the subject of debate. Since the early findings of Jacobsen in 1940s [135, 136], different functions in human and animal subjects have been linked to the prefrontal cortex. These function include and is not limited to motor planning and control, short-term memory, attention, response inhibition, decision making, strategy set shifting etc [95, 219]. In this dissertation I explored the role of rat medial prefrontal cortex in *action selection*.

The vast repertoire of human motion and dexterous control over movement is all executed through some 650 skeletal muscles, all of which are under the control of the central nervous system. Arguably, motor processing starts with an internal representation[1]: a desire to move and a motor goal. Following Schall [210], here I distinguish between *decisions* and *goals*. In this framework, decisions are perceptions based on sensory evidences, but goals are the locations or objects that the subject chooses as a target for their *action*. The motor system is believed to be organized in a functional hierarchy [112, 137, 203, 249]. The highest

[1]These internal representations however are not fixed and need to be continuously updated via the incoming sensory input and the efference copy of the motor commands to maintain accurate movement.

and most abstract level, which is affiliated with prefrontal cortex, is supposedly dealing with the *purpose of a movement*. This is shown in a schematic by Haggard in Figure 5.1.

As illustrated in Figure 5.1, primary motor cortex (M1) which is considered to be the final cortical stage of motor control, receives two sets of input. One key group is reaching M1 through supplementary motor area (SMA), prefrontal cortex (PFC) and the Basal Ganglia (BG). The second network is gathering information from posterior lobe of the cortex which is mainly dedicated to sensory processing. The frontal cortical network is believed to play a critical role in motor goal initiation and maintenance. This network is considered the highest level in motor control. The next level is concerned with forming a movement plan and has anatomically been mapped to the posterior parietal and premotor cortices [112]. As shown in the schematic, premotor cortex forms the details of the movement plan based on the sensory information it receives from the sensory areas of the cortex. And the lowest level of the hierarchy coordinates spatiotemporal details related to muscle contraction which is required to execute the already planned movement.

The sixty-four-thousand dollar question here is how the sensorimotor mappings generate a movement to a desired location. Though the detailed mechanism of such sensorimotor integration remains largely unknown, one can speculate on a few required steps. For starters, the target location has to be identified and localized with respect to the body's coordinate system, aka an *egocentric* coordiante. Then the current configuration of the arms and the corresponding muscles should be determined to enable a detailed plan for muscle recruitment to be established. Thus through a series of sensory inputs, required information is collected and transformed into detailed plans of muscle recruitment.

In the presence of a barrage of incoming sensory information which may carry different information supporting conflicting choices, an *executive system*, gates irrelevant information

and supports expression of appropriate actions. A working hypothesis that has increasingly received empirical support through the past decade is that prefrontal cortex as the major player in cognitive control process, provides a mechanism for active maintenance of goals and means to achieve them in the form of persistence activity [160]. It is through this biasing influence of the prefrontal cortex that its role in input and output gating of sensory inputs and motor commands can be studied [46]. As I will describe later, attention and response selection are alternative terms for input and output gating.

The motivation behind this dissertation is to better understand the role of prefrontal cortex in sensorimotor integration. For practical and ethical reasons I have selected rats as my animal model, despite the fact that non-human primates' brain is evolutionarily closer to human brain. There has always been disputes between two groups of scientists on the anatomical and functional similarities and differences of rodent and human prefrontal cortex [62,140,173,194,213,227]. Being aware of these discussions, in my working hypothesis I chose the rat medial prefrontal cortex (mPFC) as an analogue to primate dorsolateral prefrontal cortex (dlPFC) and adopted a delayed choice task to test the sensorimotor procedure.

One major advantage of this design compared to a bulk of previous experimental setups used for PFC working memory investigation in rodents is the precise temporal control capability between different epochs of the task. A typical rodent working memory task involves some sort of maze like a T-maze, where a cue is presented in the central arm of the maze and the subject has to select either of the two arms based on the instructed cue. The lapse of the time between the instruction cue and the moment of turning towards the periphery arms where the subjects is running along the central arm of the maze is often considered as the motor planning or working memory period. However the main drawback of these designs is the poor temporal control over the behavioral events of the task which

in turn leads to smearing the temporal accuracy of the inferred results. In order to overcome these limitations, I adopted an operant conditioning task used previously to study the neural dynamics in the Basal Ganglia and premotor cortex as well as the study of attention mechanisms [21, 34, 83, 99, 211].

5.1 Working memory

By definition, *working memory* is an alternative memory system proposed by Alan Baddeley to account for some of the shortcomings of the Atkinson and Shiffrin's *short-term memory* model [12, 14, 16]. Although the model has changed dramatically over the years since it was first introduced almost 40 years ago, still it is valid model capable of answering a corpus of observed phenomenon [17]. The model is basically describing how human brain is capable of actively maintaining and manipulating a limited number of memory pieces, to be used later in order to guide a future act. Research in this field has identified a crucial role for a number of brain regions in working memory including the prefrontal cortex, parietal cortex, anterior cingulate cortex and specific nuclei of the basal ganglia. Most of this information is obtained through neuroimaging studies in human and detailed cellular knowledge of working memory mechanism has remained unknown.

Albeit the underlying mechanism is unclear and disputable, there is sort of a consensus that the prefrontal cortex (on top of other putative roles), is capable of and crucial for 'temporal bridging' between the sensory information and motor actions. This has been denoted from very early lesioning experiments and subsequent experiments reproducing the results supporting this hypothesis [95, 136, 219]. By this account, prefrontal cortex is responsible for maintaining some memory of information required to accomplish the task. This leads to the

idea of 'memory cells', showing sustained activity during the delay period. So far, two major models for maintaining a memory without an external cue in a neuronal network has been suggested [78]: recurrent excitation within cell assemblies and synfire chains, although many different models for working memory encoding have been proposed since the introduction of these two important model [23, 24, 117, 148, 149, 221, 245].

The recurrent excitation idea underlies the classical Hopfield neural network model, suggested as a mechanism for storing discrete memory items [126]. In the Hopfield model, memory items are stored in the synaptic weight matrix of a network. In this model, neurons that cooperatively encode the same pattern have higher inter-connectivity weight, forming a cell assembly, whereas neurons that are representing different items have weaker reciprocal weights (or have inhibitory connections). The weights are often calibrated through a Hebbian like learning scheme [119] that reinforces connections between two coactive neurons given the thumb rule of *'neurons that fire together, wire together'*. Adaptation of this model to describe working memory was mainly accomplished through the works of Xiao-Jing Wang and through collaborations with Patricia Goldman-Rakic and was based on the delayed task data collected from non-human primate dlPFC [55, 201, 223, 233]. One problem with such a recurrent excitatory network is instability, meaning that excitation of a portion of the network will consequently lead to more excitation which in turn drives the whole system into an unstable state. It was suggested that such instability would not occur if excitation is sufficiently slow, compared to the negative feedback, since recurrent synapses are mediated through NMDA receptors with a slow time constant of 50-100 msec.

On the other hand, an alternative method to sustain the activity within a local network in the absence of external sensory cue is a synfire chain [1,2,70], suggested by Moshe Abeles. A synfire chain is *'essentially a feed-forward network of neurons with many layers (or pools)'* [3].

A neuron in each pool receives many excitatory feeds from the previous pool and also feeds onto the a number of next pool neurons. Thus the activity is maintained throughout the ensemble in a cascade like form where a volley of spikes propagates from one pool to another.

The results I have obtained so far from the analysis of single units' activity during the delay period support the later model. As shown in Figure 4.12(a), unlike the activity of memory cells recorded from primate dlPFC(two samples of which already shown in Figures 2.5 and 2.6), units recorded from the rat mPFC (specifically layer V prelimbic cortex) do not show sustained activity throughout the delay period. On the other hand, these units become selective for one aspect of the task for a short 'lifetime'. However, as depicted in the graph, this lifetime starts at different latencies with respect to the initiation of the delay period for different cells. Similar to an Olympic torch, the responsibility of maintaining a representation required to accomplish the task is relayed from one group of cells to another. This observation is more suggesting a synfire chain like mechanism for working memory representation in the rat prelimbic cortex. The observation is also consistent with predictions of Izhikevich's polychronous model for working memory [221].

Persistent activity of prefrontal cells, has been shown to be correlated with a number of task-relevant information such as a previously presented cue, a forthcoming response or a particular contingency between the cue and response [32, 94, 97, 195, 199, 232]. An important question regarding the memory function of the prefrontal cortex is whether this memory is *prospective* or *retrospective*. Prospective memory is where the content of the represented memory is about something that is to happen in future, whereas retrospective memory is about past events. In other words retrospective memory is all about a recollection or maintaining a past episode where prospective memory is about **'remembering to remember'**, or like remembering an intended action in future.

Specifics of the experimental design in the delayed choice task I used throughout this experiment provides a good test bed to investigate the type of memory encoding in the prelimbic cortex. In a regular center out saccade task which is common among the non-human primate studies (such as the one used for By Goldman-Rakic [94]), a peripheral target on a circle is shown to the subject. The subject is required to fixate on the center of the circle until a go cue is presented and then move their gaze to the target in order to receive the reward. A similar rodent version is a delayed alternation task [127]. In this task the subject has the option to select between either of the two locations in a maze to receive a reward and is required to alternate between the options, i.e. visiting a previously visited target would not obtain a reward. In both of these tasks, the sensory cue driving the action is the same as the spatial location of the target, which makes decoding the content of the encoded memory tricky.

In our experimental design however, the sensory cues and appropriate action are completely unrelated. In other words, there is no natural or *ecologically valid* association between the sensory cues and the action goals(motor targets). The two auditory cues corresponding to two motor targets are selected arbitrarily by the experimenter. Although this choice of cue-action association is cognitively more costly and would elongate the learning period, but it serves the purpose of distinguishing the identity of the encoded memory by the prefrontal cortex cells.

The inactivation studies performed through the application of GABA agonist *muscimol* or the proton pump *archaerhodopsin* (ArchT), cast light on the encoding mechanism of memory in the prelimbic cortex. I start with describing the reversible inactivation results. Muscimol is a GABA_A agonist commonly used for reversible inactivation of a small volume of brain tissue through increasing inactivation. Certain amounts of muscimol were injected

unilaterally in the prelimbic cortex via chronically implanted cannulae, while the subjects were lightly anesthetized. After a recovery period of typically about an hour, the subjects were put in their training cage. As shown in Figure 4.8, the performance of the subjects significantly dropped under the injection effect and only for those trials where the cue was instructing towards a target on the contralateral side with respect to the injected brain hemisphere. The key to answer the question regarding the encoded memory represented in the prefrontal cortex is the lateralized suppression of performance. Lateralization is a well-known phenomenon in the nervous system. Especially in the motor system, a corpus of stimulation and inactivation studies have supported the dominant modulatory role of one brain hemisphere on the contralateral limbs [137]. Same is true for the visual system where the visual information coming from one eye changes crisscross at the optic chiasm and finally ends up being processed by the contralateral brain hemisphere. However, processing of single tone frequencies is not lateralized in the cortex. Both hemispheres have auditory cortices dedicated to processing a range of frequency and to my knowledge no evidence of frequency specific dominance in one hemisphere has been reported. Following that line of reasoning, had the prefrontal cortex been involved in retrospective encoding, we would have expected to observe either **a)** a drop in performance of both types of trials following a unilateral injection or **b)** no change in performance of either type of trials. The latter could possibly be due to one hemisphere compensating for the temporarily inactivated one and the former could have happened because of the decline in memory capacity due to inactivation of one hemisphere. However, only in trials where the target contralateral to the injection side was instructed were impaired. Thus I speculate that the memory encoding in the prelimbic circuit is a prospective one, maintaining information regarding the location of the future action. This may be interpreted as biasing effect of prefrontal cortex over the motor actions [159].

Different action plans are competing for expression and only those who receive stronger support from the executive control unit will get expressed. It is one hypothesized role of the prefrontal cortex to provide this bias signal for the motor actions, collecting continuous sensory evidence from the environment, comparing those with expectations and past motor history and finally providing this bias signal for different actions and thus enforcing a *top-down control* over the behavior. Injecting muscimol causes a temporary inactivation of the affected tissue and thus the action which is supposed to receive a support signal (which in this case is 'moving towards the contralateral side of the injection') will be dampened. Consequently the other competing action, will receive a stronger support and the subject's movement will become biased towards the ipsilateral side. This bias is then quantified as the ipsi-contra differential performance and calculated for different scenarios of the experiment.

Shown in Figure 4.9 is the dosage curve showing the biasing effect of the muscimol application as the function of the amount injected. The more volume injected, the stronger the bias effect until a point where almost all responses on the contralateral side to the injection side were suppressed and the subject is totally biased towards the ipsilateral targets.

Prelimbic cortex is a relatively big brain region. Following Paxinos and Watson's measurement of the prelimbic cortex [187], it extends in the anterior-posterior direction from +2.5-5mm (AP), 0-1.5mm in the mediolateral (ML) and 2-4mm in the dorsoventral (DV) direction. Different methods have been suggested to indirectly quantify the spatial extent of muscimol effect such as glucose uptake [154], evoked field potentials [242], multi-unit activity levels [11, 79] and finally a more direct method of using fluorescent muscimol [9]. As a rule of thumb, $1\mu L$ of injection will spread into about 1mm of the tissue[2].

[2]However this does not indicate the level of inactivation in the tissue with respect to the injection site

One possible explanation for the volume dependent differential bias effect is that as more muscimol volume is injected in the tissue larger prelimbic regions will get suppressed and thus the differential effect will grow as a function of the volume muscimol injected.

Results of the optogenetic suppression of the activity also support the findings of muscimol inactivation. Subsets of trials were selected and green light was delivered intracortically to the transfected tissue to suppress the prefrontal activity during the trial. Rest of the trials did not receive any light or the blue light with an spectrum far from the excitation wavelength of the ArchT channels was delivered. In consistence with the above mentioned results performance of the subject was affected only during those trials where suppression has occurred on the contralateral prefrontal cortex. This further supports our argument that the content of the memory encoded by the prefrontal cortex is motor related, rather than a mere sensory memorandem.

5.2 A 4-Hz oscillation

Spectral analysis of the local field potential signal throughout the task, shows a modulation in low frequency ($\approx 4Hz$) during the choice epoch of the task as illustrated in Figure 4.15. The role of neural oscillations in information processing is not yet fully clear [40, 43, 235]. However, there is a consensus on that oscillations represent a brain mechanism for sculpting temporal coordination of neural activity among different brain networks [230, 234]. Inter-areal communication between different brain regions are believed to be coordinated through synchronous activity of a population of cells that gives rise to coherent neural oscillations. Lower frequency oscillation (4-8 Hz) conventionally known as *theta* has been well studied in the hyppocampus during spatial exploration and navigation [29, 38, 228]. It is hypothesized

that theta oscillation in hippocampus is a mechanism of forming and retrieval of spatial information by the so called pyramidal *place cells*. Theta oscillation has also been observed in human neocortex during working memory task [157, 197].

A recent study of Fujisawa and Buzsaki [93], studied the role of 4-Hz oscillation in prefrontal cortex, hippocampus and ventral tegmental area (VTA) in rodents during a working memory maze navigation task. Results of the study showed that the neuronal activity in three regions is coordinated via a 4-Hz oscillation. It was also observed that goal-predicting cells in both PFC and hyppocampus are phase-locked to the oscillation. These results suggested 4-Hz oscillation as a means of retrieving spatial memory.

The observation of target selective modulation of 4-Hz oscillation throughout the trial, is in accordance with the results reported by Buzsaki et al. and suggests that the role of oscillation in retrieving spatial memories and exploiting on the motor memories of goal-achieving motor actions.

5.3 Possible role of prefrontal cortex in action selection

I talked earlier on the conflict between two important roles of the prefrontal circuit, one is to provide a flexible online mechanism for updating the goals in presence of continuously changing environment and the other being robustly maintaining the same goals. One possible solution to this conflict is the idea of working memory *gating* [35, 57, 91]. Such 'input' and 'output' gating of the working memory are hypothesized to be relying on the corticostriatal loops [46]. This new hypothesis speculates that similar to the input gating mechanism (also denoted as *attention*) where only task relevant sensory information are gated in the working memory pool, there should exist an output gating mechanism that selectively chooses

the top-down control of the prefrontal cortex on behavior. When the gate is closed, the working memory content will be maintained but would not have the top-down influence on the actions [54, 124, 130].

Prefrontal cortex is reciprocally connected to the basal ganglia through its input structure, striatum. Patterns of that connectivity is illustrated in the schematic of Figure 5.2.

A major principle of the cortico-basal ganglia relations is the parallel organization of the connections from prefrontal cortex to basal ganglia to thalamus and back to prefrontal cortex [104] (Figure 5.3 for detailed pathways). As depicted in Figure 5.2 , the striatal projections from cytoarchitecturally and functionally distinct prefrontal cortical areas are distributed in a somatotopical fashion along the entire longitudinal axis of the striatum. The medial prefrontal areas project to the ventral and medial parts of the nucleus accumbens, the so called 'shell' region, and to the medial parts of the caudate-putamen complex. These projections concentrate in the most rostral part of the striatum and diminish caudally. Thus a ventral-to-dorsal axis in the medial prefrontal cortex corresponds to a ventromedial-to-dorsolateral axis in the striatum. The information derived from distinct prefrontal cortical fields will remain fairly segregated in the striatum.

There is a recurrent idea in the literature that one main role of the basal ganglia is action selection [56, 69, 81, 200]. The 'action selection' becomes an issue whenever two or more competing actions are competing for limited motor resources [3]. In this framework different action compete for expression and the one that receive more higher level support will get expressed and the rest will get suppressed. This model is often called a 'winner-take-all' mechanism where only one out of many different actions will get implemented. Basal ganglia has been shown to provide suppression of the prepotent but inappropriate actions

[3]'Decision making' is also synonymous to action selection in this context.

during the 'choice' epoch of a task [99].

Recent models of the basal ganglia take advantage of the great deal of inhibitory connections in the basal ganglia to explain action selection [161]. Stewart and Eliasmith proposed a model for such action selection in basal ganglia [81, 218]. The underlying assumption is that action selection is context-dependent, meaning that different actions do not have inherent priority over others, but the context of the task attributes different utilities to different actions. Then the task of the basal ganglia is to incorporate the utility value and suppress the low-utility actions. A toy example of the proposed model is shown in Figure 5.4.

In this model, there are three different action that have different 'utility' or 'desirability', 0.3, 0.8 and 0.5. The model's task would be to choose one of them. Since the output from basal ganglia is inhibitory, the desired action should produce a near zero output that would consequently lead to suppression of all the other actions but the one with the highest utility. The model shows both direct and indirect pathways. As shown, the one action with highest utility will produce a zero output. It is evident that the proposed model is functional only and only if the input utilities provided through cortex are valid. If the value of utilities are close to each other or zero, the circuit will not function. One speculation of this dissertation is the role of prefrontal cortex in maintaining robust and distinguishable representation of the action values associated with prepotent actions in the context of the sensory input.

Gage et al. used a very similar experimental design to my experiment and recorded multiple unit activities from multiple brain regions specifically fast spiking inhibitory (FSI) striatal cells [99]. They reported a fast increase in selective recruitment of FSI cells during the choice epoch. It was thus suggested that the FSI cells in sensorimotor striatum are involved in the process of suppressing the prepotent but inappropriate action. The data presented here constitute an empirical evidence to the long-debated problem of action selection and

suppression in basal ganglia at a cellular level.

Whatever the input to the basal ganglia, setting the values for the actions remain unknown. In the data shown in Figure 4.12, it is shown that the majority of prefrontal cells are selective slightly prior and during the choice epoch. In fact peak of population selectivity (17%) occurs at the moment of action selection, aka 'the point of no return' [175]. The timing of this functional population selectivity, patterns of reciprocal connectivity between the prefrontal cortex and basal ganglia and the evidence of striatal selectivity during the choice epoch prompts me to suggest that the prefrontal cortex provides a robust representation of the action goals to downstream structures.

This suggestion is in accordance with the hypothesis about the cortical-basal ganglio-thalamic loop. In this model, cortex provides, stores and manipulates representations, basal ganglia maps brain states into courses of action and the thalamus performs real-time monitoring of body state and applies routing signals to cortical pathways [81].

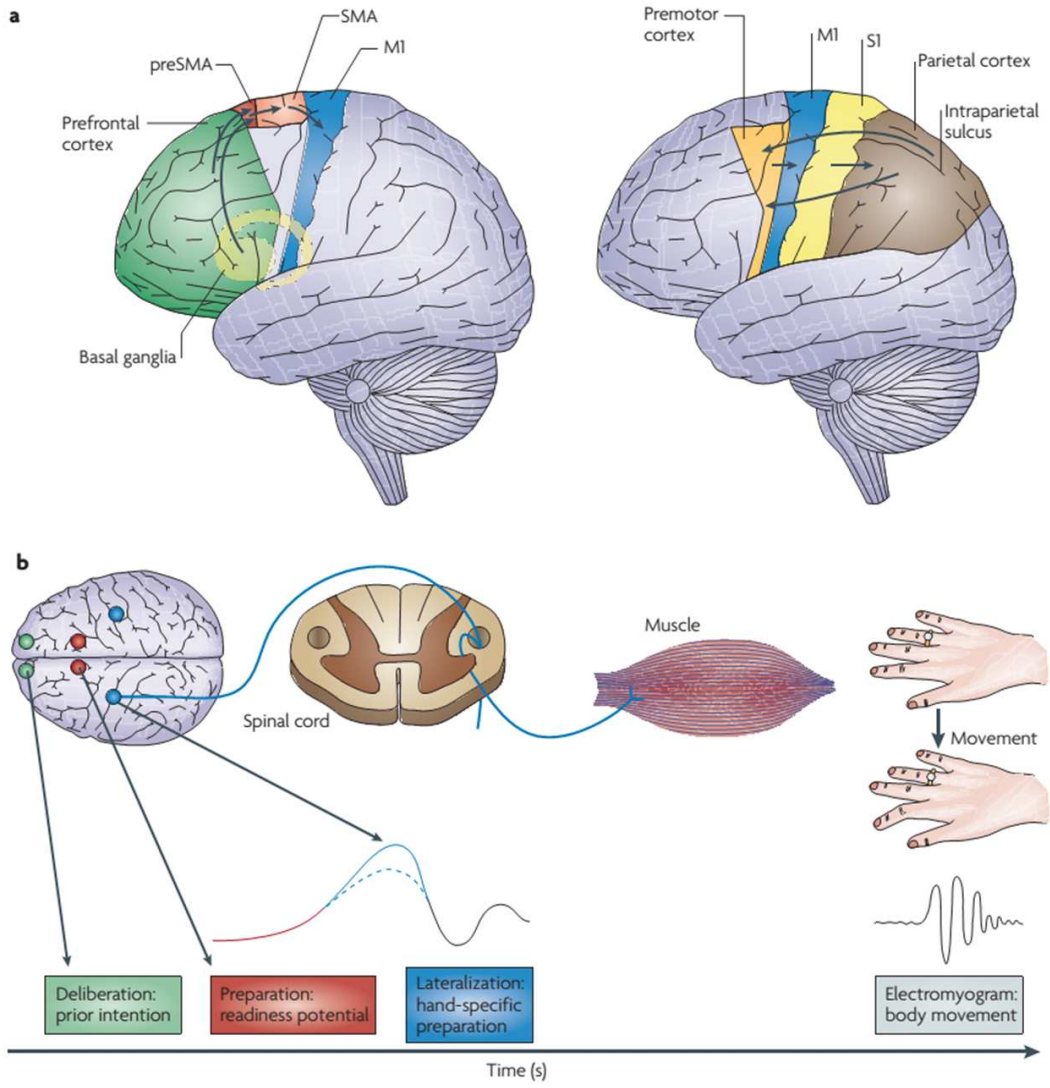

Figure 5.1: **Brain circuits involved in voluntary action**, **a)** Primary motor cortex receives two sets of inputs. The first is routed through the SMA area which itself receives inputs from the prefrontal cortex and the basal ganglia and the other loop relays sensory information through primary sensory cortex, parietal cortex and the premotor cortex **b)** brain activity recorded in different brain regions preceding a movement in the right hand. Adapted from [112]

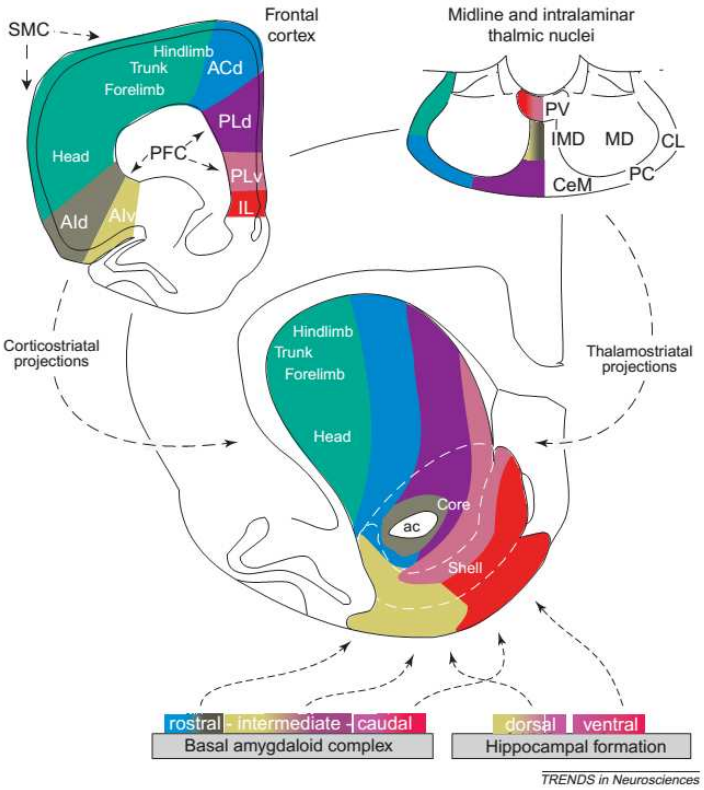

Figure 5.2: **Cortical and thalamic inputs to the striatum** distributed in dorsomedial to ventrolateral regions. Note that the topographical organization in the corticostriatal projections is the leading organizational principle. Adapted from [231]

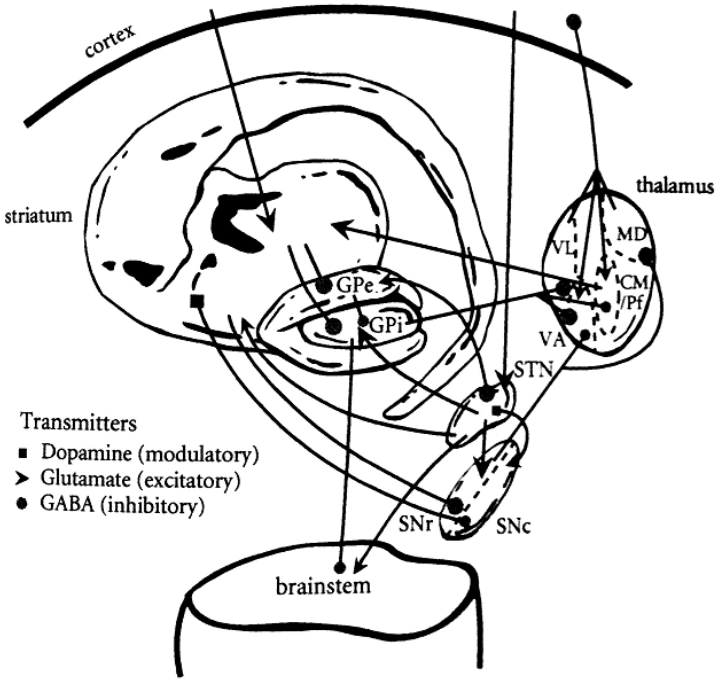

Figure 5.3: **Corticostriatal thalamic loop**, illustrating the direct and indirect pathways. Adapted from [81]

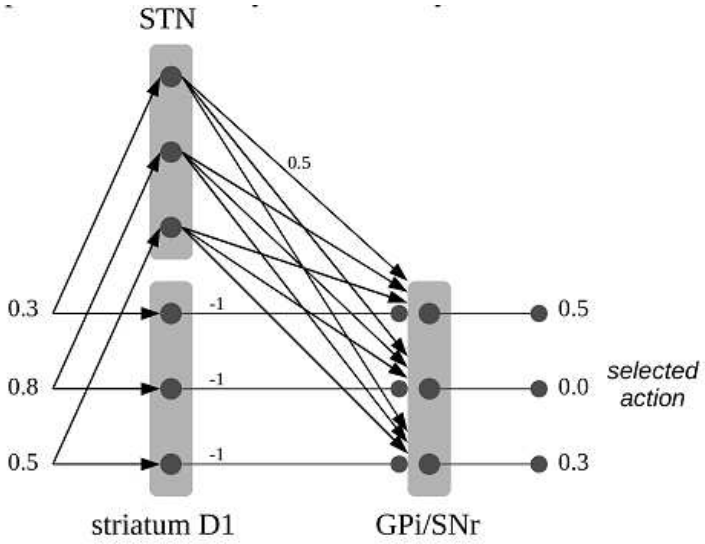

Figure 5.4: **Model for action selection via striatal D1 cells and the subthalamic nucleus**, cortical input provides utility values for the actions which in turn leads to the basal ganglia to release inhibition on the action with highest value, suppressing the rest. Adapted from [218]

Chapter 6

Concluding Remarks

Plato's point is that we can never have true knowledge of anything that is in a constant state of change. We can only have ***opinions****.*
— Jostein Gaarder*, Sophie's World*

Initiating a movement goal and maintaining that goal throughout the planning and execution of a goal-directed action is an essential element of all goal-directed behavior. Prefrontal cortex has been implicated in the neural mechanisms underlying goal initiation and maintenance. Patients with frontal lobe damage have been reported to suffer from 'wandering off the tasks'. The neural code for goal initiation and maintenance should be robust against potential distracting cues and the continuous barrage of sensory information that could hinder the organism from fully executing the task.

In the context of brain-machine interfaces (BMIs) aimed at restoring motor function to motor impaired subjects, decoders aim to translate an ongoing pattern of neural activity into control signals to actuate artificial - or natural, non functioning- limbs. However, decoding has been primarily restricted to moment-by-moment kinematic variables of an intended movement from premotor or motor cortical neurons without knowledge of the goals. These conventional decoders suffer from a number of drawbacks such as the continuous need for subjects attention and slowness. It is important to determine the latency of movement initiation to inform decoders of neural activity. On the other hand, advances in robotics have

enabled very fast dexterous control of artificial limbs given a motor goal. Insights from this study can be utilized in the design of next generation BMIs driven by decoding a cognitive signal (representing motor intent) rather than moment-by-moment kinematics of a motor task.

In this thesis, I have adopted an instructed delayed response task to study the neural mechanism of motor goal initiation and maintenance in the prelimbic circuit of the rat medial prefrontal cortex (mPFC). While the tuning characteristics of cortical neurons in early sensory and late motor areas can be revealed by classical linear and nonlinear regression analysis, the mixed selectivity of PFC neurons requires new machine learning algorithms that can unveil their heterogeneous responses characteristics. Thus I have applied state-of-the-art machine learning algorithms to the analysis of the mPFC neurons activity collected using chronically implanted microelectrode arrays.

As shown and discussed earlier, lateralized inactivation of the prelimbic cortex using muscimol results in lateralized deficit in the subject's responses. These results strongly support my hypothesis that this area of the brain contributes to the execution of the delayed choice task. However there are a number of limitation to this approach, some of which were described earlier. First is the unknown extent of brain inactivation using reversible inactivation. Even, the recently suggested application of fluorescent muscimol, only shows the extent of drug diffusion and would not help determining the spatial spread of inactivation. Second is the poor temporal resolution of the inactivation using muscimol. The effects may last up to hours after the injection (at variable degrees). Ideally to dissect the fine engagement of brain circuits in action selection, we need to be able to suppress the activity with a temporal precision not slower than ten millisecond which obviously in orders of magnitude faster of the muscimol response.

In this dissertation, I have shown the feasibility of using optogenetic techniques to suppress the activity of prefrontal cells using brief flashes of green light to the extent that a behavioral effects is obtained in awake behaving subjects (results shown in Figure 4.19). I have shown that the effect is dependent on the activation of light-activated proton pumps since now effect was observed under the blue laser trials. The lateralized deficit was observed while the light pulse was flashed throughout the trial, from the onset of the fixation period until hitting the target.

Although I have collected some pilot data for an experiment where the optogenetic suppression of activity was limited to individual epochs of the task, this experiment is beyond the scopes of this dissertation. In this experiment during each session, a subset of trials were selected and light was flashed during a given epoch, as illustrated in Figure . Preliminary data (shown in the appendix) replicates the previous results regarding the differential lateralized deficit when the light was flashed throughout the trial and no effect under the control trials.

The data also suggests a lateralized deficit during trials where the light was flashed through the delay and choice epochs, however this is part of an ongoing collaborative project and it is premature at this stage to draw any conclusions before running enough controls and collecting enough data from sufficient number of subjects to compensate for across subjects variability. Results of this experiment may establish a temporally precise causal link between the activity in the prefrontal cortex and the performance of the delayed choice task and may be informative in the long-debated causality vs. correlation debate of neuronal responses.

Another extension to this study would be to simultaneously record from multiple brain regions supposedly involved in this task and compare and contrast the response properties of different units. Throughout the conduct of this project I intended to collect some prelim-

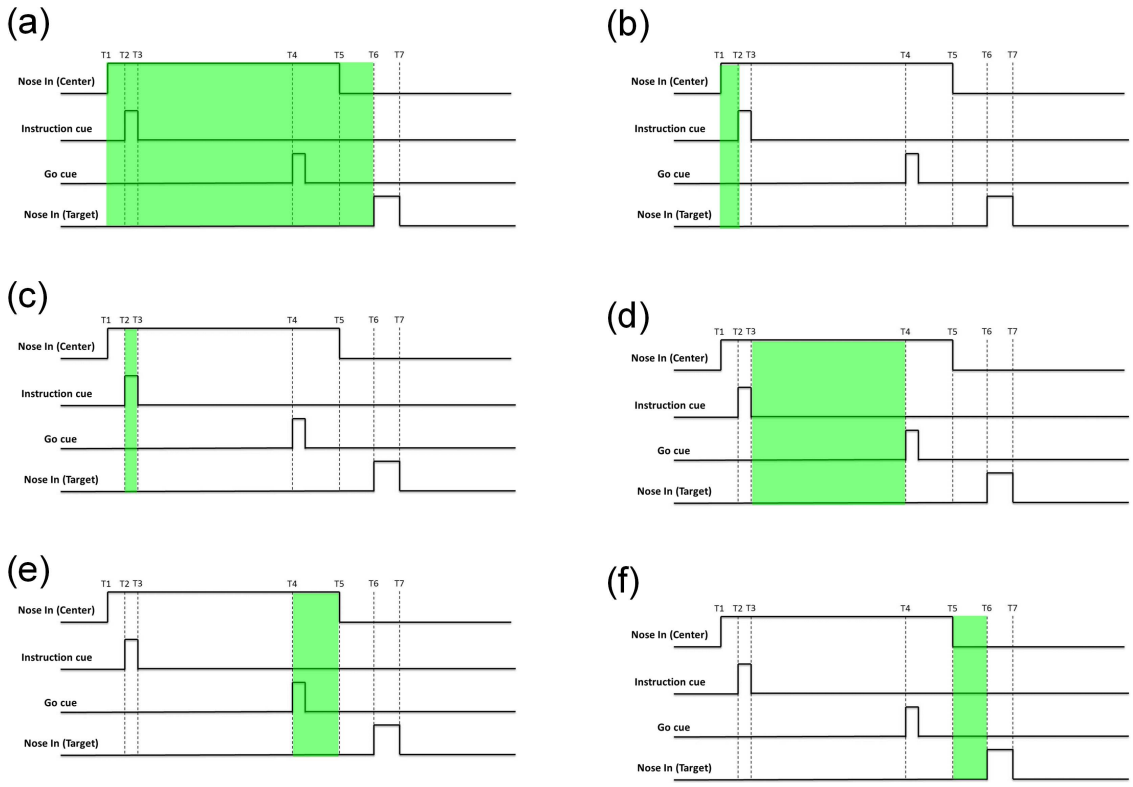

Figure 6.1: **Selective inactivation of the prelimbic circuit using optogenetics toolbox: ArchT and green light (520 nm)** Inhibiting the activity of prelimbic cells **a)**throughout the trial and during **b)** fixation period, **c)** the instruction cue presentation, **d)** delay period, **e)** reaction epoch and **f)** choice epoch.

inary data where the activity is simultaneously recorded both in the prelimbic cortex and secondary motor cortex (M2), where Erlich et al. have shown motor encoding signals during the delay period [83]. However during these simultaneous recording, the quality of the M2 recordings was quite poor, which I speculate was due to the probe design used. I would suggest developing a custom designed microdrive device specifically to target the prelimbic and secondary motor cortices. This would hopefully provide means of fair comparison between different functional properties of prefrontal and premotor neurons.

APPENDICES

Appendix A. Animal Subjects

Order ID	Animal ID	Experiment	End Date
1	A4	Electrophysiology (Pilot)	04/06/2012
2	A26	Electrophysiology (Pilot)	02/22/2013
3	A28	Electrophysiology (Pilot)	05/05/2013
4	A39	Electrophysiology	02/11/2014
5	PFC2	Electrophysiology	04/30/2014
6	PFC3	Electrophysiology	06/01/2014
7	A35	Inactivation (Pilot)	08/01/2013
8	A27	Inactivation (Pilot)	09/23/2013
9	A36	Inactivation	12/02/2013
10	A37	Inactivation	04/11/2014
11	A45	Inactivation	02/07/2014
12	A47	Inactivation	04/28/2014
13	PFC4	Inactivation	07/01/2014
14	PFC5	Inactivation	07/01/2014
15	PFC12	Inactivation	07/01/2014
16	PFC13	Inactivation	07/01/2014
17	A19	Optogenetics (Pilot)	08/11/2012
18	A38	Optogenetics	01/17/2014
19	A48	Optogenetics	04/30/2014
20	PFC1	Optogenetics	04/30/2014
21	PFC14	Optogenetics	07/15/2014
22	PFC15	Optogenetics	07/15/2014
23	PFC16	Optogenetics	07/15/2014
24	PFC17	Optogenetics	07/15/2014

Table 1: List of animal subject recruited for different experiments.

Electrophysiology

Subject ID: A39

Session	Date	Number of Units	Performance
1	01/29/2014	12	71.11
2	01/30/2014	33	71.11
3	01/30/2014	18	78.05
4	01/31/2014	27	82.65
5	02/01/2014	37	72.27
6	02/03/2014	36	79.90
7	02/04/2014	25	79.29

Table 2: Detail session information about A39.

Subject ID: PFC2

Session	Date	Number of Units	Performance
1	04/01/2014	19	82.82
2	04/02/2014	10	80
3	04/03/2014	13	82.51
4	04/09/2014	11	83.17
5	04/11/2014	11	81.81
6	04/16/2014	13	79.66
7	04/17/2014	10	79.13
8	04/21/2014	9	82.43

Table 3: Detail session information about PFC2.

Subject ID: PFC3

Session	Date	Number of Units	Performance
1	05/07/2014	9	80.98
2	05/08/2014	5	78.77
3	05/12/2014	8	81.28
4	05/13/2014	6	77.83
5	05/14/2014	4	82.08
6	05/15/2014	2	80.76
7	05/16/2014	8	78.83
8	05/19/2014	5	78.68
9	05/20/2014	2	80.31

Table 4: Detail session information about PFC3.

Appendix B. Video tracking of head orientation

From very early on, one of the main concerns of the delayed reaction tasks was the identification of the means of accomplishing the task [76, 132]. One possible suggestion was that the subjects may use postural mediation and orient their body towards the target preparing for a movement toward the target, whereas the other other hypothesis suggests the use of a memory mechanism to maintain a plan for the forthcoming behavior.

To investigate the underlying means of performing the task, we used two LEDs on attached to the recording headstage and obtained high speed video recording to extract the location of the LEDs and thus infer the head orientation. Details of the method are described in Appendix 6.

Figure 2 shows the head orientation averaged across many trials during a session for right and left trials. The two trajectories share their pre-movement segments where the head is almost at zero angle with respect to the midline. Trajectories start to diverge after the Go cue. This suggest a strategy other than the use of body posture for task accomplishment.

To track the head orientation during the task performance, I used two LEDs(red and green) on top of subjects head. Images were captured using a uEye camera at 87 fps rate

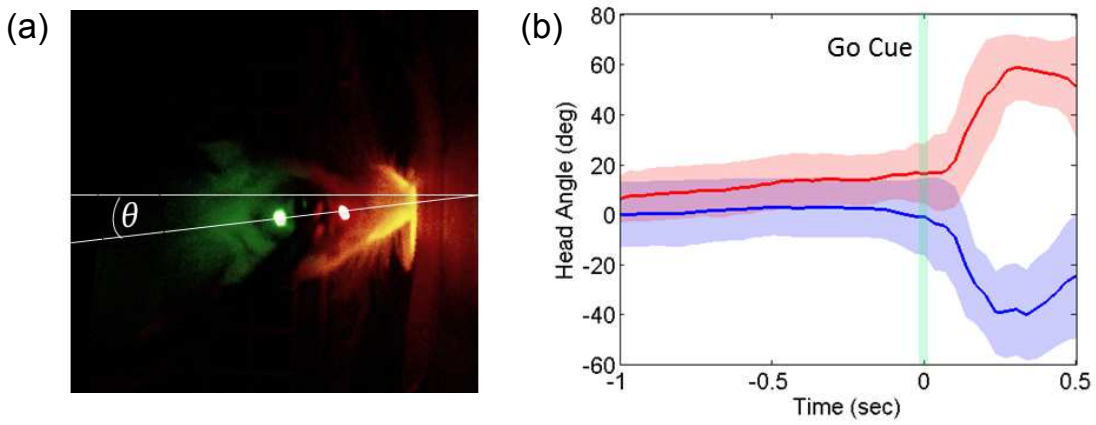

Figure 2: **Tracking head orientation a** One captured frame during the delay period of the subject performing the task, showing the midline, two LEDs and the head orientation angle θ. **b** Head orientation throughout different epoch of the task, averaged across right and left trials.

and saved on a local computer for further offline analysis. Figure 3 shows the flowchart of the analysis used to extract the spatial location of the LEDs through time and infer the head orientation.

Briefly, each frame was acquired and the color image was converted to a grayscale image. Using the Otsu's method [176] a threshold was determined to segment the background and the detected objects(presumably the LEDs). Following image segmentation, a black and white is acquired. Morphological operations were used to detemine the number of objects [108]. If exactly two objects are detected in the field of view (the two LEDs), the centroid of each is determined and the head orientation is determined geometrically. In case less than two objects were detected (e.g. when the subjects is out of the field of view or one of the LEDs is blocked by the wires) or more than two objects are detected (e.g. by reflection of one the LEDs), the algorithms returned a N/A. The N/A were estimated by a linear interpolation during the postprocessing. Sample images recorded while the subject performing the task is shown in Figure 4.

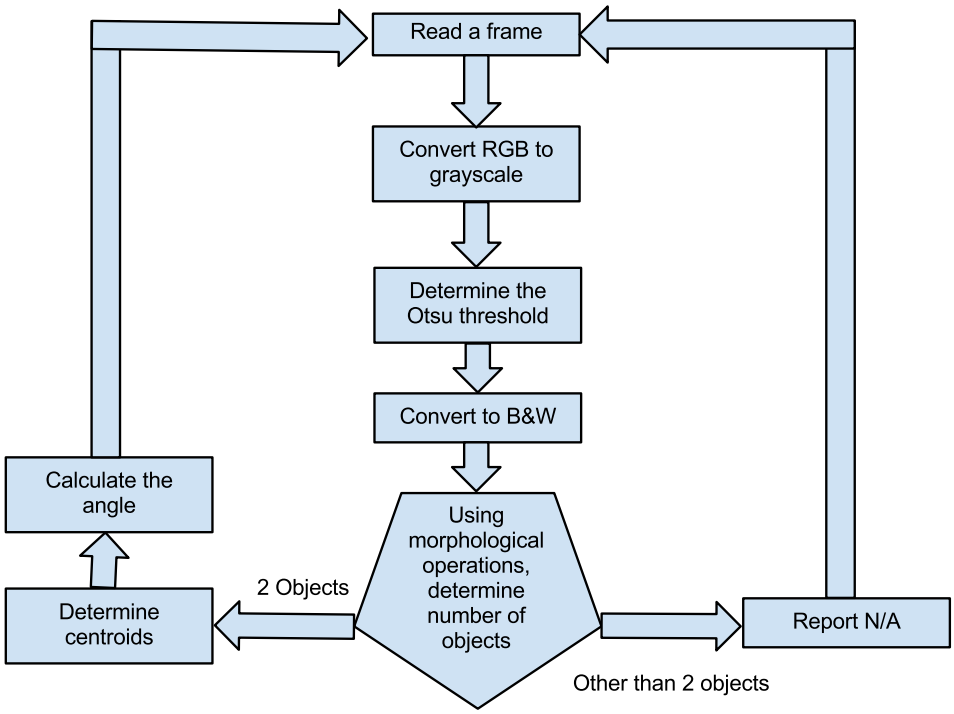

Figure 3: **Flowchart of the algorithms developed to track the head orientation**, using colored images captured at 87 fps.

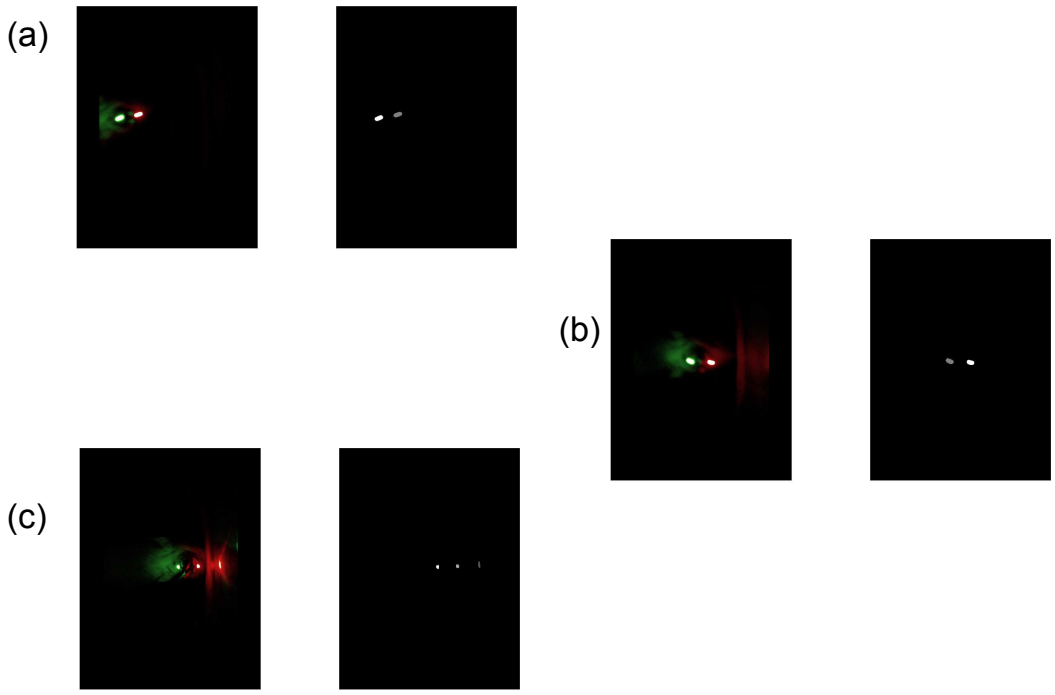

Figure 4: **Samples of video tracking** Right panel shows the raw image captured while the subject performed the task and the left panel is the final output of the algorithm that shows the location of the LEDs. **(a)** The subject is moving toward the fixation hole **(b)** the subject inside the fixation whole during a delay period **(c)** reflection of the red LED causing the detection of a third object.

Appendix C. Behavior-locked suppression of neuronal activity

In this dissertation, it has been shown that suppression of prefrontal cortex activity using an optogenetic approach that enables a suppression temporally limited to the duration of the trial results in lateralized deficit in subject's performance. Furthermore I designed another experiment where the suppression of activity was limited to individual epochs of the task. In particular, subsets of trials throughout a session were selected in which the light was delivered only fixation, instruction, delay, reaction and choice epochs. Also different subsets of trials were selected in which light was either delivered throughout the trial or no light was delivered at all. The latter was used as a negative control while the former was a positive control to ensure that the light is effective.

To my surprise, effectiveness of optogenetic suppression dropped dramatically with consecutive suppression sessions. This rate of decline is shown for one subject in Figure , suggesting that after n=5 sessions the effect is almost negligible.

Following these results, to calculate the performance drop due to epoch-limited optogenetic suppression of activity, I only included the first 5 sessions for each subjects. Results are shown in Figure 6.

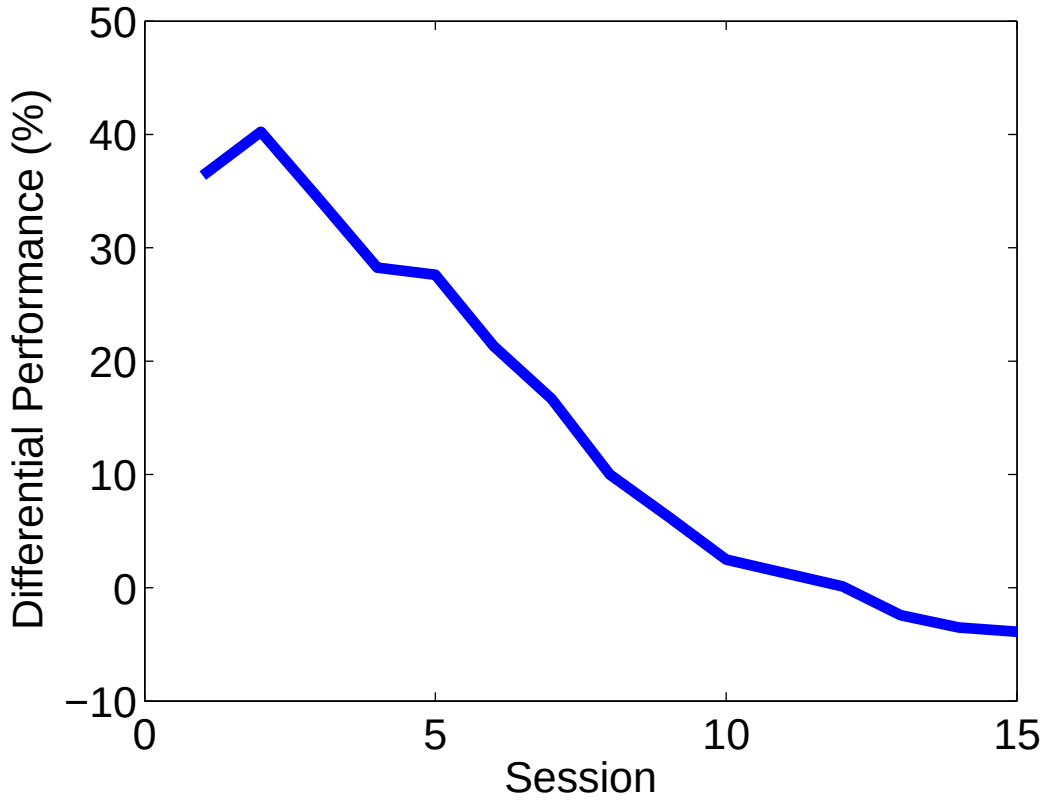

Figure 5: **Changes in lateralized performance deficit**, lateralized performance deficit is one metric of suppression effectiveness. As shown here, this measure is declining throught consecutive repetition of optogenetic suppression.

Although the data depicts a trend towards differential performance during choice, reaction and delay suppression, but there exists no statistically significant difference between the contralateral and ipsilateral trials. This can be in part due to the decline observed in effectiveness of the optogenetic suppression. Long-term effects of optogenetics perturbation of neuronal activity has not yet been fully studied. One possible hypothesis for the decline in effectiveness of the suppression is the engagement of compensatory mechanisms that get activated during artificial perturbation of neuronal activity [248]. However, more has to be studied to fully explain the effects observed in this pilot dataset.

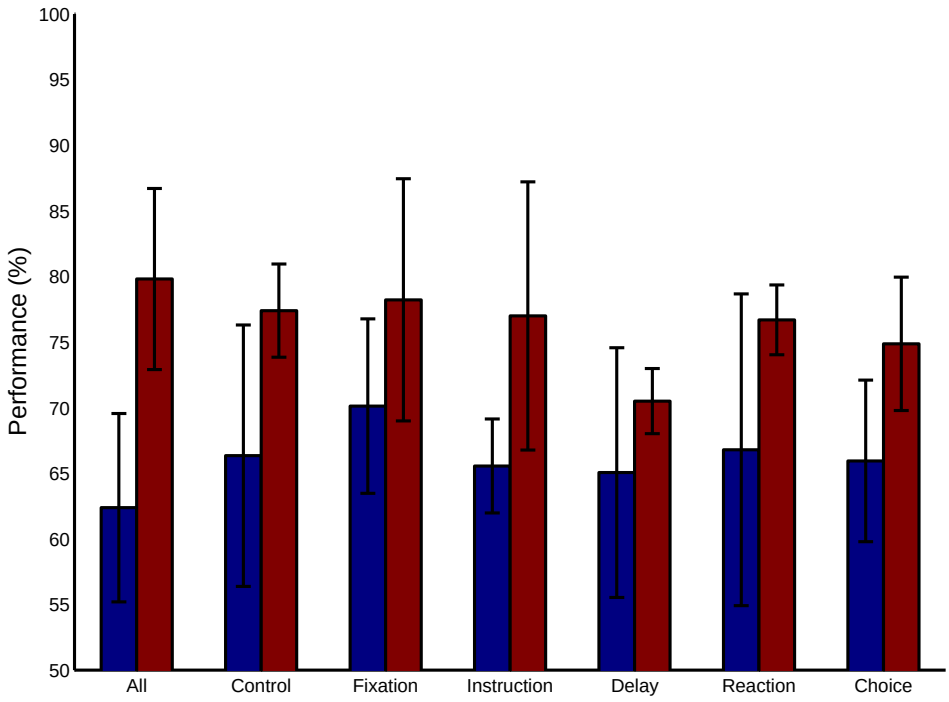

Figure 6: **Performances under epoch specific suppression of activity**, n=4 subjects, 2,000 trials.

BIBLIOGRAPHY

BIBLIOGRAPHY

[1] Abeles, M. *Local cortical circuits*. Springer, 1982.

[2] Abeles, M. *Corticonics: Neural circuits of the cerebral cortex*. Cambridge University Press, 1991.

[3] Abeles, M. Synfire chains. 1441. revision 91850.

[4] Afshar, A., Santhanam, G., Yu, B. M., Ryu, S. I., Sahani, M., and Shenoy, K. V. Single-trial neural correlates of arm movement preparation. *Neuron 71*, 3 (2011), 555–564.

[5] Aghagolzadeh, M., Eldawlatly, S., and Oweiss, K. Synergistic coding by cortical neural ensembles. *Information Theory, IEEE Transactions on 56*, 2 (2010), 875–889.

[6] Aghagolzadeh, M., and Oweiss, K. Compressed and distributed sensing of neuronal activity for real time spike train decoding. *Neural Systems and Rehabilitation Engineering, IEEE Transactions on 17*, 2 (2009), 116–127.

[7] Akirav, I., Raizel, H., and Maroun, M. Enhancement of conditioned fear extinction by infusion of the gabaa agonist muscimol into the rat prefrontal cortex and amygdala. *European Journal of Neuroscience 23*, 3 (2006), 758–764.

[8] Alexander, G. E., and Crutcher, M. D. Preparation for movement: neural representations of intended direction in three motor areas of the monkey. *Journal of Neurophysiology 64*, 1 (1990), 133–150.

[9] Allen, T. A., Narayanan, N. S., Kholodar-Smith, D. B., Zhao, Y., Laubach, M., and Brown, T. H. Imaging the spread of reversible brain inactivations using fluorescent muscimol. *Journal of neuroscience methods 171*, 1 (2008), 30–38.

[10] Andersen, R., Burdick, J., Musallam, S., Pesaran, B., and Cham, J. Cognitive neural prosthetics. *Trends in Cognitive Sciences 8*, 11 (2004), 486–493.

[11] Arikan, R., Blake, N. M., Erinjeri, J. P., Woolsey, T. A., Giraud, L., and Highstein, S. M. A method to measure the effective spread of focally injected muscimol into the central nervous system with electrophysiology and light microscopy. *Journal of neuroscience methods 118*, 1 (2002), 51–57.

[12] Atkinson, R. C., and Shiffrin, R. M. Human memory: A proposed system and its control processes. *The psychology of learning and motivation 2* (1968), 89–195.

[13] Babadi, B., and Brown, E. A review of multi-taper spectral analysis.

[14] Baddeley, A. The episodic buffer: a new component of working memory? *Trends in cognitive sciences 4*, 11 (2000), 417–423.

[15] Baddeley, A., Chincotta, D., Stafford, L., and Turk, D. Is the word length effect in stm entirely attributable to output delay? evidence from serial recognition. *The Quarterly Journal of Experimental Psychology: Section A 55*, 2 (2002), 353–369.

[16] Baddeley, A. D., and Hitch, G. Working memory. *The psychology of learning and motivation 8* (1974), 47–89.

[17] Baddely, A. Working memory: theories, models, and controversies. *Annual review of psychology 63* (2012), 1–29.

[18] Balleine, B. W., and O'Doherty, J. P. Human and rodent homologies in action control: corticostriatal determinants of goal-directed and habitual action. *Neuropsychopharmacology 35*, 1 (2009), 48–69.

[19] Banich, M. T., and Compton, R. J. *Cognitive neuroscience*. Wadsworth Publishing Company, 2010.

[20] Bansal, A. K., Truccolo, W., Vargas-Irwin, C. E., and Donoghue, J. P. Decoding 3d reach and grasp from hybrid signals in motor and premotor cortices: spikes, multiunit activity, and local field potentials. *Journal of neurophysiology 107*, 5 (2012), 1337–1355.

[21] Bari, A., Dalley, J. W., and Robbins, T. W. The application of the 5-choice serial reaction time task for the assessment of visual attentional processes and impulse control in rats. *Nature protocols 3*, 5 (2008), 759–767.

[22] Barthó, P., Hirase, H., Monconduit, L., Zugaro, M., Harris, K. D., and Buzsáki, G. Characterization of neocortical principal cells and interneurons by net-

work interactions and extracellular features. *Journal of neurophysiology 92*, 1 (2004), 600–608.

[23] Bays, P. M. Noise in neural populations accounts for errors in working memory. *The Journal of Neuroscience 34*, 10 (2014), 3632–3645.

[24] Bekolay, T., Laubach, M., and Eliasmith, C. A spiking neural integrator model of the adaptive control of action by the medial prefrontal cortex. *The Journal of Neuroscience 34*, 5 (2014), 1892–1902.

[25] BeMent, S. L., Wise, K. D., Anderson, D. J., Najafi, K., and Drake, K. L. Solid-state electrodes for multichannel multiplexed intracortical neuronal recording. *Biomedical Engineering, IEEE Transactions on*, 2 (1986), 230–241.

[26] Bialek, W., Rieke, F., Van Steveninck, R. d. R., and Warland, D. Reading a neural code. *Science 252*, 5014 (1991), 1854–1857.

[27] Bishop, C., et al. *Pattern recognition and machine learning*, vol. 4. springer New York, 2006.

[28] Blanche, T. J., Spacek, M. A., Hetke, J. F., and Swindale, N. V. Polytrodes: high-density silicon electrode arrays for large-scale multiunit recording. *Journal of neurophysiology 93*, 5 (2005), 2987–3000.

[29] Bland, B. H. The physiology and pharmacology of hippocampal formation theta rhythms. *Progress in neurobiology 26*, 1 (1986), 1–54.

[30] Boashash, B. *Time frequency analysis*. Gulf Professional Publishing, 2003.

[31] Bokil, H., Andrews, P., Kulkarni, J. E., Mehta, S., and Mitra, P. P. Chronux: a platform for analyzing neural signals. *Journal of neuroscience methods 192*, 1 (2010), 146–151.

[32] Boussaoud, D., and Wise, S. Primate frontal cortex: effects of stimulus and movement. *Experimental Brain Research 95*, 1 (1993), 28–40.

[33] Boyden, E. S., Zhang, F., Bamberg, E., Nagel, G., and Deisseroth, K. Millisecond-timescale, genetically targeted optical control of neural activity. *Nature neuroscience 8*, 9 (2005), 1263–1268.

[34] Brasted, P. J., Dunnett, S. B., and Robbins, T. W. Unilateral lesions of the medial agranular cortex impair responding on a lateralised reaction time task. *Behavioural brain research 111*, 1 (2000), 139–151.

[35] Braver, T. S., and Cohen, J. D. 31 on the control of control: The role of dopamine in regulating prefrontal function and working memory.

[36] Brodal, P. *The central nervous system: structure and function*. Oxford University Press, 2004.

[37] Brown, E. N., Kass, R. E., and Mitra, P. P. Multiple neural spike train data analysis: state-of-the-art and future challenges. *Nature neuroscience 7*, 5 (2004), 456–461.

[38] Buzsáki, G. Theta oscillations in the hippocampus. *Neuron 33*, 3 (2002), 325–340.

[39] Buzsáki, G. Large-scale recording of neuronal ensembles. *Nature neuroscience 7*, 5 (2004), 446–451.

[40] Buzsaki, G. *Rhythms of the Brain*. Oxford University Press, USA, 2009.

[41] Buzsáki, G. Neural syntax: cell assemblies, synapsembles, and readers. *Neuron 68*, 3 (2010), 362–385.

[42] Buzsáki, G., Anastassiou, C. A., and Koch, C. The origin of extracellular fields and currentseeg, ecog, lfp and spikes. *Nature Reviews Neuroscience 13*, 6 (2012), 407–420.

[43] Buzsáki, G., and Wang, X.-J. Mechanisms of gamma oscillations. *Annual review of neuroscience 35* (2012), 203–225.

[44] Carmena, J. M., Lebedev, M. A., Crist, R. E., O'Doherty, J. E., Santucci, D. M., Dimitrov, D. F., Patil, P. G., Henriquez, C. S., and Nicolelis, M. A. Learning to control a brain–machine interface for reaching and grasping by primates. *PLoS biology 1*, 2 (2003), e42.

[45] Carter, M., and Shieh, J. *Guide to research techniques in neuroscience*. Academic Press, 2009.

[46] Chatham, C. H., Frank, M. J., and Badre, D. Corticostriatal output gating during selection from working memory. *Neuron 81*, 4 (2014), 930–942.

[47] Christopher, and Foundation, D. R. One degree of separation, Paralysis and Spinal cord injury in the united states. Tech. rep., 01 2009.

[48] Churchland, M. M., Afshar, A., and Shenoy, K. V. A central source of movement variability. *Neuron 52*, 6 (2006), 1085–1096.

[49] Cisek, P., and Kalaska, J. F. Neural correlates of reaching decisions in dorsal premotor cortex: specification of multiple direction choices and final selection of action. *Neuron 45*, 5 (2005), 801–814.

[50] Cohen, A., Daubechies, I., and Feauveau, J.-C. Biorthogonal bases of compactly supported wavelets. *Communications on pure and applied mathematics 45*, 5 (1992), 485–560.

[51] Cohen, L. *Time-frequency analysis*, vol. 778. Prentice Hall PTR Englewood Cliffs, NJ:, 1995.

[52] Cohen, M. X. *Analyzing Neural Time Series Data: Theory and Practice*. MIT Press, 2014.

[53] Collinger, J. L., Wodlinger, B., Downey, J. E., Wang, W., Tyler-Kabara, E. C., Weber, D. J., McMorland, A. J., Velliste, M., Boninger, M. L., and Schwartz, A. B. High-performance neuroprosthetic control by an individual with tetraplegia. *The Lancet 381*, 9866 (2013), 557–564.

[54] Collins, A. G., and Frank, M. J. Cognitive control over learning: creating, clustering, and generalizing task-set structure. *Psychological review 120*, 1 (2013), 190.

[55] Compte, A., Brunel, N., Goldman-Rakic, P. S., and Wang, X.-J. Synaptic mechanisms and network dynamics underlying spatial working memory in a cortical network model. *Cerebral Cortex 10*, 9 (2000), 910–923.

[56] Cools, A. Role of the neostriatal dopaminergic activity in sequencing and selecting behavioural strategies: facilitation of processes involved in selecting the best strategy in a stressful situation. *Behavioural brain research 1*, 5 (1980), 361–378.

[57] Cools, R., Sheridan, M., Jacobs, E., and D'Esposito, M. Impulsive personality predicts dopamine-dependent changes in frontostriatal activity during component processes of working memory. *The Journal of neuroscience 27*, 20 (2007), 5506–5514.

[58] Cowen, S. L., and McNaughton, B. L. Selective delay activity in the medial prefrontal cortex of the rat: contribution of sensorimotor information and contingency. *Journal of neurophysiology 98*, 1 (2007), 303–316.

[59] Crick, F., and Koch, C. Towards a neurobiological theory of consciousness. In *Seminars in the Neurosciences* (1990), vol. 2, p. 203.

[60] Crick, F., and Koch, C. A framework for consciousness. *Nature neuroscience 6*, 2 (2003), 119–126.

[61] Csicsvari, J., Henze, D. A., Jamieson, B., Harris, K. D., Sirota, A., Barthó, P., Wise, K. D., Buzsáki, G., et al. Massively parallel recording of unit and local field potentials with silicon-based electrodes. *Journal of neurophysiology 90*, 2 (2003), 1314–1323.

[62] Dalley, J. W., Cardinal, R. N., and Robbins, T. W. Prefrontal executive and cognitive functions in rodents: neural and neurochemical substrates. *Neuroscience & Biobehavioral Reviews 28*, 7 (2004), 771–784.

[63] Daubechies, I. Orthonormal bases of compactly supported wavelets. *Communications on pure and applied mathematics 41*, 7 (1988), 909–996.

[64] Daubechies, I. Orthonormal bases of compactly supported wavelets ii. variations on a theme. *SIAM Journal on Mathematical Analysis 24*, 2 (1993), 499–519.

[65] Daubechies, I., et al. *Ten lectures on wavelets*, vol. 61. SIAM, 1992.

[66] Dayan, P., and Abbott, L. F. *Theoretical neuroscience*, vol. 31. MIT press Cambridge, MA, 2001.

[67] Deller, J. R., Proakis, J. G., and Hansen, J. H. *Discrete-time processing of speech signals*. IEEE New York, NY, USA:, 2000.

[68] Dempster, A. P., Laird, N. M., Rubin, D. B., et al. Maximum likelihood from incomplete data via the em algorithm. *Journal of the Royal statistical Society 39*, 1 (1977), 1–38.

[69] Denny-Brown, D., and Yanagisawa, N. The role of the basal ganglia in the initiation of movement. *Research publications-Association for Research in Nervous and Mental Disease 55* (1976), 115.

[70] Diesmann, M., Gewaltig, M.-O., and Aertsen, A. Stable propagation of synchronous spiking in cortical neural networks. *Nature 402*, 6761 (1999), 529–533.

[71] DiStefano III, J. *Dynamic Systems Biology Modeling and Simulation*. Academic Press, 2014.

[72] Donoghue, J. P. Connecting cortex to machines: recent advances in brain interfaces. *nature neuroscience 5* (2002), 1085–1088.

[73] Donoho, D. L., and Johnstone, J. M. Ideal spatial adaptation by wavelet shrinkage. *Biometrika 81*, 3 (1994), 425–455.

[74] Druckmann, S., and Chklovskii, D. B. Neuronal circuits underlying persistent representations despite time varying activity. *Current Biology* (2012).

[75] Duda, R., Hart, P., and Stork, D. Pattern classification. *New York: John Wiley, Section 10* (2001), l.

[76] Dudchenko, P. A. An overview of the tasks used to test working memory in rodents. *Neuroscience & Biobehavioral Reviews 28*, 7 (2004), 699–709.

[77] DUNCAN, R. *Response times: Their role in inferring elementary mental organization*. Oxford University Press, USA, 1991.

[78] Durstewitz, D., Seamans, J. K., and Sejnowski, T. J. Neurocomputational models of working memory. *Nature neuroscience 3* (2000), 1184–1191.

[79] Edeline, J.-M., Hars, B., Hennevin, E., and Cotillon, N. Muscimol diffusion after intracerebral microinjections: a reevaluation based on electrophysiological and autoradiographic quantifications. *Neurobiology of learning and memory 78*, 1 (2002), 100–124.

[80] Eichenbaum, H. *Learning & memory*. WW Norton & Company, 2008.

[81] Eliasmith, C. *How to build a brain: A neural architecture for biological cognition*. Oxford University Press, 2013.

[82] Elixhauser, A., Cost, H., Project, U., et al. *Hospitalization in the United States, 1997*. Agency for Healthcare Research and Quality, 2000.

[83] Erlich, J. C., Bialek, M., and Brody, C. D. A cortical substrate for memory-guided orienting in the rat. *Neuron 72*, 2 (2011), 330–343.

[84] Ethier, C., Oby, E. R., Bauman, M., and Miller, L. E. Restoration of grasp following paralysis through brain-controlled stimulation of muscles. *Nature 485*, 7398 (2012), 368–371.

[85] Euston, D. R., and McNaughton, B. L. Apparent encoding of sequential context in rat medial prefrontal cortex is accounted for by behavioral variability. *The Journal of neuroscience 26*, 51 (2006), 13143–13155.

[86] Eysenck, M. W. *Cognitive psychology: A student's handbook*. Taylor & Francis, 2000.

[87] Feller, W. Probability theory and its applications. *New York* (1950), 118–123.

[88] Fetz, E., and Baker, M. Response properties of precentral neurons in awake monkeys. *Physiologist 12*, 3 (1969), 223.

[89] Fetz, E. E. Operant conditioning of cortical unit activity. *Science 163*, 3870 (1969), 955–958.

[90] Fetz, E. E., and Finocchio, D. V. Operant conditioning of specific patterns of neural and muscular activity. *Science 174*, 4007 (1971), 431–435.

[91] Frank, M. J., Loughry, B., and OReilly, R. C. Interactions between frontal cortex and basal ganglia in working memory: a computational model. *Cognitive, Affective, & Behavioral Neuroscience 1*, 2 (2001), 137–160.

[92] Fujisawa, S., Amarasingham, A., Harrison, M. T., and Buzsáki, G. Behavior-dependent short-term assembly dynamics in the medial prefrontal cortex. *Nature neuroscience 11*, 7 (2008), 823–833.

[93] Fujisawa, S., and Buzsáki, G. A 4 hz oscillation adaptively synchronizes prefrontal, vta, and hippocampal activities. *Neuron 72*, 1 (2011), 153–165.

[94] Funahashi, S., Bruce, C. J., and Goldman-Rakic, P. S. Mnemonic coding of visual space in the monkey's dorsolateral prefrontal cortex. *Journal of neurophysiology 61*, 2 (1989), 331–349.

[95] Fuster, J. *The prefrontal cortex*. Academic Press, 2008.

[96] Fuster, J. M., Alexander, G. E., et al. Neuron activity related to short-term memory. *Science 173*, 997 (1971), 652–654.

[97] Fuster, J. M., Bodner, M., and Kroger, J. K. Cross-modal and cross-temporal association in neurons of frontal cortex. *Nature 405*, 6784 (2000), 347–351.

[98] Gabor, D. Theory of communication. part 1: The analysis of information. *Journal of the Institution of Electrical Engineers-Part III: Radio and Communication Engineering 93*, 26 (1946), 429–441.

[99] Gage, G. J., Stoetzner, C. R., Wiltschko, A. B., and Berke, J. D. Selective activation of striatal fast-spiking interneurons during choice execution. *Neuron 67*, 3 (2010), 466–479.

[100] Gerardin, E., Pochon, J.-B., Poline, J.-B., Tremblay, L., Van de Moortele, P.-F., Levy, R., Dubois, B., Le Bihan, D., and Lehéricy, S. Distinct striatal regions support movement selection, preparation and execution. *Neuroreport 15*, 15 (2004), 2327.

[101] Ghil, M., Allen, M., Dettinger, M., Ide, K., Kondrashov, D., Mann, M., Robertson, A. W., Saunders, A., Tian, Y., Varadi, F., et al. Advanced spectral methods for climatic time series. *Reviews of geophysics 40*, 1 (2002), 3–1.

[102] Gilja, V., Chestek, C. A., Diester, I., Henderson, J. M., Deisseroth, K., and Shenoy, K. V. Challenges and opportunities for next-generation intracortically based neural prostheses. *Biomedical Engineering, IEEE Transactions on 58*, 7 (2011), 1891–1899.

[103] Gisquet-Verrier, P., and Delatour, B. The role of the rat prelimbic/infralimbic cortex in working memory: not involved in the short-term maintenance but in monitoring and processing functions. *Neuroscience 141*, 2 (2006), 585–596.

[104] Glowinski, J., and Christen, P. G.-R. Y. *Motor and cognitive functions of the prefrontal cortex*. Springer, 1994.

[105] Gold, C., Henze, D. A., Koch, C., and Buzsáki, G. On the origin of the extracellular action potential waveform: a modeling study. *Journal of neurophysiology 95*, 5 (2006), 3113–3128.

[106] Goldstein, E. *Cognitive psychology: Connecting mind, research and everyday experience*. Cengage Learning, 2010.

[107] Golgi, C. The neuron doctrine: theory and facts. *Nobel lecture 1921* (1906), 190–217.

[108] Gonzalez, R. C., Woods, R. E., and Eddins, S. L. *Digital image processing using MATLAB*, vol. 2. Gatesmark Publishing Tennessee, 2009.

[109] Goodman, L. A. Kolmogorov-smirnov tests for psychological research. *Psychological bulletin 51*, 2 (1954), 160.

[110] Grossmann, A., and Morlet, J. Decomposition of hardy functions into square integrable wavelets of constant shape. *SIAM journal on mathematical analysis 15*, 4 (1984), 723–736.

[111] Gustus, A., Stillfried, G., Visser, J., Jörntell, H., and van der Smagt, P. Human hand modelling: kinematics, dynamics, applications. *Biological cybernetics 106*, 11-12 (2012), 741–755.

[112] Haggard, P. Human volition: towards a neuroscience of will. *Nature Reviews Neuroscience 9*, 12 (2008), 934–946.

[113] Hahn, S. L. *Hilbert transforms in signal processing*. Artech House, 1996.

[114] Han, Y. K., Köver, H., Insanally, M. N., Semerdjian, J. H., and Bao, S. Early experience impairs perceptual discrimination. *Nature neuroscience 10*, 9 (2007), 1191–1197.

[115] Harris, K. D. Neural signatures of cell assembly organization. *Nature Reviews Neuroscience 6*, 5 (2005), 399–407.

[116] Harris, K. D., Henze, D. A., Csicsvari, J., Hirase, H., and Buzsáki, G. Accuracy of tetrode spike separation as determined by simultaneous intracellular and extracellular measurements. *Journal of Neurophysiology 84*, 1 (2000), 401–414.

[117] Hasselmo, M. E. A model of prefrontal cortical mechanisms for goal-directed behavior. *Journal of cognitive neuroscience 17*, 7 (2005), 1115–1129.

[118] Hatsopoulos, N. G., and Donoghue, J. P. The science of neural interface systems. *Annual review of neuroscience 32* (2009), 249.

[119] Hebb, D. The organization of behavior; a neuropsychological theory.

[120] Heffner, H. E., and Heffner, R. S. Hearing ranges of laboratory animals. *Journal of the American Association for Laboratory Animal Science 46*, 1 (2007), 20–22.

[121] Hervey, A. S., Epstein, J. N., Curry, J. F., Tonev, S., Eugene Arnold, L., Keith Conners, C., Hinshaw, S. P., Swanson, J. M., and Hechtman, L. Reaction time distribution analysis of neuropsychological performance in an adhd sample. *Child Neuropsychology 12*, 2 (2006), 125–140.

[122] Hjort, N., and Jones, M. Locally parametric nonparametric density estimation. *The Annals of Statistics* (1996), 1619–1647.

[123] Hochberg, L. R., Bacher, D., Jarosiewicz, B., Masse, N. Y., Simeral, J. D., Vogel, J., Haddadin, S., Liu, J., Cash, S. S., van der Smagt, P., et al. Reach and grasp by people with tetraplegia using a neurally controlled robotic arm. *Nature 485*, 7398 (2012), 372–375.

[124] Hochreiter, S., and Schmidhuber, J. Long short-term memory. *Neural computation 9*, 8 (1997), 1735–1780.

[125] Hodgkin, A. L., and Huxley, A. F. A quantitative description of membrane current and its application to conduction and excitation in nerve. *The Journal of physiology 117*, 4 (1952), 500.

[126] Hopfield, J. J. Neural networks and physical systems with emergent collective computational abilities. *Proceedings of the national academy of sciences 79*, 8 (1982), 2554–2558.

[127] Horst, N. K., and Laubach, M. Reward-related activity in the medial prefrontal cortex is driven by consumption. *Frontiers in neuroscience 7* (2013).

[128] Hramov, A. *Wavelets in Neuroscience (Springer Series in Synergetics)*. Springer, 2014.

[129] Hsu, C., and Lin, C. A comparison of methods for multiclass support vector machines. *Neural Networks, IEEE Transactions on 13*, 2 (2002), 415–425.

[130] Huang, T.-R., Hazy, T. E., Herd, S. A., and O'Reilly, R. C. Assembling old tricks for new tasks: A neural model of instructional learning and control. *Journal of cognitive neuroscience 25*, 6 (2013), 843–851.

[131] Hung, C. P., Kreiman, G., Poggio, T., and DiCarlo, J. J. Fast readout of object identity from macaque inferior temporal cortex. *Science 310*, 5749 (2005), 863–866.

[132] Hunter, W. S. The delayed reaction in animals and children. *Animal Behavior Monographs* (1913).

[133] Hyman, R. Stimulus information as a determinant of reaction time. *Journal of experimental psychology 45*, 3 (1953), 188.

[134] Izaki, Y., Maruki, K., Hori, K., and Nomura, M. Effects of rat medial prefrontal cortex temporal inactivation on a delayed alternation task. *Neuroscience letters 315*, 3 (2001), 129–132.

[135] Jacobsen, C. F. Functions of frontal association area in primates. *Archives of Neurology and Psychiatry 33*, 3 (1935), 558.

[136] Jacobsen, C. F., and Nissen, H. W. Studies of cerebral function in primates. iv. the effects of frontal lobe lesions on the delayed alternation habit in monkeys. *Journal of Comparative Psychology 23*, 1 (1937), 101.

[137] Kandel, E. R., Schwartz, J. H., Jessell, T. M., et al. *Principles of neural science*, vol. 4. McGraw-Hill New York, 2000.

[138] Kaneko, K. *Life: an introduction to complex systems biology*. Springer, 2006.

[139] Kelly, R. C., Smith, M. A., Samonds, J. M., Kohn, A., Bonds, A., Movshon, J. A., and Lee, T. S. Comparison of recordings from microelectrode arrays and single electrodes in the visual cortex. *The Journal of neuroscience 27*, 2 (2007), 261–264.

[140] Kesner, R. P., and Churchwell, J. C. An analysis of rat prefrontal cortex in mediating executive function. *Neurobiology of learning and memory 96*, 3 (2011), 417–431.

[141] Kesner, R. P., Hunt, M. E., Williams, J. M., and Long, J. M. Prefrontal cortex and working memory for spatial response, spatial location, and visual object information in the rat. *Cerebral Cortex 6*, 2 (1996), 311–318.

[142] Koralek, A. C., Jin, X., Long II, J. D., Costa, R. M., and Carmena, J. M. Corticostriatal plasticity is necessary for learning intentional neuroprosthetic skills. *Nature 483*, 7389 (2012), 331–335.

[143] Kwon, K. Y., Eldawlatly, S., and Oweiss, K. Neuroquest: A comprehensive analysis tool for extracellular neural ensemble recordings. *Journal of neuroscience methods 204*, 1 (2012), 189–201.

[144] Lacouture, Y., and Cousineau, D. How to use matlab to fit the ex-gaussian and other probability functions to a distribution of response times. *Tutorials in Quantitative Methods for Psychology 4*, 1 (2008), 35–45.

[145] Lapish, C. C., Durstewitz, D., Chandler, L. J., and Seamans, J. K. Successful choice behavior is associated with distinct and coherent network states in anterior cingulate cortex. *Proceedings of the National Academy of Sciences 105*, 33 (2008), 11963–11968.

[146] Lebedev, M. A., and Nicolelis, M. A. Brain–machine interfaces: past, present and future. *TRENDS in Neurosciences 29*, 9 (2006), 536–546.

[147] Lewicki, M. S. A review of methods for spike sorting: the detection and classification of neural action potentials. *Network: Computation in Neural Systems 9*, 4 (1998), R53–R78.

[148] Lim, S., and Goldman, M. S. Balanced cortical microcircuitry for maintaining information in working memory. *Nature neuroscience* (2013).

[149] Lo, C.-C., Boucher, L., Paré, M., Schall, J. D., and Wang, X.-J. Proactive inhibitory control and attractor dynamics in countermanding action: a spiking neural circuit model. *The Journal of Neuroscience 29*, 28 (2009), 9059–9071.

[150] Loader, C. R. Local likelihood density estimation. *The Annals of Statistics* (1996), 1602–1618.

[151] Lu, C. W., Patil, P. G., Chestek, C. A., et al. Current challenges to the clinical translation of brain machine interface technology. *International review of neurobiology 107* (2012), 137–160.

[152] Mallat, S. *A wavelet tour of signal processing*. Academic press, 1999.

[153] Mallat, S. G. A theory for multiresolution signal decomposition: the wavelet representation. *Pattern Analysis and Machine Intelligence, IEEE Transactions on 11*, 7 (1989), 674–693.

[154] Martin, J. H. Autoradiographic estimation of the extent of reversible inactivation produced by microinjection of lidocaine and muscimol in the rat. *Neuroscience letters 127*, 2 (1991), 160–164.

[155] Meck, W. H., Penney, T. B., and Pouthas, V. Cortico-striatal representation of time in animals and humans. *Current opinion in neurobiology 18*, 2 (2008), 145–152.

[156] Mehring, C., Rickert, J., Vaadia, E., de Oliveira, S. C., Aertsen, A., and Rotter, S. Inference of hand movements from local field potentials in monkey motor cortex. *Nature neuroscience 6*, 12 (2003), 1253–1254.

[157] Meltzer, J. A., Zaveri, H. P., Goncharova, I. I., Distasio, M. M., Papademetris, X., Spencer, S. S., Spencer, D. D., and Constable, R. T. Effects of working memory load on oscillatory power in human intracranial eeg. *Cerebral Cortex 18*, 8 (2008), 1843–1855.

[158] Miesenböck, G., and Kevrekidis, I. G. Optical imaging and control of genetically designated neurons in functioning circuits. *Annu. Rev. Neurosci. 28* (2005), 533–563.

[159] Miller, E. The prefrontal cortex and cognitive control. *Nature reviews neuroscience 1*, 1 (2000), 59–66.

[160] Miller, E., and Cohen, J. An integrative theory of prefrontal cortex function. *Annual review of neuroscience 24*, 1 (2001), 167–202.

[161] Mink, J. W. The basal ganglia: focused selection and inhibition of competing motor programs. *Progress in neurobiology 50*, 4 (1996), 381–425.

[162] Mischel, W., and Metzner, R. Preference for delayed reward as a function of age, intelligence, and length of delay interval. *The Journal of Abnormal and Social Psychology 64*, 6 (1962), 425.

[163] Mitra, P., and Bokil, H. *Observed brain dynamics*. Oxford University Press, USA, 2007.

[164] Mitra, P. P., and Pesaran, B. Analysis of dynamic brain imaging data. *Biophysical journal 76*, 2 (1999), 691–708.

[165] Mohebi, A., and G., O. K. Neural ensemble correlates of working memory in the rat medial prefrontal cortex. In *41st Annual Meeting of Society for Neuroscience (SfN)* (Nov 2012).

[166] Musallam, S., Corneil, B., Greger, B., Scherberger, H., and Andersen, R. Cognitive control signals for neural prosthetics. *Science 305*, 5681 (2004), 258–262.

[167] Narayanan, N. S., and Laubach, M. Delay activity in rodent frontal cortex during a simple reaction time task. *Journal of neurophysiology 101*, 6 (2009), 2859–2871.

[168] Negrotti, M. Artificial limbs: History and current trends. In *The Reality of the Artificial*. Springer, 2012, pp. 109–113.

[169] Nicolelis, M. A. Brain–machine interfaces to restore motor function and probe neural circuits. *Nature Reviews Neuroscience 4*, 5 (2003), 417–422.

[170] Nicolelis, M. A. *Methods for neural ensemble recordings*. CRC press, 2007.

[171] Nicolelis, M. A. Mind in motion. *Scientific American 307*, 3 (2012), 58–63.

[172] ny Cajal, R. S.(1899). textura del sistema nervioso del hombre y de los vertebrados.

[173] Öngür, D., and Price, J. The organization of networks within the orbital and medial prefrontal cortex of rats, monkeys and humans. *Cerebral cortex 10*, 3 (2000), 206–219.

[174] Oppenheim, A. V., Schafer, R. W., Buck, J. R., et al. *Discrete-time signal processing*, vol. 2. Prentice-hall Englewood Cliffs, 1989.

[175] Osman, A., Kornblum, S., and Meyer, D. E. The point of no return in choice reaction time: controlled and ballistic stages of response preparation. *Journal of Experimental Psychology: Human Perception and Performance 12*, 3 (1986), 243.

[176] Otsu, N. A threshold selection method from gray-level histograms. *Automatica 11*, 285-296 (1975), 23–27.

[177] Oweiss, K. G. *Multiresolution analysis of multichannel neural recordings in the context of signal detection, estimation, classification and noise suppression*. PhD thesis, University of Michigan, 2002.

[178] Oweiss, K. G. *Statistical signal processing for neuroscience and neurotechnology*. Academic Press, 2010.

[179] Oweiss, K. G., and Anderson, D. J. A new technique for blind source separation using subband subspace analysis in correlated multichannel signal environments. In

Acoustics, Speech, and Signal Processing, 2001. Proceedings.(ICASSP'01). 2001 IEEE International Conference on (2001), vol. 5, IEEE, pp. 2813–2816.

[180] Oweiss, K. G., and Anderson, D. J. Noise reduction in multichannel neural recordings using a new array wavelet denoising algorithm. *Neurocomputing 38* (2001), 1687–1693.

[181] Oweiss, K. G., Mason, A., Suhail, Y., Kamboh, A. M., and Thomson, K. E. A scalable wavelet transform vlsi architecture for real-time signal processing in high-density intra-cortical implants. *Circuits and Systems I: Regular Papers, IEEE Transactions on 54*, 6 (2007), 1266–1278.

[182] Owings, M. F., and Kozak, L. J. Ambulatory and inpatient procedures in the united states, 1996. *Vital and health statistics. Series 13, Data from the National Health Survey*, 139 (1998), 1–119.

[183] Padhi, A. K. *Development of a Limb prosthesis by reverse mechanotransduction*. PhD thesis, 2013.

[184] Pal, N. R., and Bezdek, J. C. On cluster validity for the fuzzy c-means model. *Fuzzy Systems, IEEE Transactions on 3*, 3 (1995), 370–379.

[185] Paninski, L., Pillow, J., and Lewi, J. Statistical models for neural encoding, decoding, and optimal stimulus design. *Progress in brain research 165* (2007), 493–507.

[186] Parmesan, C., and Yohe, G. A globally coherent fingerprint of climate change impacts across natural systems. *Nature 421*, 6918 (2003), 37–42.

[187] Paxinos, G., and Watson, C. *The rat brain in stereotaxic coordinates*. Academic press, 2007.

[188] Peckham, P. H., Kilgore, K. L., Keith, M. W., Bryden, A. M., Bhadra, N., and Montague, F. W. An advanced neuroprosthesis for restoration of hand and upper arm control using an implantable controller. *The Journal of hand surgery 27*, 2 (2002), 265–276.

[189] Pesaran, B., Musallam, S., and Andersen, R. Cognitive neural prosthetics. *Current Biology 16*, 3 (2006), R77–R80.

[190] Pesaran, B., Pezaris, J. S., Sahani, M., Mitra, P. P., and Andersen, R. A. Temporal structure in neuronal activity during working memory in macaque parietal cortex. *arXiv preprint q-bio/0309034* (2002).

[191] Pillow, J. W., Ahmadian, Y., and Paninski, L. Model-based decoding, information estimation, and change-point detection techniques for multineuron spike trains. *Neural Computation 23*, 1 (2011), 1–45.

[192] Polikov, V. S., Tresco, P. A., and Reichert, W. M. Response of brain tissue to chronically implanted neural electrodes. *Journal of neuroscience methods 148*, 1 (2005), 1–18.

[193] Poor, H. V. *An introduction to signal detection and estimation*. Springer, 1994.

[194] Preuss, T. Do rats have prefrontal cortex? the rose-woolsey-akert program reconsidered. *Cognitive Neuroscience, Journal of 7*, 1 (1995), 1–24.

[195] Quintana, J., and Fuster, J. M. From perception to action: temporal integrative functions of prefrontal and parietal neurons. *Cerebral Cortex 9*, 3 (1999), 213–221.

[196] Quiroga, R. Q., Nadasdy, Z., and Ben-Shaul, Y. Unsupervised spike detection and sorting with wavelets and superparamagnetic clustering. *Neural computation 16*, 8 (2004), 1661–1687.

[197] Raghavachari, S., Kahana, M. J., Rizzuto, D. S., Caplan, J. B., Kirschen, M. P., Bourgeois, B., Madsen, J. R., and Lisman, J. E. Gating of human theta oscillations by a working memory task. *The journal of Neuroscience 21*, 9 (2001), 3175–3183.

[198] Rangel, A., Camerer, C., and Montague, P. R. A framework for studying the neurobiology of value-based decision making. *Nature Reviews Neuroscience 9*, 7 (2008), 545–556.

[199] Rao, S. C., Rainer, G., and Miller, E. K. Integration of what and where in the primate prefrontal cortex. *Science 276*, 5313 (1997), 821–824.

[200] Redgrave, P., Prescott, T. J., and Gurney, K. The basal ganglia: a vertebrate solution to the selection problem? *Neuroscience 89*, 4 (1999), 1009–1023.

[201] Renart, A., Song, P., and Wang, X.-J. Robust spatial working memory through homeostatic synaptic scaling in heterogeneous cortical networks. *Neuron 38*, 3 (2003), 473–485.

[202] Rieke, F., Warland, D., De Ruyter van Steveninck, R., and Bialek, W. Exploring the neural code. *Cambridge, Massachusetts: Institute of Technology* (1996).

[203] Roskies, A. L. How does neuroscience affect our conception of volition? *Annual review of neuroscience 33* (2010), 109–130.

[204] Rosner, B. *Fundamentals of biostatistics*. Cengage Learning, 2010.

[205] Ross, S. M. *Introduction to probability models*. Academic press, 2006.

[206] Rousche, P. J., Normann, R. A., et al. Chronic recording capability of the utah intracortical electrode array in cat sensory cortex. *Journal of neuroscience methods 82*, 1 (1998), 1.

[207] Rutishauser, U., Schuman, E. M., and Mamelak, A. N. Online detection and sorting of extracellularly recorded action potentials in human medial temporal lobe recordings, in vivo. *Journal of neuroscience methods 154*, 1 (2006), 204–224.

[208] SAMEJIMA, K., and DOYA, K. Multiple representations of belief states and action values in corticobasal ganglia loops. *Annals of the New York Academy of Sciences 1104*, 1 (2007), 213–228.

[209] Samson, H. H., and Chappell, A. Muscimol injected into the medial prefrontal cortex of the rat alters ethanol self-administration. *Physiology & behavior 74*, 4 (2001), 581–587.

[210] Schall, J. D. Neural basis of deciding, choosing and acting. *Nature Reviews Neuroscience 2*, 1 (2001), 33–42.

[211] Schmidt, R., Leventhal, D. K., Mallet, N., Chen, F., and Berke, J. D. Canceling actions involves a race between basal ganglia pathways. *Nature neuroscience 16*, 8 (2013), 1118–1124.

[212] Schneidman, E., Berry, M. J., Segev, R., and Bialek, W. Weak pairwise correlations imply strongly correlated network states in a neural population. *Nature 440*, 7087 (2006), 1007–1012.

[213] Seamans, J. K., Lapish, C. C., and Durstewitz, D. Comparing the prefrontal cortex of rats and primates: insights from electrophysiology. *Neurotoxicity research 14*, 2-3 (2008), 249–262.

[214] Serruya, M. D., Hatsopoulos, N. G., Paninski, L., Fellows, M. R., and Donoghue, J. P. Brain-machine interface: Instant neural control of a movement signal. *Nature 416*, 6877 (2002), 141–142.

[215] Shlens, J. A tutorial on principal component analysis. *Systems Neurobiology Laboratory, University of California at San Diego 82* (2005).

[216] Sonuga-Barke, E., Taylor, E., Sembi, S., and Smith, J. Hyperactivity and delay aversioni. the effect of delay on choice. *Journal of Child Psychology and Psychiatry 33*, 2 (1992), 387–398.

[217] Sternberg, S. Memory-scanning: Mental processes revealed by reaction-time experiments. *American scientist* (1969), 421–457.

[218] Stewart, T. C., Choo, X., and Eliasmith, C. Dynamic behaviour of a spiking model of action selection in the basal ganglia. In *Proceedings of the 10th international conference on cognitive modeling* (2010), Citeseer, pp. 235–40.

[219] Stuss, D. T., and Knight, R. T. *Principles of frontal lobe function*. Oxford University Press, 2013.

[220] Sul, J. H., Kim, H., Huh, N., Lee, D., and Jung, M. W. Distinct roles of rodent orbitofrontal and medial prefrontal cortex in decision making. *Neuron 66*, 3 (2010), 449–460.

[221] Szatmáry, B., and Izhikevich, E. M. Spike-timing theory of working memory. *PLoS computational biology 6*, 8 (2010), e1000879.

[222] Taylor, D. M., Tillery, S. I. H., and Schwartz, A. B. Direct cortical control of 3d neuroprosthetic devices. *Science 296*, 5574 (2002), 1829–1832.

[223] Tegnér, J., Compte, A., and Wang, X.-J. The dynamical stability of reverberatory neural circuits. *Biological cybernetics 87*, 5-6 (2002), 471–481.

[224] Thomson, D. J. Spectrum estimation and harmonic analysis. *Proceedings of the IEEE 70*, 9 (1982), 1055–1096.

[225] Thomson, D. J. Multitaper analysis of nonstationary and nonlinear time series data. *Nonlinear and nonstationary signal processing* (2000), 317–394.

[226] Tye, K. M., and Deisseroth, K. Optogenetic investigation of neural circuits underlying brain disease in animal models. *Nature Reviews Neuroscience 13*, 4 (2012), 251–266.

[227] Uylings, H., Groenewegen, H. J., and Kolb, B. Do rats have a prefrontal cortex? *Behavioural brain research 146*, 1 (2003), 3–17.

[228] Vanderwolf, C. Hippocampal electrical activity and voluntary movement in the rat. *Electroencephalography and clinical neurophysiology 26*, 4 (1969), 407–418.

[229] Varela, F. J. *The embodied mind: Cognitive science and human experience*. MIT press, 1993.

[230] Von der Malsburg, C., Phillips, W. A., and Singer, W. *Dynamic coordination in the brain: from neurons to mind*. MIT Press, 2010.

[231] Voorn, P., Vanderschuren, L. J., Groenewegen, H. J., Robbins, T. W., and Pennartz, C. Putting a spin on the dorsal–ventral divide of the striatum. *Trends in neurosciences 27*, 8 (2004), 468–474.

[232] Wallis, J. D., Anderson, K. C., and Miller, E. K. Single neurons in prefrontal cortex encode abstract rules. *Nature 411*, 6840 (2001), 953–956.

[233] Wang, X.-J. Discovering spatial working memory fields in prefrontal cortex. *Journal of Neurophysiology 93*, 6 (2005), 3027–3028.

[234] Wang, X.-J. Neurophysiological and computational principles of cortical rhythms in cognition. *Physiological reviews 90*, 3 (2010), 1195–1268.

[235] Wang, X.-J., and Buzsáki, G. Gamma oscillation by synaptic inhibition in a hippocampal interneuronal network model. *The journal of Neuroscience 16*, 20 (1996), 6402–6413.

[236] Ward, M. P., Rajdev, P., Ellison, C., and Irazoqui, P. P. Toward a comparison of microelectrodes for acute and chronic recordings. *Brain research 1282* (2009), 183–200.

[237] Whelan, R. Effective analysis of reaction time data. *The Psychological Record 58*, 3 (2010), 9.

[238] Whishaw, I. Q., et al. *The Behavior of the Laboratory Rat: A Handbook with Tests: A Handbook with Tests*. Oxford University Press, USA, 2004.

[239] Wiener, M. C., and Richmond, B. J. Model based decoding of spike trains. *Biosystems 67*, 1 (2002), 295–300.

[240] Wilcox, R. R. Some practical reasons for reconsidering the kolmogorov-smirnov test. *British Journal of Mathematical and Statistical Psychology 50*, 1 (1997), 9–20.

[241] Wild, J., Sieger, T., Novak, D., and Jech, R. Spike sorting algorithms comparison. In *2nd INCF Congress of Neuroinformatics, Pilsner, Czech Republic* (2009).

[242] Wilensky, A. E., Schafe, G. E., Kristensen, M. P., and LeDoux, J. E. Rethinking the fear circuit: the central nucleus of the amygdala is required for the acquisition, consolidation, and expression of pavlovian fear conditioning. *The Journal of neuroscience 26*, 48 (2006), 12387–12396.

[243] Willcocks, A. L., and McNally, G. P. The role of medial prefrontal cortex in extinction and reinstatement of alcohol-seeking in rats. *European Journal of Neuroscience 37*, 2 (2013), 259–268.

[244] Wiltschko, A. B., Gage, G. J., and Berke, J. D. Wavelet filtering before spike detection preserves waveform shape and enhances single-unit discrimination. *Journal of neuroscience methods 173*, 1 (2008), 34–40.

[245] Wimmer, K., Nykamp, D. Q., Constantinidis, C., and Compte, A. Bump attractor dynamics in prefrontal cortex explains behavioral precision in spatial working memory. *Nature neuroscience* (2014).

[246] Yilmaz, Ö. *Seismic data analysis*, vol. 1. Society of Exploration Geophysicists Tulsa, 2001.

[247] Zalocusky, K., and Deisseroth, K. Optogenetics in the behaving rat: integration of diverse new technologies in a vital animal model. *Optogenetics 1*, 1–17.

[248] Zanto, T. P., Chadick, J. Z., Satris, G., and Gazzaley, A. Rapid functional reorganization in human cortex following neural perturbation. *The Journal of Neuroscience 33*, 41 (2013), 16268–16274.

[249] Zhu, J. Understanding volition. *Philosophical Psychology 17*, 2 (2004), 247–273.

[250] Zhuang, J., Truccolo, W., Vargas-Irwin, C., and Donoghue, J. P. Decoding 3-d reach and grasp kinematics from high-frequency local field potentials in primate primary motor cortex. *Biomedical Engineering, IEEE Transactions on 57*, 7 (2010), 1774–1784.

[251] Ziegler-Graham, K., MacKenzie, E. J., Ephraim, P. L., Travison, T. G., and Brookmeyer, R. Estimating the prevalence of limb loss in the united states: 2005 to 2050. *Archives of physical medicine and rehabilitation 89*, 3 (2008), 422–429.